Atomic Energy Control Board
P.O. Box 1046
Ottawa, Canada
K1P 5S9

Commission de contrôle de l'énergie atomique
C.P. 1046
Ottawa, Canada
K1P 5S9

INFO-0209

# ANALYSIS OF DATA OBTAINED IN TWO-PHASE FLOW TESTS OF PRIMARY HEAT TRANSPORT PUMPS

by

T.C. Currie
Carleton University

A research report prepared for the
Atomic Energy Control Board
Ottawa, Canada

Project Number 85.1.6

June, 1986

Canada

Research report

# ANALYSIS OF DATA OBTAINED IN TWO-PHASE FLOW TESTS OF PRIMARY HEAT TRANSPORT PUMPS


## ABSTRACT

This report analyzes data obtained in two-phase flow tests of primary heat transport pumps performed during the period 1980-1983. Phenomena which have been known to cause pump-induced flow oscillations in pressurized piping systems under two-phase conditions are reviewed and the above-mentioned data analyzed to determine whether any of the identified phenomena could have been responsible for the instabilities observed in those tests. Tentative explanations for the most severe instabilities are given based on those analyses. It is shown that suction pipe geometry probably plays an important role in promoting instabilities, so additional experiments to investigate the effect of suction pipe geometry on the stability of flow in a closed pipe loop under two-phase conditions are recommended.

## RÉSUMÉ

Le présent rapport analyse les données obtenues au cours d'essais d'écoulement diphasique des pompes du circuit de caloportage primaire, effectués entre 1980 et 1983. Il examine les phénomènes connus responsables de l'oscillation de l'écoulement provoquée par les pompes dans les systèmes de canalisation sous pression dans des conditions d'écoulement diphasique et il analyse les données mentionnées ci-dessus pour déterminer si l'un ou l'autre des phénomènes identifiés pourrait avoir causé les instabilités observées lors des essais. Il suggère certaines explications possibles des instabilités les plus graves d'après ces données. Il montre que la disposition des conduites d'aspiration pourrait être largement responsable des instabilités et recommande donc de procéder à des expériences supplémentaires pour étudier l'effet de la disposition des conduites d'aspiration sur la stabilité de l'écoulement dans des canalisations à boucle fermée, placées dans des conditions d'écoulement diphasique.



## DISCLAIMER

The Atomic Energy Control Board is not responsible for the accuracy of the statements made or opinions expressed in this publication and neither the Board nor the author assumes liability with respect to any damage or loss incurred as a result of the use made of the information contained in this publication.

## EXECUTIVE SUMMARY

During the period 1980-1983, two-phase flow tests of full-scale Bruce and Pickering PHT pumps were conducted by Ontario Hydro in large test loops constructed especially for that purpose. During the course of those tests, periodic head and flow variations which resulted in limited vibration of the test loop piping were observed under certain conditions. The peak-to-peak amplitude of the head pulsations reached 450 kPa in some of the Bruce pump tests and 2 MPa in some of the Pickering pump tests, figures that correspond to approximately 25% and 150% of the respective pump differential pressures with single-phase liquid flow at design conditions.

The abovementioned periodic head pulsations occurred at loop temperatures below 180°C in the Pickering pump tests and at temperatures above 170°C in the Bruce pump tests. Since the Pickering and Bruce pump tests were performed in different loops, the differences between the results of the two series of tests could have been caused by the use of different pumps, differences in loop geometry, or both of these factors.

By analyzing the results of the Bruce pump tests, it has been concluded that the head instabilities which occurred at test temperatures greater than 170°C probably resulted from the passage of plug or slug flow through the pump, although there is a possibility that some of the instabilities were caused by self-excitation of a low order acoustic mode in the test loop. If the pulsations were caused by plug or slug flow, it is believed that their absence at test temperatures below 170°C probably resulted primarily from the steepness of the void gradient at the pump suction at such temperatures. Increases in this gradient as the test temperature was lowered would have reduced the voided length upstream of the inlet for a given pump suction void fraction and therefore the length available for plug or slug flow to develop. It is assumed in the report that the ingestion of plug or slug flow by the pump would not have caused large head variations once the head became fully degraded and that the pump suction void fraction at the completion of head degradation would have been approximately 30% in the low temperature tests. With these assumptions, it is shown that at temperatures below 170°C, the voided length upstream of the pump probably did not extend beyond the roughly 2m length of vertical pipe that preceded the pump before the pump head became fully degraded (i.e., before the pump

suction void fraction reached 30%). Since this voided length would have corresponded to fewer than four pipe diameters, the large vapor bubbles characteristic of the slug flow regime in vertical upflow would probably not have had an opportunity to form.

At temperatures above 170°, the analysis described in the report shows that the voided length probably extended into the horizontal return header upstream of the 2m length of vertical pipe before the head became fully degraded, permitting plug or slug flow to form at a void fraction much lower than the figure of 20-30% normally assumed to apply to vertical upflows. Once the flashing front had reached the horizontal return header, the voided length would have increased much more rapidly than it did when the void was restricted to the vertical pipe immediately upstream of the pump because the gravitational head loss component that would have predominated in the vertical riser would have been absent. It is assumed that the much greater voided lengths that would have existed in the tests performed at temperatures above 170°C before the pump head become fully degraded combined with the fact that most of the voided length would then have been horizontal caused plug or slug flow to form in those tests, resulting in head pulsations.

In the case of the Pickering pump tests, a suction tee located just upstream of the pump would have had a homogenizing effect on the flow passing through it and thus have prevented idealized slug or plug flow from reaching the pump inlet. This is the most probable explanation for the fact that head pulsations did not occur in the Pickering pump tests performed at loop temperatures of 180°C and above even though they were observed at those temperatures in the Bruce pump tests.

It is believed that the head pulsations observed in the Pickering pump tests performed at temperatures below 180°C resulted either from choking of the flow at some point between the suction tee and the pump inlet or from cavitation or cavitation choking within the pump. The former cause is suspected because at temperatures below 180°C, the flow velocity at the pump suction at 100% rated flow would have exceeded the homogeneous two-phase sound speed of the mixture produced when void started to form at that location. The instabilities could also have been produced by a sound speed related phenomenon other than choking, however, since large hydraulic losses and hence extensive vapor production

and flow redistribution would have occurred at the pump inlet if shock waves had formed on the anti-rotation vanes upstream of the pump and/or on the leading edges of the impeller blades.

As noted previously, the instabilities observed in the low temperature Pickering pump tests could also have resulted from cavitation or cavitation choking within the pump since these phenomena are most severe at low temperatures. Pump cavitation could have caused self-excited (self-sustaining) oscillations involving a low order acoustic mode or simply transitory oscillations that would eventually have died out even if bleeding of the loop had been discontinued. There are numerous accounts in the literature of instances in which cavitating turbopumps of other types (e.g., liquid-fueled rocket motor pumps, boiler feed pumps) have caused self-excited flow oscillations of the type just mentioned. The limited test data available for the Pickering pump tests are not sufficient to determine whether the instabilities observed in those tests were of this type, however.

It was concluded that the instabilities observed in the low temperature Pickering pump tests could not have been caused by the passage of plug or slug flow through the pump.

The analysis of the Bruce and Pickering pump tests indicates that some of the differences between the results of those tests probably resulted from differences in suction pipe geometry. For that reason, it is recommended that an experimental program be initiated to investigate the effect of suction pipe geometry on the stability of two-phase flow in a closed pipe loop. In particular, tests should be performed with and without a suction tee and with different lengths of vertical pipe upstream of the pump. A length of horizontal pipe should be provided upstream of the vertical pipe to enable the flow regimes characteristic of horizontal flow to form.

Because the peak-to-peak amplitude of the head pulsations that occurred in the Pickering pump tests performed at temperatures below 180°C was occasionally as large as 1 1/2 times the single-phase pump head, as mentioned previously, tests to identify the most probable cause of those pulsations should be given the highest priority. The low temperature instabilities were probably caused by cavitation or cavitation choking within the pump/suction tee assembly so this possibility should be investigated first.

# TABLE OF CONTENTS


| | | page |
|---|---|---|
| ABSTRACT/RÉSUMÉ | | i |
| EXECUTIVE SUMMARY | | ii |
| A | INTRODUCTION | 1 |
| A.1 | Background | 1 |
| A.2 | Bruce A Pump Tests | 2 |
| A.2.1 | Pump Design | 2 |
| A.2.2 | Test Loop Geometry | 5 |
| A.2.3 | Loop Instrumentation | 5 |
| A.2.4 | Test Procedure | 9 |
| A.2.5 | Results of the Bruce A Pump Tests | 10 |
| A.3 | Bruce B Pump Tests | 15 |
| A.4 | Pickering B Pump Tests | 19 |
| A.4.1 | Pump Design | 19 |
| A.4.2 | Test Loop Geometry | 19 |
| A.4.3 | Loop Instrumentation | 19 |
| A.4.4 | Results of the Pickering B Pump Tests | 25 |
| A.5 | Darlington PHT Pump Tests | 30 |
| A.6 | Summary | 31 |
| B | FLOW INSTABILITIES IN PRESSURIZED PIPING SYSTEMS | 32 |
| B.1 | Introduction | 32 |
| B.2 | Self-Excited (Acoustic) Flow Oscillations | 34 |
| B.2.1 | Quasi-Steady Pump Operation | 36 |
| B.2.2 | Non-Steady Pump Operation | 44 |
| B.3 | Flow Oscillations Caused By Choking of a Flow Restriction Upstream of a Pump | 53 |
| C | ANALYSIS OF BRUCE PUMP TESTS | 59 |
| C.1 | Introduction | 59 |
| C.2 | High Temperature Tests | 59 |
| C.2.1 | Possibility of Mechanical-Hydraulic Interaction | 66 |
| C.3 | Low Temperature Tests | 66 |
| C.3.1 | Reasons for the Cessation of Any Instabilities Caused By Plug or Slug Flow | 66 |
| C.3.1.1 | Reduction in the Pump Suction Void Fraction Required for Head Degradation | 67 |

| | | |
|---|---|---|
| C.3.1.2 | Decrease in the Voided Length Upstream of the Pump | 67 |
| C.3.2 | Reasons for the Cessation of Any Instabilities Caused By Self-Excitation of a Low Order Acoustic Mode | 71 |
| C.3.2.1 | Changes in the Pump's Two-Phase Performance Characteristics | 71 |
| C.3.2.2 | Concentration of Void at the Pump Suction | 71 |
| C.3.2.3 | Supersonic Flow in the Suction Pipe | 72 |
| C.4 | Summary | 78 |
| D | ANALYSIS OF PICKERING PUMP TESTS | 80 |
| D.1 | Introduction | 80 |
| D.2 | High Temperature Tests | 80 |
| D.3 | Low Temperature Tests | 82 |
| D.3.1 | Instabilities Caused By Choking Between the Suction Tee and the Pump Inlet | 83 |
| D.3.2 | Instabilities Caused By Cavitation Within the Pump | 88 |
| D.3.3 | Other Effects | 90 |
| D.4 | Summary | 92 |
| E | CONCLUSIONS | 94 |
| F | RECOMMENDATIONS | 97 |
| REFERENCES | | R1 |

APPENDICES

| | |
|---|---|
| A | Comparison of the Work Required to Isentropically Collapse the Void in a Two-Phase Mixture With the Work Required to Compress Liquid Water Between the Same Initial and Final Pressures |
| B | Analysis of Pump Surge in a Pipe Connecting Two Reservoirs |
| C | Analysis of Surge in a Simple Pipe Loop |
| D | Modified ANC Model for the Bruce Pump |
| E | Small Perturbation Analysis of Surge |

F Voided Length Calculations

G Oscillatory Void Volume Calculation

## FIGURES


| | | page |
|---|---|---|
| 1 | Cut Away View of the Bruce GS PHT Pump Used in the Pump Test Loop [Ref.1] | 3 |
| 2 | Bruce B PHT Pump Performance Characteristics [Ref.13] | 4 |
| 3 | Piping Diagram for the Bruce Pump Test Loop [Ref.4] | 6 |
| 4 | Bruce Pump Test Loop-Flow Diagram [Ref.1] | 7 |
| 5 | Transducer Locations on Bruce Pump Test Loop [Ref.7] | 8 |
| 6 | Results of Bruce Pump Test 69 (Performed at 235°C) [Ref.7] | 11 |
| 7 | Results of Bruce Pump Test 71 (Performed at 215°C) [Ref.7] | 13 |
| 8 | Oscillogram for Bruce Pump Test 85 [Ref.7] | 14 |
| 9 | Classification of Instabilities Observed in the Bruce Pump Tests [Ref.10] | 16 |
| 10 | Bruce Test Pressure Pulsation Amplitudes vs. Test Temperature [Ref.9] | 18 |
| 11 | Pickering B GS PHT Pump Cross-Section Showing Instrumentation and Auxiliary Circuits [Ref.13] | 20 |
| 12 | Pickering GS B PHT Pump Performance Characteristics [Ref.5] | 21 |
| 13 | Pickering B Test Loop and Structure Arrangement [Ref.11] | 22 |
| 14 | Pickering B PHT Pump Test Loop Flow Schematic Diagram [Ref.11] | 23 |

| | | |
|---|---|---|
| 15 | Transducer Locations on Pickering Pump Test Loop [Ref.10] | 24 |
| 16 | Pressure Pulse Amplitude vs. Test Temperature for the Pickering Void Matrix Tests [Ref.11] | 27 |
| 17 | Head Pulsation Amplitude and Frequency vs. Time in Test 202 [Ref.10] | 29 |
| 18 | Location of the Air Pocket in the Impeller of the Pump Tested by Murakami and Minemura [Ref.18] | 33 |
| 19 | First and Second Quarter Wave Acoustic Modes in a Straight Pipe Connecting Two Constant Head Reservoirs | 40 |
| 20 | First Half-Wave Acoustic Mode in a Straight Pipe Connecting Two Constant Head Reservoirs | 40 |
| 21 | Crossplot of Pump Performance Data From Air-Water Tests of Rothe and Runstadler [Ref.29] | 43 |
| 22 | Test Loop Used in Air-Water Tests Performed By Rothe and Runstadler [Ref.29] | 43 |
| 23 | Head Degradation at Different Flows for a 1:5 Scale Model of a KWU PWR Pump [Ref.30] | 45 |
| 24a | Flow Velocity Relative to the Impeller at Design Conditions | 48 |
| 24b | Void Formation and Bubble Accumulation Caused By Flow Incidence at Low Flow Coefficients | 48 |
| 25 | Loop Modelled in the Numerical Simulation of Surge | 51 |
| 26 | Results of the Numerical Simulation of Surge-Mass Flowrate ($\dot{m}$) and Pressure (p) Variations at the Pump Suction and Discharge | 51 |

| | | |
|---|---|---|
| 27 | Test Facility of Outa et al. [Ref.23] | 55 |
| 28 | Oscillogram of Flowrates and Pressures Recorded During A Period of Instability in the Tests of Outa et al. [Ref.23] | 55 |
| 29 | Sequential Flow Patterns Between the Choked Orifice and the Pump Suction in the Tests of Outa et al. [Ref.23] | 56 |
| 30 | Flow Regime Map Proposed by Mandhane et al. [Ref.39] | 63 |
| 31 | Effect of Pipe Diameter on Transition Boundaries [Ref.42] | 63 |
| 32 | Possible Path of Conditions in the Suction Pipe Assuming $U_L^S$ is Large Enough for Bubbly Flow to be the First Flow Regime to Form | 65 |
| 33 | Rapid Change in Head Pulsation Frequency Observed in Bruce GS A Pump Test 68 (240°C) [Ref.8] | 66 |
| 34 | Effect of Pressure on the Two-Phase Performance of a 1:5 Scale Model of a KWU PWR Pump at 45% Rated Flow [Ref.30] | 68 |
| 35 | Voided Length Upstream of the Pump Suction (L) | 68 |
| 36 | Voided Length Upstream of the Pump vs. Test Temperature | 70 |
| 37 | Loop Studied By Hobson and Marshall [Ref.20] With the Cavitation Volume Upstream of the Pump | 73 |
| 38 | Speed of Sound in a Homogeneous Steam-Water Mixture in Thermodynamic Equilibrium vs. Temperature at Void Fractions of 0.3, 3 and 30% | 73 |
| 39 | Possible Effect of Test Temperature on the Pump Head At Which Head Pulsations Start | 75 |

| | | |
|---|---|---|
| 40 | Oscillogram Recorded in Test 131 (Performed at 180°C) [Ref.8] | 76 |
| 41 | Void Fraction Downstream of the Suction Tee at Which Void First Appears Upstream vs. Saturation Temperature | 81 |
| 42 | Results of Test 202 [Ref.11] | 84 |

## TABLES


| | | page |
|---|---|---|
| 1 | Bruce NGS A Pump Nominal Operating Conditions and Characteristics | 5 |
| 2 | Transducer Identification Codes | 9 |
| 3 | Pickering NGS B Nominal Operating Conditions and Performance Characteristics | 19 |
| 4 | Summary of Pickering NGS B PHT Pumpset Simulated Loss of Coolant Accident Tests | 26 |
| 5 | Pressure Pulsation Data for Low Temperature Void Matrix Tests | 29 |
| 6 | Nominal Operating Conditions and Peak-to-Peak Amplitudes of Oscillatory Parameters During Surge | 52 |
| 7 | Parameter Ranges for the Flow Regime Map Proposed By Mandhane et al. [Ref.39] | 62 |
| E.1 | Data Used in the Small Perturbation Stability Calculation | E4 |
| E.2 | Values of $\sigma$ and $\omega$ for the First Four Roots of Eq.E.14 (i.e., modes of oscillation) | E5 |

# A. INTRODUCTION

## A.1 Background

During the period 1980-1983, two-phase flow tests of full-scale Bruce and Pickering primary heat transport (PHT) pumps were conducted by Ontario Hydro in test loops located at the Ontario Hydro Research Pump Test Complex (RPTC) described in [Ref.1]. During the course of those tests, which are described in detail in [Refs.2-12]*, periodic head and flow variations accompanied by vibrations of the test loop piping were observed under certain conditions. Although the tests were performed primarily to assess the survivability of the pumps under simulated loss-of-coolant accident conditions and were completed with the pumps sustaining very little damage, the cause of the observed flow instabilities was not clear in most instances.

In the earliest of the Simulated Loss-of-Coolant Accident (SLOCA) tests just referred to, a PHT pump of the type used in Bruce Nuclear Generating Station (NGS) A was tested under two-phase conditions in a test loop that will be described in a subsequent section. Tests of a Bruce NGS A PHT pump fitted with a Bruce B motor were performed later in the same test loop, followed by tests of a Pickering B PHT pump in a different loop. The conditions under which periodic head pulsations were observed in the tests of the Pickering pump, specifically at loop temperatures <u>below</u> 180°C, were not consistent with the results of the Bruce pump tests where the most severe periodic pulsations were observed at temperatures <u>above</u> 170°C. Since the Pickering and Bruce pump tests were performed in different loops, it was not clear whether the results of the tests were inconsistent in the sense just mentioned because the pumps were different, the loops were different, or both. Because of these uncertainties and because the contradictory results referred to above were never explained, the extent to which the results of the pump tests could be applied (if at all) to hypothetical accident scenarios was completely unknown.

---

* These tests were followed by tests of a Darlington PHT pump. Since no reports describing the results of the Darlington pump tests had been released by the time this report was written, those tests will be referred to only briefly in this document.

In previous work performed under contract for the Atomic Energy Control Board, Guthrie and Currie [Ref.13] reviewed the international literature on pump-related flow instabilities and resulting piping vibrations along with the results of the Ontario Hydro pump tests mentioned earlier. One of the recommendations of that study was that the results of the Ontario Hydro pump tests be analysed with the aim of gaining an improved understanding of the causes of the severe head pulsations observed in the tests and particularly why the instabilities occurred under certain conditions in the Bruce pump test loop and not under seemingly similar conditions in the Pickering pump test loop and vice-versa. This report describes such an analysis and offers tentative explanations for many of the apparently inconsistent results of the Ontario Hydro tests.

The manner in which the Bruce and Pickering SLOCA tests were performed and the results of those tests are reviewed briefly in subsequent sections.

## A.2 Bruce A Pump Tests

### A.2.1 Pump Design

A Bruce NGS A PHT pumpset uses a Byron Jackson pump and a Westinghouse motor. The pump itself is a single stage double volute design with a 72.5 cm (28.5") diameter impeller, a 56 cm (22") I.D. vertical suction pipe and a 56 cm I.D. horizontal discharge. A cut-away view of the pump, as installed in the Research Pump Test Complex in which Ontario Hydro performed the SLOCA tests, is shown in Figure 1.

The single phase performance characteristics of a Bruce NGS (A or B)* pumpset are shown in Figure 2 and the pump's nominal operating conditions and performance characteristics are summarized in Table 1.

---

* The pumps used in Bruce NGS A and B differ significantly in mechanical design but have essentially identical hydraulic performance characteristics.

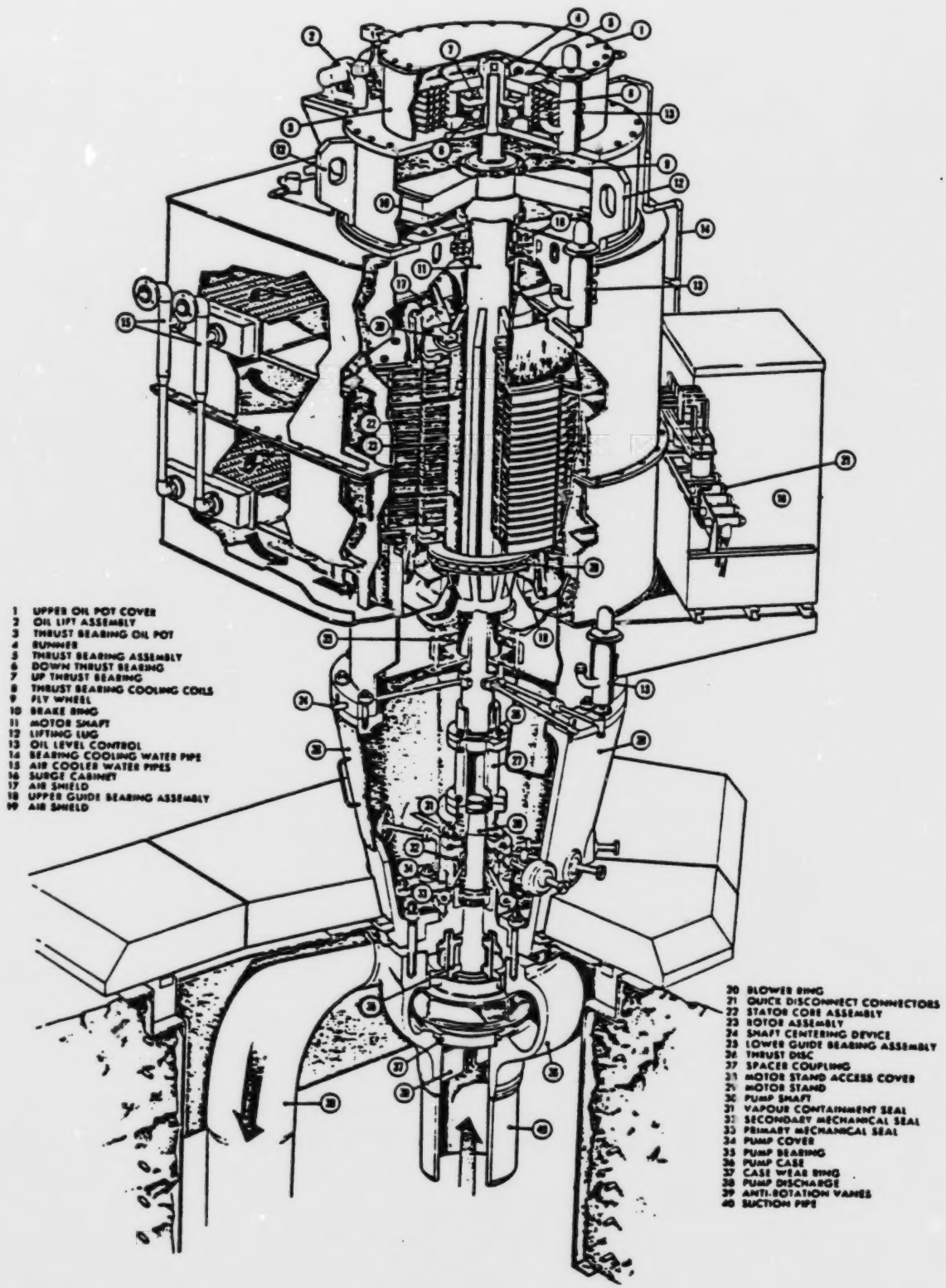


Figure 1 Cut Away View of the Bruce GS PHT Pump Used in the Pump Test Loop [from Ref.1]

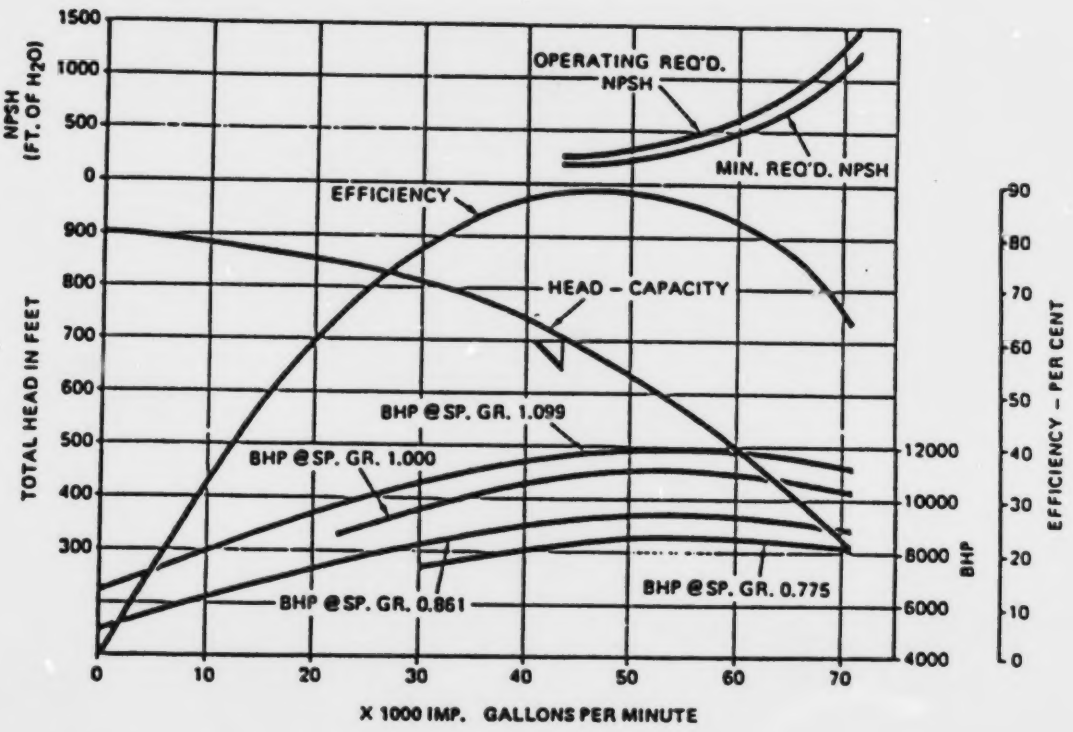


Figure 2 Bruce B PHT Pump Performance Characteristics [Ref.13]

Table 1: Bruce NGS A Pump Nominal Operating Conditions and Characteristics [Ref.1]

| | |
|---|---|
| Operating temperature | 264 C |
| Operating suction pressure | 8.83 MPa |
| Rated flow | 3.3 $m^3$/sec. |
| Rated head | 213 m |
| Motor rating | 8.5 MW |
| Motor speed | 1800 rpm |
| Specific speed | 3220 rpm US $gpm^{1/2}$ / $ft^{3/4}$ |

### A.2.2 Test Loop Geometry

The test loop in which the Bruce pump tests were performed is shown in Figures 3 and 4. As illustrated, the suction and discharge headers were connected by three inverted U-shaped pipes, or "hairpins", each of which was fitted with a throttling valve located approximately 2.5 m above a horizontal length of pipe (the return header) leading to a vertical section rising to the pump suction. At design flow, more than 80% of the total pressure drop in the loop occurred across the throttling valves.

The test loop did not duplicate Bruce PHT piping in any respect.

### A.2.3 Loop Instrumentation

The RPTC Bruce pump test loop was equipped with several pressure transducers in the suction and discharge pipes and several accelerometers to measure vibration levels at different points in the piping network. A venturi meter was installed at the top of each loop hairpin to measure the flowrate through the hairpin. The locations of most of the above-mentioned transducers on the test loop support frame and piping are shown in Figure 5. The identification codes for the transducers shown in Figure 5 are defined in Table 2.

In later tests, annubars were installed to measure flowrates at the pump suction and discharge.

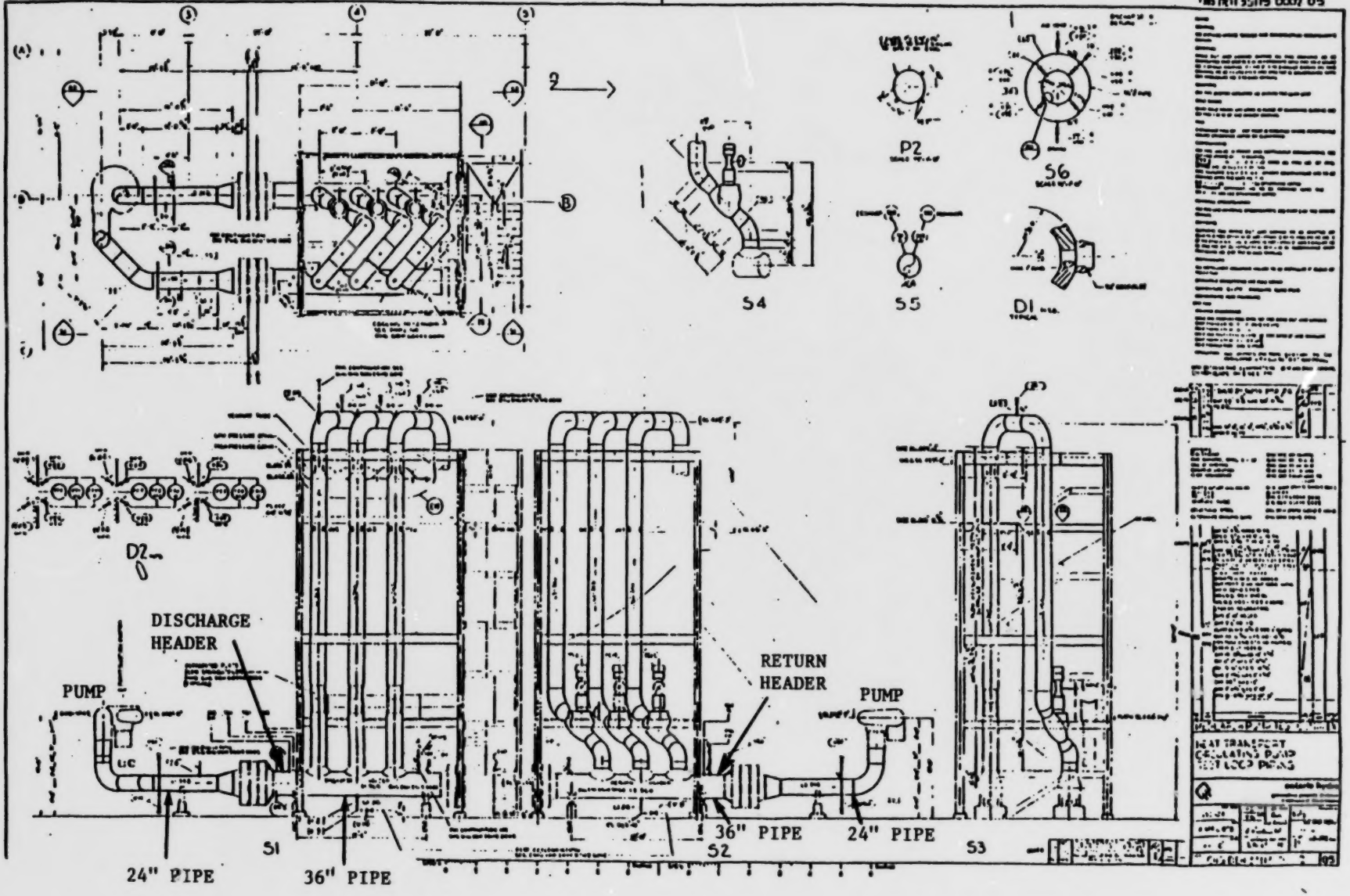


Figure 3 Piping Diagram for the Bruce Pump Test Loop
[from Ref.4]

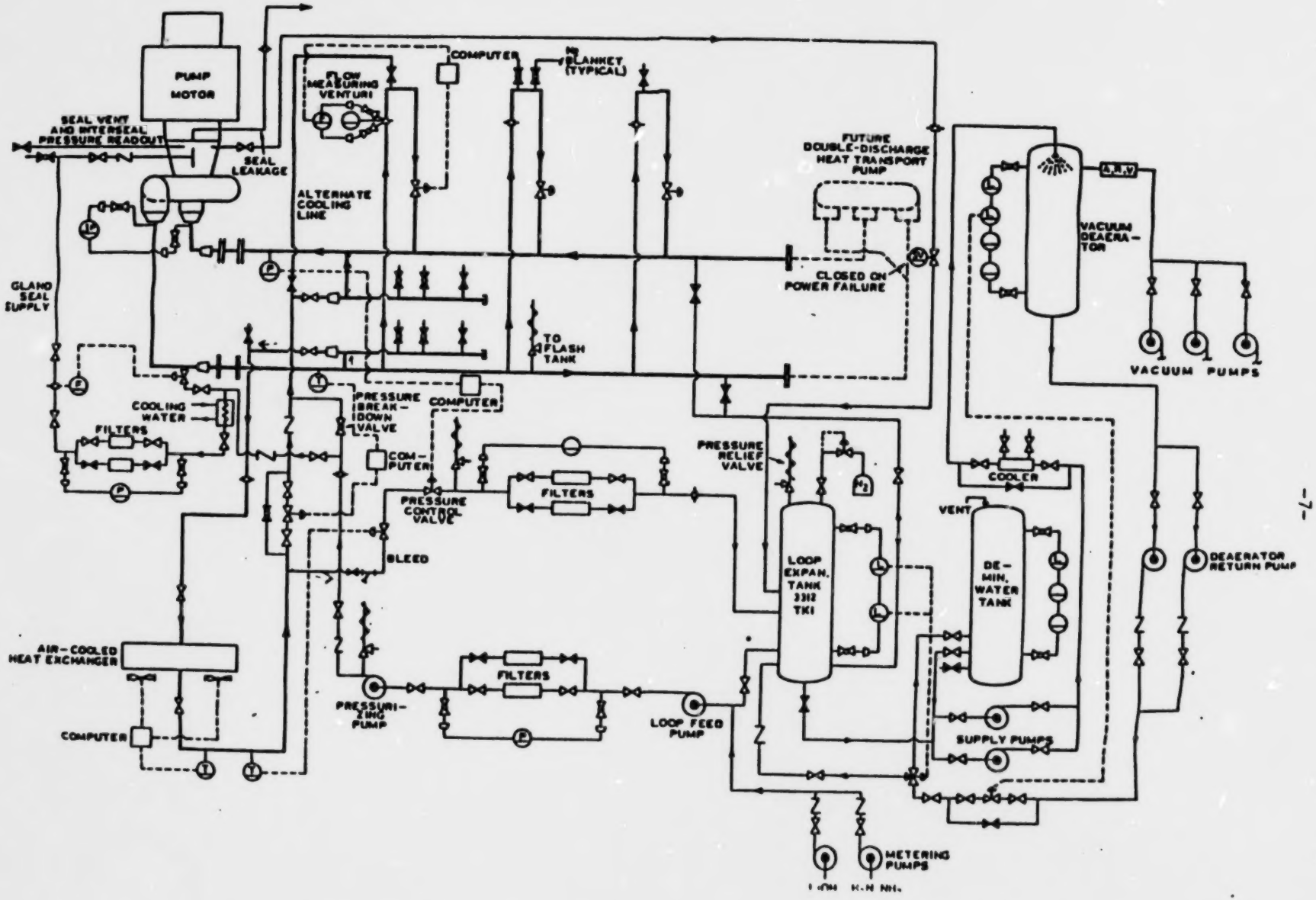


Figure 4 Bruce Pump Test Loop - Flow Diagram [from Ref.1]

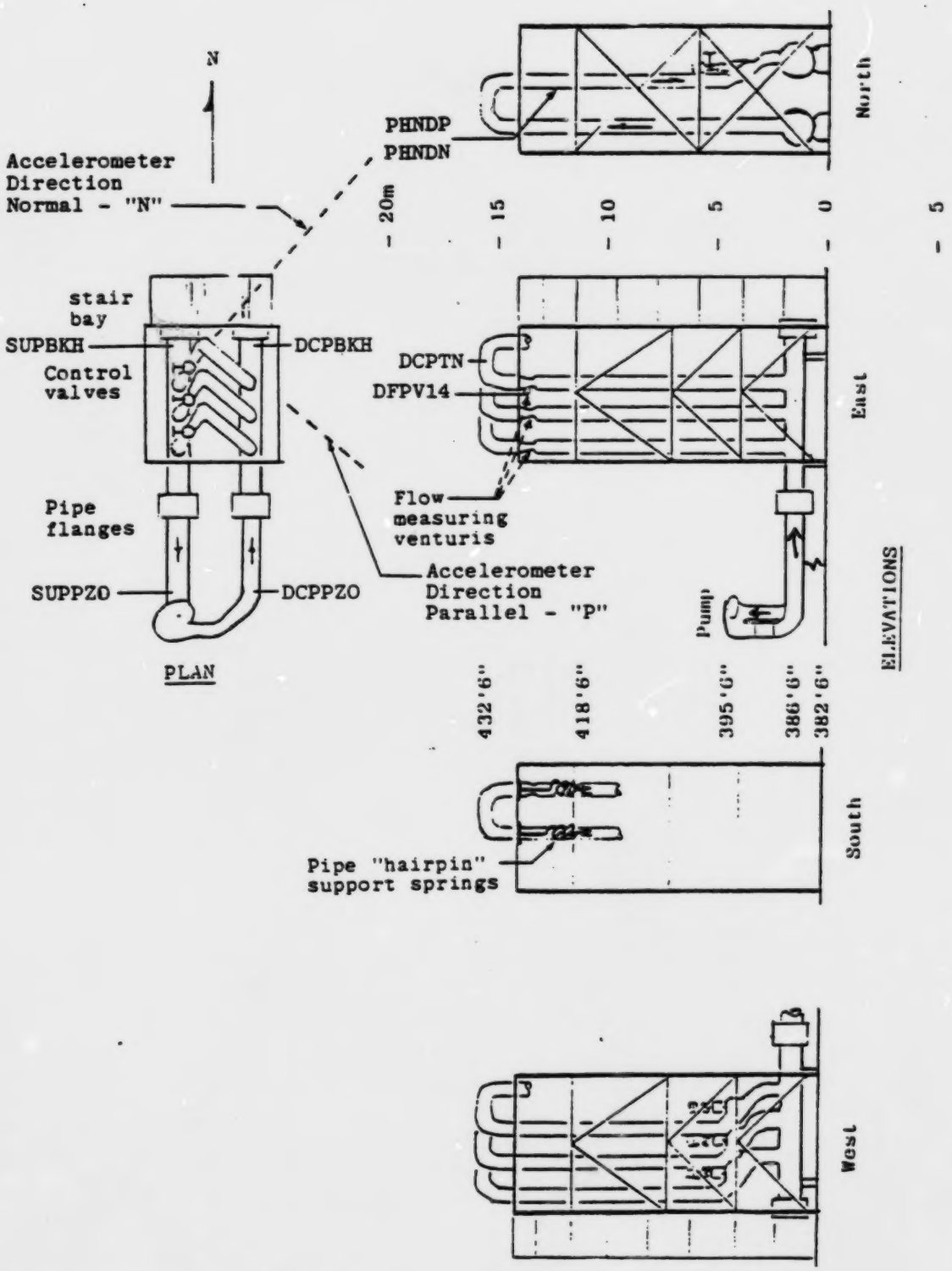


Figure 5 Transducer Locations on Bruce Pump Test Loop
[from Ref.7]

Table 2: Transducer Identification Codes [Ref.7]

| Transducer Identification Code | |
|---|---|
| DCPTN | Discharge pressure at the top of the north hairpin |
| DCPPZO | Discharge pressure at the piezometric ring |
| SUPPZO | Suction pressure at the piezometric ring |
| DFPV14 | Venturi differential pressure, north hairpin |
| PHNDN | Hairpin pipe vibration, normal |
| PHNDP | Hairpin pipe vibration, parallel |
| SUPBKH | Suction pressure at the bulkhead |
| DCPBKH | Discharge pressure at the bulkhead |

In addition to the instrumentation described above, temperature sensors were installed to monitor temperatures at different points in the loop, in particular at the pump suction and discharge. Instrumentation was also provided for measuring pump torque.

The loop was depressurized by bleeding water from the discharge header into an expansion tank maintained at approximately atmospheric pressure. To prevent the bleed water from flashing when it was throttled from the loop pressure to the tank pressure, it was first cooled to a temperature <100°C in the loop heat exchanger. The average void fraction in the loop at any time was then calculated by dividing the volume of water collected (after correcting for the difference in density between the cool water collected and the hot water in the loop) by the total loop volume. No attempt was made to measure local void fractions, for instance at the pump suction.

### A.2.4 Test Procedure

The only energy source in the loop was the pump itself (i.e., heaters were not used), so a typical test began by running the test pump at full speed (1800 rpm) with the loop suction pressure held at 9 MPa until the desired test temperature was reached.

The pump speed was then set to the desired value and water was gradually bled from the loop. When the loop average void reached a value large enough to cause the flow in the loop to stop (typically 50%), cold water was pumped back into the loop at a rate of 6 l/s by the pressurizing pump. The test was terminated when the pump suction pressure reached 9 MPa. Because of the test procedure adopted, the test temperature varied slightly as the loop was bled and dropped to 100°C or less (typically) during refill.

### A.2.5 Results of the Bruce A Pump Tests

Tests of the Bruce A pump were performed at pump speeds of 400 to 1800 rpm[a] [Ref.7]. Although it was initially intended to perform tests at temperatures ranging from 265°C to 115°C over the full range of pump speeds just mentioned, full speed (1800 rpm) tests at temperatures below 205°C could not be performed because of excessive vibration of the loop piping (hairpins) during refill.

Large amplitude (>100 kPa) periodic head pulsations were observed during both draining and refilling of the loop in all of the full speed tests that were attempted. In test 69, for instance, which was performed at a loop temperature of 235°C, head pulsations starting at a frequency of 3.5 Hz and later decreasing to less than 1 Hz were observed while the loop was draining and the pump head was degrading, as shown in Figure 6. During refill, a similar sequence of events occurred only in reverse since head pulsation frequencies were initially less than 1 Hz and subsequently increased to more than 3.5 Hz before refilling was completed.

The most severe pipe vibrations occurred when the frequency of the head pulsations was near to the fundamental frequency of the

---

[a] The results of the low speed tests are not described in detail in the referenced report. The report mentions only that flow stoppages due to steam segregation caused the low speed tests to be fore-shortened, as noted below.
From [Ref.7]:
(i) @ 262°C, 575 rpm - flow stopped at 21% steam void; suction header filled with steam (inadequate NPSH).
(ii) Test No.8, @ 400 rpm - flow stoppage in hairpins.
(iii) Test No.81, 550-1300 rpm - intermittent flow stoppages with increase in pump speed.

BRUCE GS "A" PRIMARY HEAT TRANSPORT PUMP TEST AT RPTC
SLOCAT PUMP HEAD AND PIPE VIBRATION vs TIME
TEST 69 81-08-20 STARTED AT 235° C 1792 rev/min

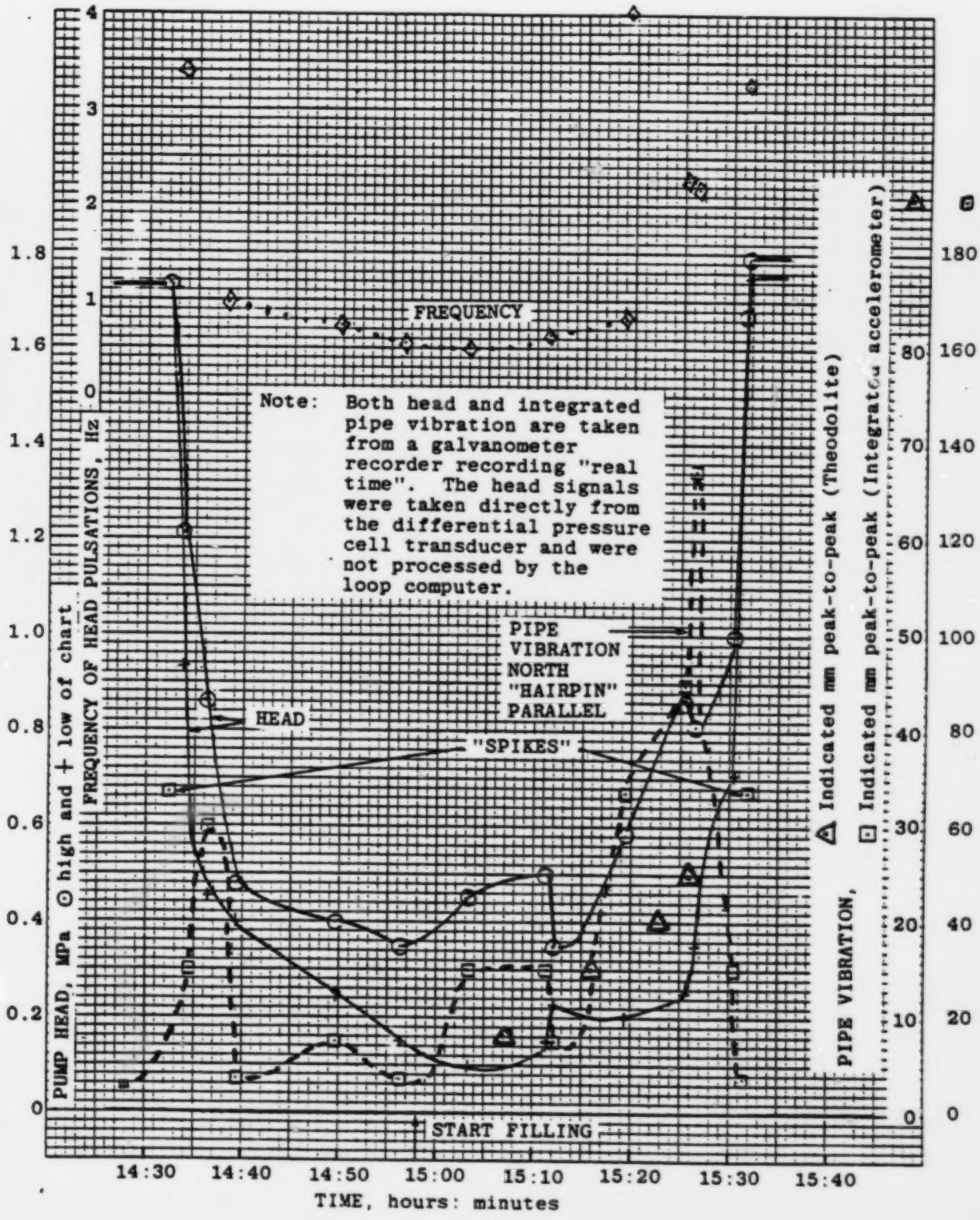
PUMP HEAD, MPa ⊙ high and + low of chart
FREQUENCY OF HEAD PULSATIONS, Hz
PIPE VIBRATION, △ Indicated mm peak-to-peak (Theodolite) ⊡ Indicated mm peak-to-peak (Integrated accelerometer)
FREQUENCY
Note: Both head and integrated pipe vibration are taken from a galvanometer recorder recording "real time". The head signals were taken directly from the differential pressure cell transducer and were not processed by the loop computer.
PIPE VIBRATION NORTH "HAIRPIN" PARALLEL
HEAD
"SPIKES"
START FILLING
14:30
14:40
14:50
15:00
15:10
15:20
15:30
15:40
TIME, hours: minutes

Figure 6 Results of Bruce Pump Test 69 (Performed at 235°C) [from Ref.7]

loop piping, 1.5 Hz [Ref.4]. Proof of this statement can be found in Figure 7, which shows that very severe vibrations occurred at a time of 15:15 during refill in test 71 (215°C) when the frequency of the head pulsations was very closely matched to the abovementioned piping fundamental frequency. Similarly, although the record of head pulsation frequency shown in Figure 6 for test 69 is not continuous, the small peak in piping vibration recorded at a time of 14:37 during draining probably occurred as the head pulsation frequency passed through 1.5 Hz. A similar observation applies to the high vibrations measured at 15:25 during refill in the same test.

An oscillograph of several parameters measured during a period of high vibrations in the full speed test performed at 205°C is given in [Ref.7] and included here as Figure 8. (Full speed tests were not performed at temperatures below 205°C because of excessive piping vibration, as mentioned previously.) The oscillograph shown in Figure 8 was obtained during refill of the loop when the loop temperature had dropped to 182°C.

The center chart of the oscillograph shown in Figure 8 displays, among other things, the pump discharge, suction and differential pressures as functions of time. The top three traces of the center chart are pressures measured at different points in the discharge pipe while the two traces directly beneath them show pressures measured in the suction pipe. The oscillograph shows that the pump suction pressure remained fairly constant with time but that the discharge and pump differential pressures varied periodically with a frequency of approximately 1.5 Hz, as did the in-plane and normal vibrations of the north hairpin (traces 6 and 7). The pressures in the discharge pipe at the piezometric ring, the bulkhead and the top of the north hairpin (obtained with the transducers labelled DCPPZO, DCPTN and DCPBKH respectively in Figure 5) appear to be out of phase in Figure 8, suggesting that there was void present in the discharge pipe over at least part of each surge cycle[a].

---

[a] Since the speed of sound in single-phase liquid water is approximately 1350 m/sec. at 182°C [Ref.14] and the three pressure transducers in the discharge pipe were no more than 25-30 m apart, the pressures at the transducers would have been almost perfectly in phase if the discharge pipe had been filled with liquid water for the entire duration of each surge cycle.

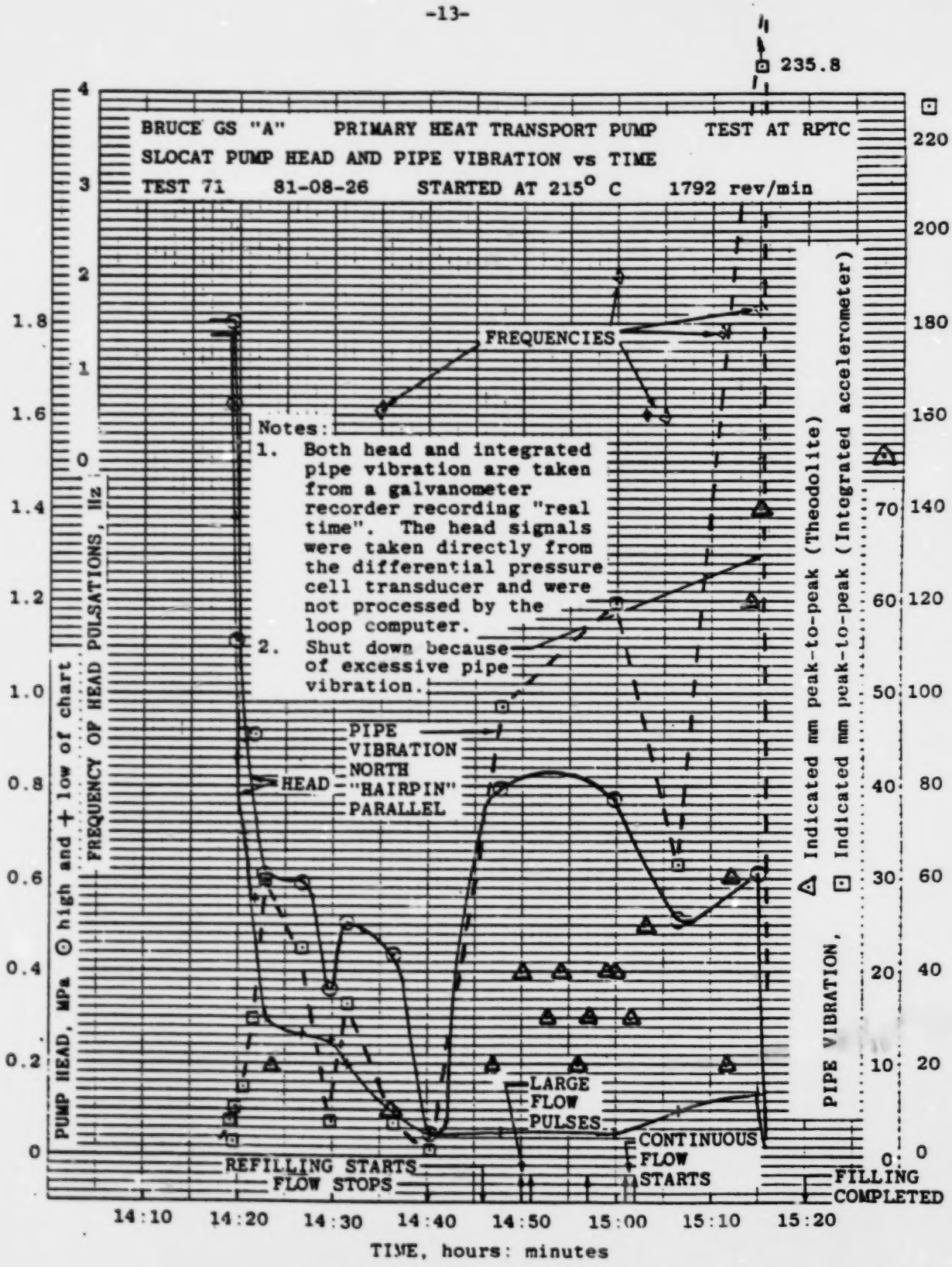
BRUCE GS "A" PRIMARY HEAT TRANSPORT PUMP TEST AT RPTC
SLOCAT PUMP HEAD AND PIPE VIBRATION vs TIME
TEST 71 81-08-26 STARTED AT 215° C 1792 rev/min
235.8
FREQUENCIES
Notes:
1. Both head and integrated pipe vibration are taken from a galvanometer recorder recording "real time". The head signals were taken directly from the differential pressure cell transducer and were not processed by the loop computer.
2. Shut down because of excessive pipe vibration.
PIPE VIBRATION NORTH "HAIRPIN" PARALLEL
HEAD
LARGE FLOW PULSES
CONTINUOUS FLOW STARTS
REFILLING STARTS
FLOW STOPS
FILLING COMPLETED
PUMP HEAD, MPa ⊙ high and + low of chart
FREQUENCY OF HEAD PULSATIONS, Hz
PIPE VIBRATION, △ Indicated mm peak-to-peak (Theodolite) ⊡ Indicated mm peak-to-peak (Integrated accelerometer)
TIME, hours: minutes
14:10 14:20 14:30 14:40 14:50 15:00 15:10 15:20

Figure 7 Results of Bruce Pump Test 71 (Performed at 215°C) [from Ref.7]

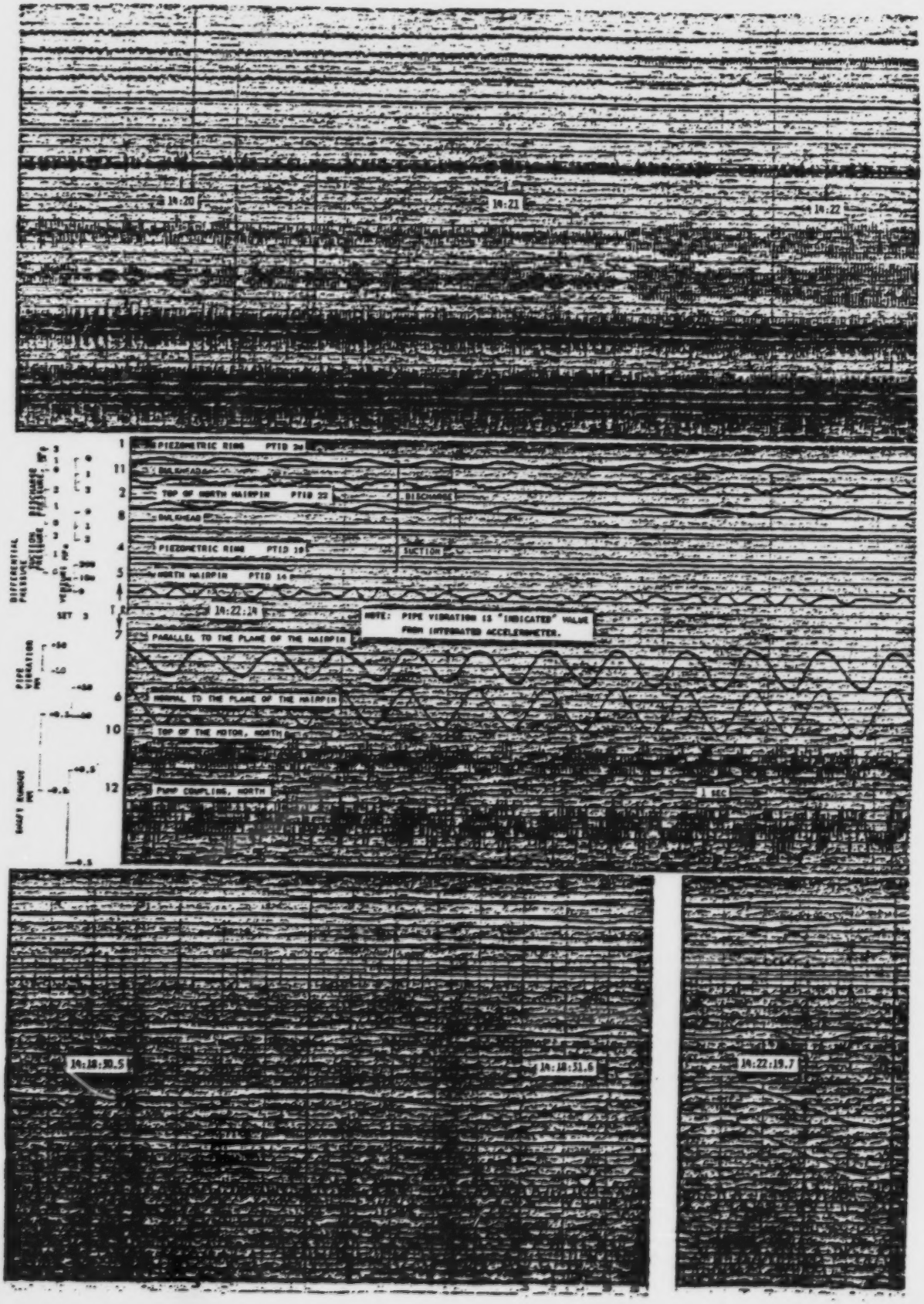
14:20
14:21
14:22
PIEZOMETRIC RING PTID 20
BULKHEAD
TOP OF NORTH HAIRPIN PTID 23
DISCHARGE
BULKHEAD
PIEZOMETRIC RING PTID 19
SUCTION
NORTH HAIRPIN PTID 14
14:22:24
NOTE: PIPE VIBRATION IS "INDICATED" VALUE FROM INTEGRATED ACCELEROMETER.
PARALLEL TO THE PLANE OF THE HAIRPIN
NORMAL TO THE PLANE OF THE HAIRPIN
TOP OF THE MOTOR, NORTH
PUMP COUPLING, NORTH
1 SEC
14:18:30.5
14:18:31.6
14:22:19.7

# FIGURE 8 (REF. 7)

. BRUCE GS 'A' PRIMARY HEAT TRANSPORT PUMP TEST

Oscillogram of discharge and suction pressures, venturi head, hairpin displacements, and shaft runouts at the top of the motor and at the pump coupling

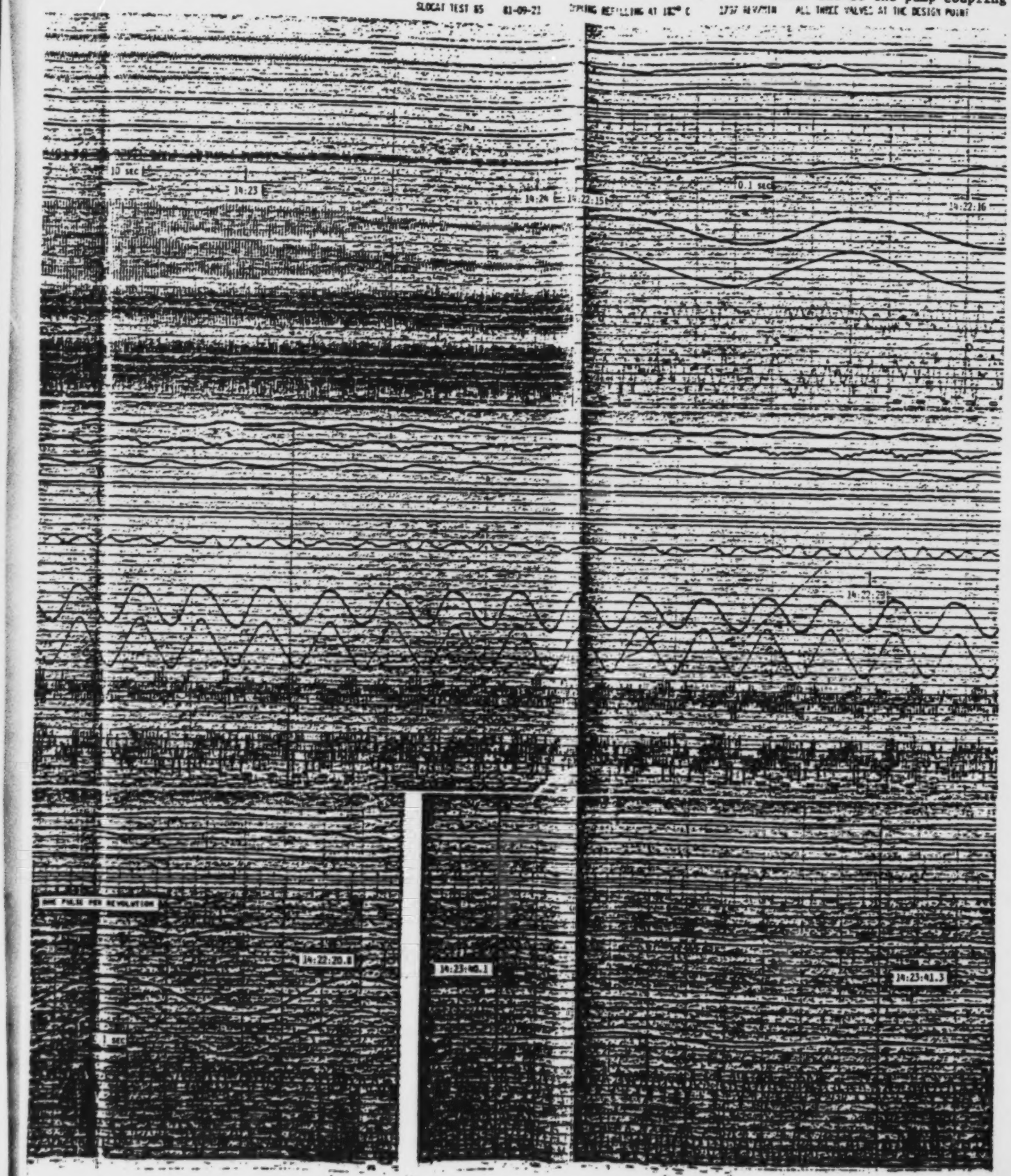

BLANK

The tests to which Figures 6 to 8 apply were performed with the flow control valves in the three hairpins set to give approximately equal flowrates in the hairpins at the pump's design flow of 3.3 $m^3/s$ (i.e., the flow in each hairpin would have been 1.1 $m^3/s$). Other tests were performed with the flow control valves adjusted to give different flows in the hairpins and different overall flows. Although head pulsations were observed in all of these tests, it was determined that the severity of the resulting pipe vibrations decreased as flowrate increased [Ref.4].

**A.3 Bruce B Pump Tests**

Following the tests of the Bruce A pumpset, the Bruce A pump was fitted with a Bruce B motor and retested in the loop described in Section 1.1.2. In addition to the transducers listed in Table 2 and shown in Figure 5, sixteen additional pressure transducers were installed in the discharge pipe to permit pressure pulse propagation velocities to be measured and annubars were added at the pump suction and discharge to measure the flowrates at those locations, as mentioned previously.

Although the results of the SLOCA tests of the Bruce A pump described in the preceding section suggested that vibrations of the loop piping would get progressively worse as the loop temperature was lowered, the SLOCA tests of the Bruce B pump showed that the vibrations were most severe when the loop temperature was approximately 180°C. The worst vibrations usually occurred during refill and, if periodic, were invariably produced by head pulsations with a frequency close to the piping fundamental frequency of 1.5 Hz.

According to Burchett [Ref.9], the instabilities observed in the Bruce B pump SLOCA tests could be classified into the four basic types shown in Figure 9. Since Burchett describes each type of instability in considerable detail, their characteristics will only be summarized here. The four classifications are as follows:

(a) Pump Head Instability - This type of instabilty was observed at test temperatures above 170°C while the pump head was degrading or recovering. The associated pressure pulsations were periodic with amplitudes as high as 450 kPa and were accompanied by flow oscillations of the same

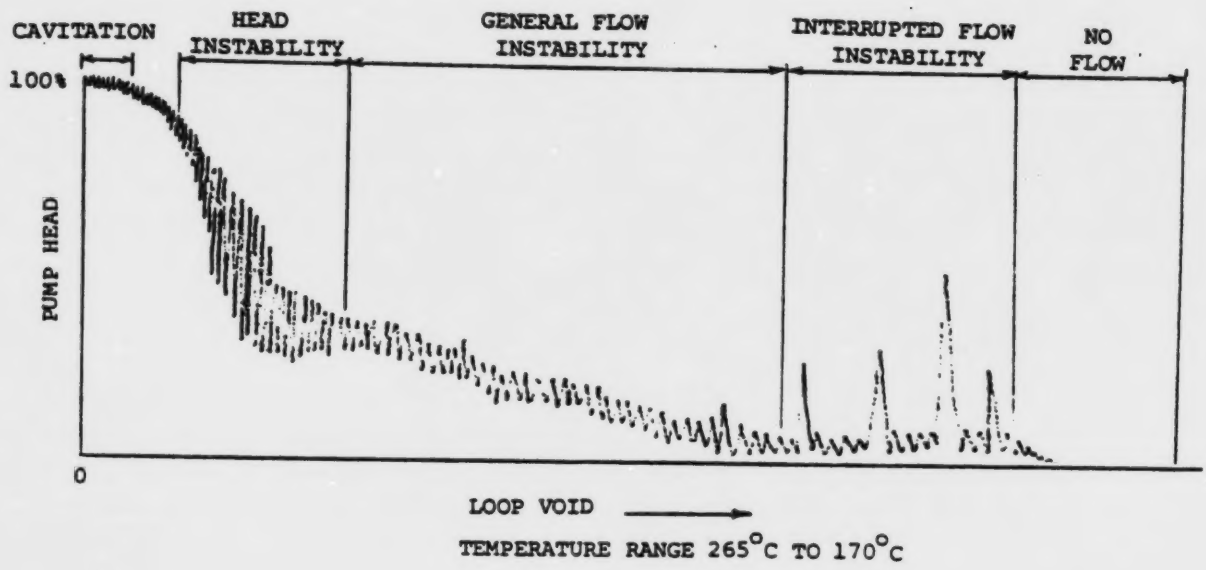


PICTORIAL PRESENTATION - PUMP HEAD VARIATION VS VOID SHOWING AREAS OF INSTABILITY OBSERVED DURING THE BRUCE NGS B PHT PUMP TESTS

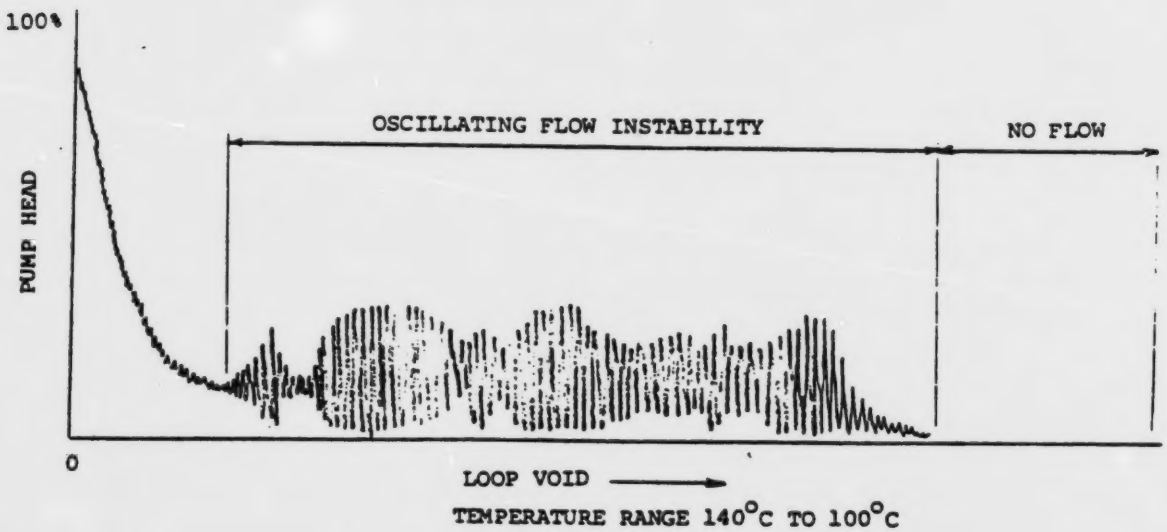


Figure 9 Classification of Instabilities Observed in the Bruce Pump Tests [from Ref.10]

frequency. The frequency of the pressure pulsations, which increased as the system void decreased, ranged from 1 to 4 Hz.

(b) General Flow Instability - Instabilities of this type were observed at higher void fractions than the pump head instabilities and were probably churn flow-induced.

(c) Interrupted Flow Instability - This type of instability produced large pressure spikes at the pump discharge and was attributed to isolated slugs of liquid travelling around the loop. The magnitude of the spike was as large as 0.95 MPa in one instance and the elapsed time between spikes ranged from 10 to 120 seconds [Ref.4]. Interrupted flow instabilities occurred when the flow in the loop had almost stopped.

(d) Oscillating Flow Instability - This type of instability was observed after the liquid and vapor in the loop had stratified and measurable flow occurred only in the discharge pipe. The frequency of the head pulsations ranged from 0.6 to 1.1 Hz. A plausible explanation of the mechanism responsible for this type of instability is advanced by Burchett in [Ref.9].

The highest pressure pulse amplitudes measured at a number of test temperatures within the range of temperatures investigated in the SLOCA B tests are shown in Figure 10, taken from [Ref.9]. The data points to the right of the dashed line in that figure apply to pump head instabilities while those to the left apply to oscillating flow instabilities. Figure 10 shows that high amplitude pressure pulsations occurred over essentially the entire range of loop temperatures investigated even though the resulting pipe vibrations were most severe at temperatures near to 180°C. Head instabilities caused the worst vibrations because the frequency of the head pulsations produced by oscillating flow instabilities, 0.6 to 1.1 Hz, was significantly less than the piping fundamental frequency of 1.5 Hz.

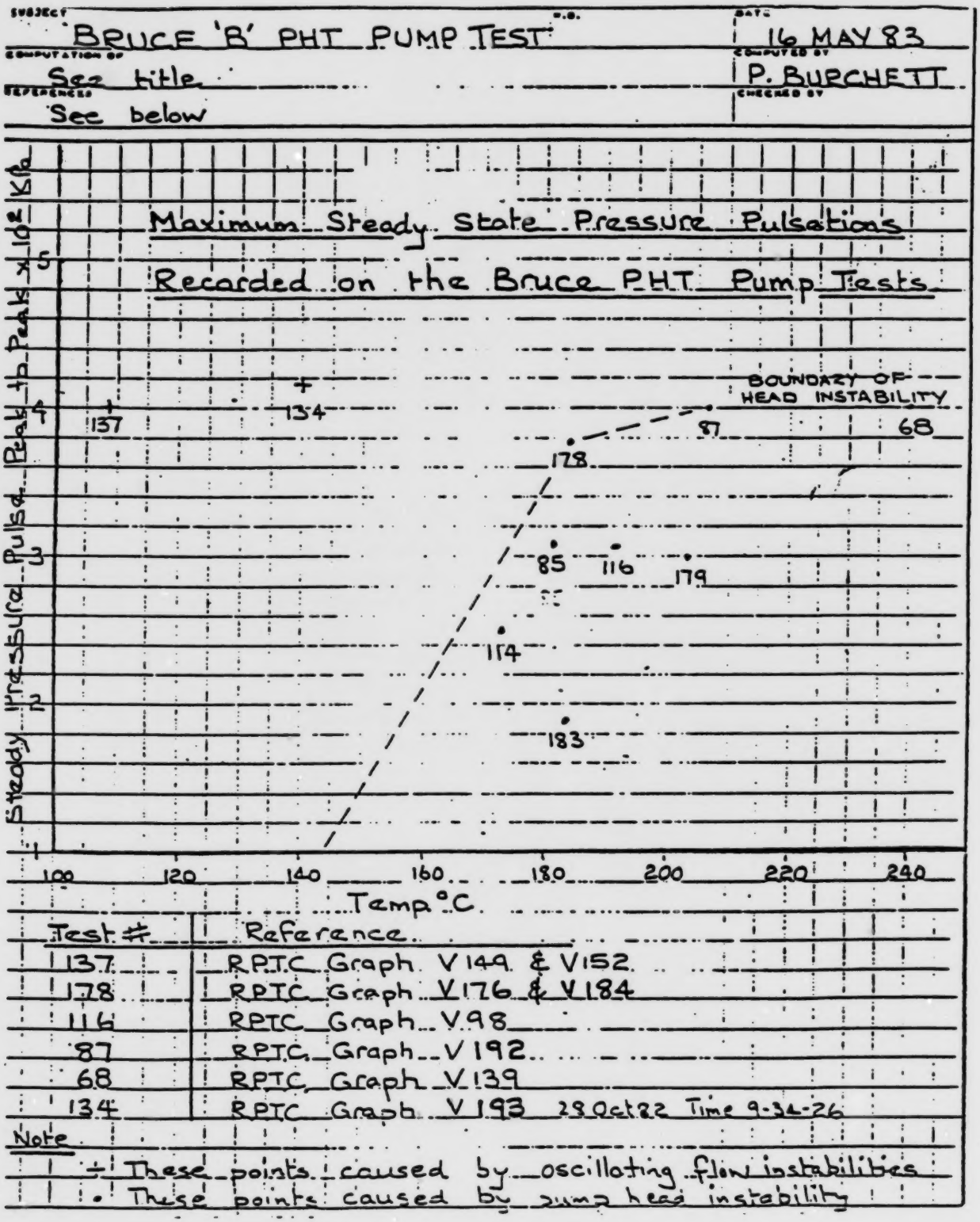


Figure 10 Bruce Test Pressure Pulsation Amplitudes vs. Test Temperature [from Ref.9]

## A.4 Pickering B Pump Tests

### A.4.1 Pump Design

A Pickering B pumpset uses a single stage, Byron Jackson pump with a 61 cm (24") diameter impeller and 35.5 cm (14") diameter vertical suction and horizontal discharge pipes. The suction pipe is connected to a tee, as shown in Figure 11.

The single phase performance characteristics of a Pickering NGS B pump are shown in Figure 12 and the pump's nominal operating conditions and performance characteristics are summarized in Table 3.

Table 3: Pickering NGS B Pump Nominal Operating Conditions and Performance Characteristics [Ref.13]

| | |
|---|---|
| Operating Temperature | 249°C |
| Operating Suction Pressure | 8.48 MPa |
| Rated Flow | 0.765 $m^3/s$ |
| Rated Head | 143 m |
| Motor Rating | 1.42 MW |
| Motor Speed | 1800 rpm |
| Specific Speed | 1960 rpm US $gpm^{1/2}$ / $ft^{3/4}$ |

### A.4.2 Test Loop Geometry

The test loop in which the Pickering pump tests were performed is shown in Figures 13 and 14. The piping on the discharge side of the pump up to the first tee replicated the geometry of a Pickering B PHT piping system from the pump to the reactor inlet header and the suction tee geometry was the same as that of the PHT system, but the mechanical and hydraulic characteristics of the test loop and PHT system were otherwise different.

### A.4.3 Loop Instrumentation

Test loop temperatures, pressures, flow rates and vibration levels were monitored with the transducers shown in Figures 14 and 15. Loop depressurization was accomplished in the same

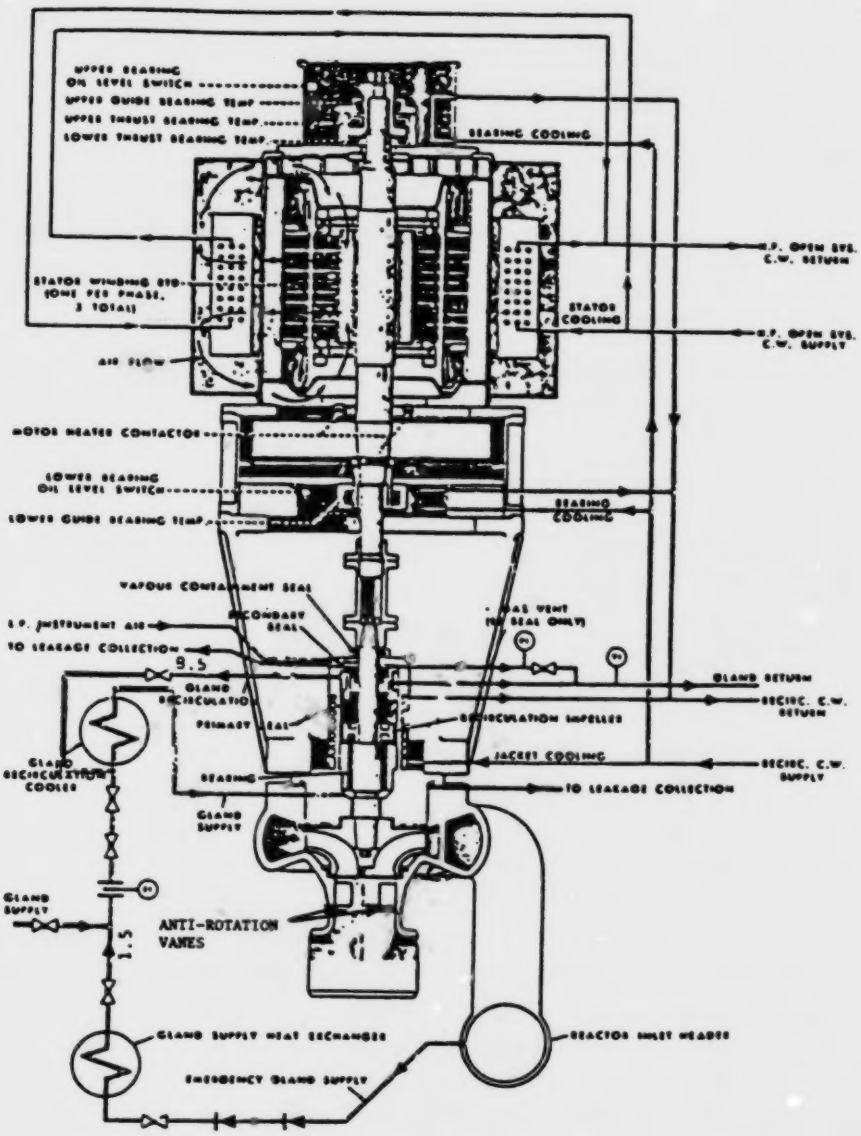


Figure 11 Pickering B GS PHT Pump Cross-Section Showing Instrumentation and Auxiliary Circuits [from Ref.13]

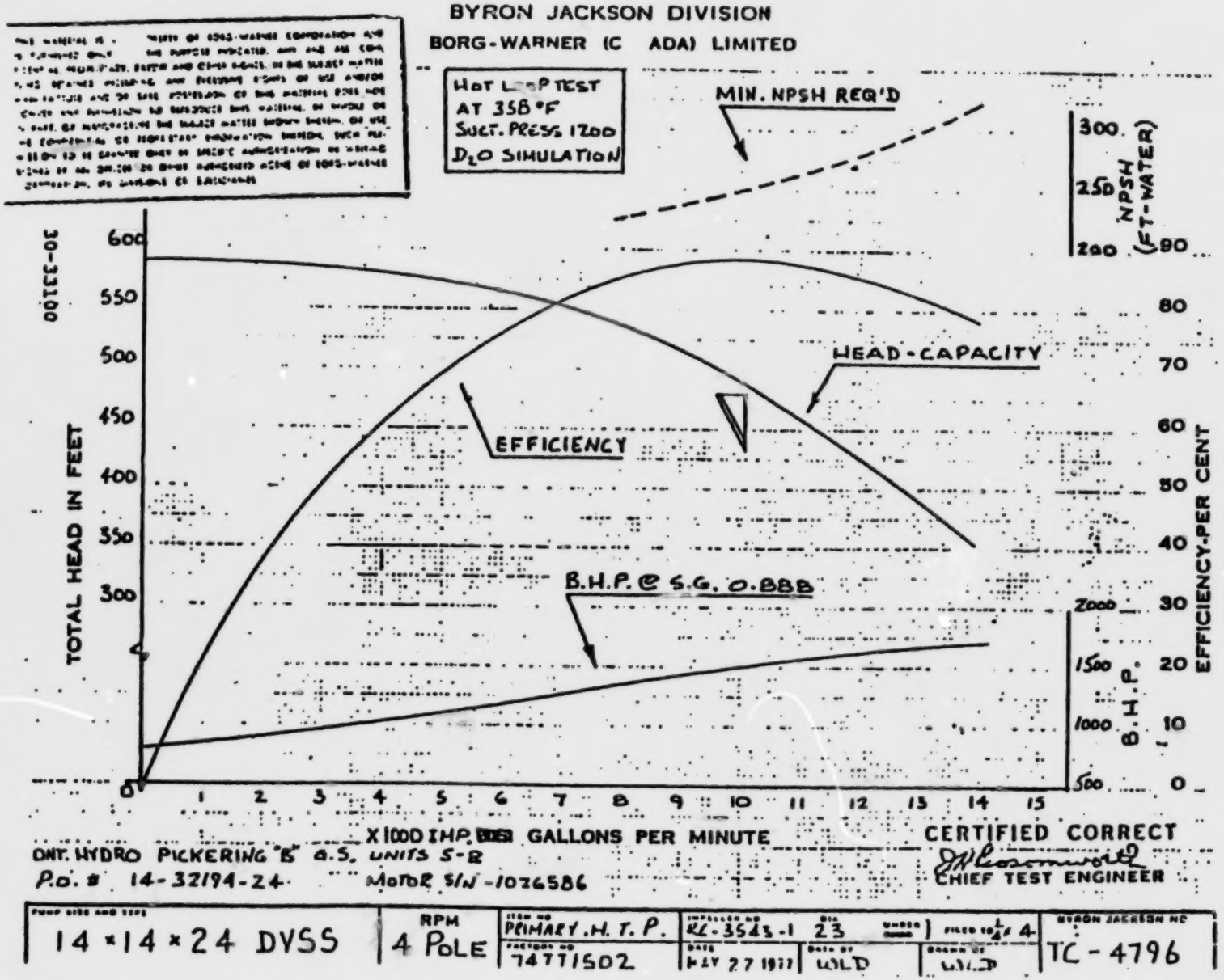


Figure 12 Pickering GS B PHT Pump Performance Characteristics [from Ref.5]

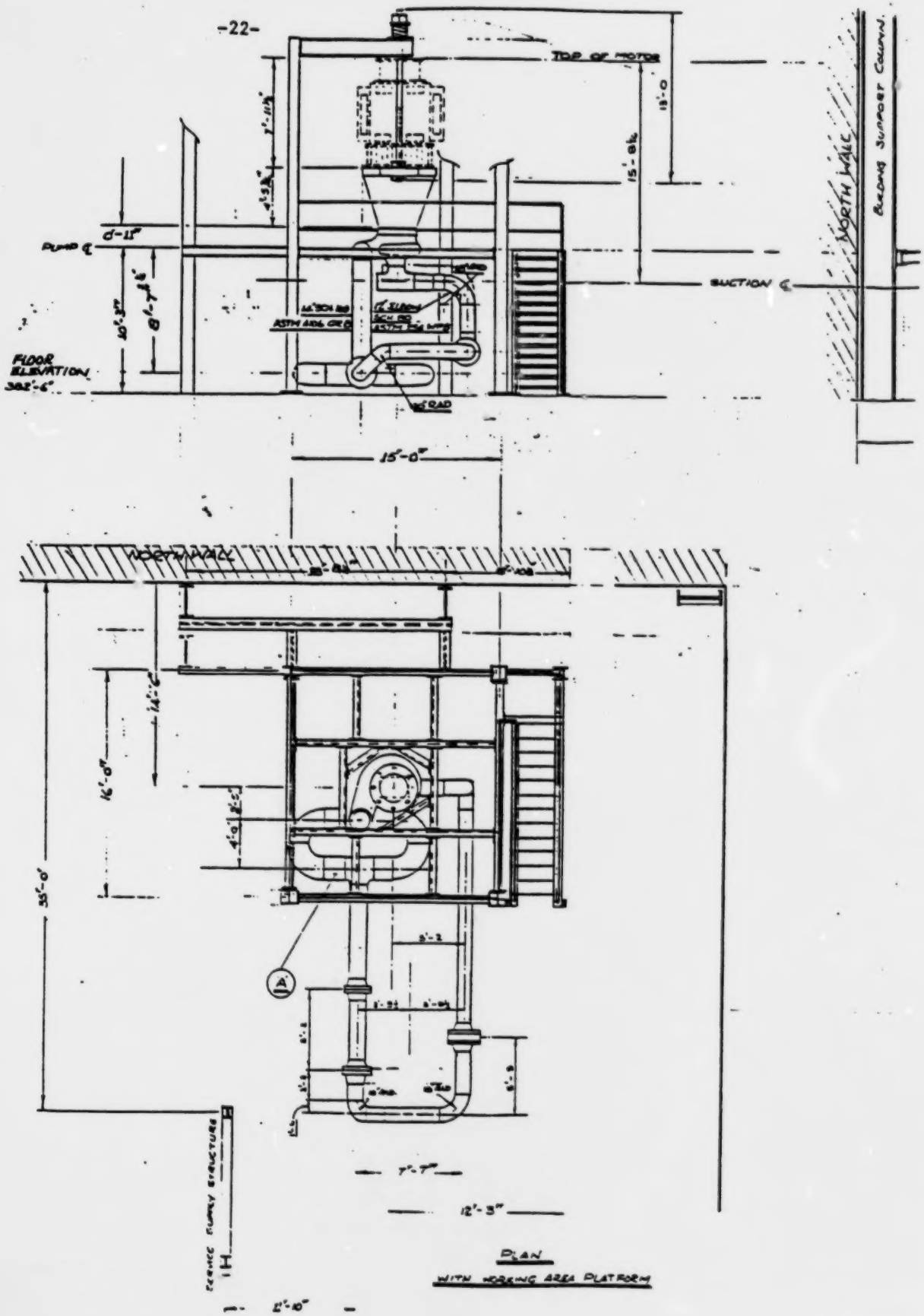


PLAN
WITH WORKING AREA PLATFORM

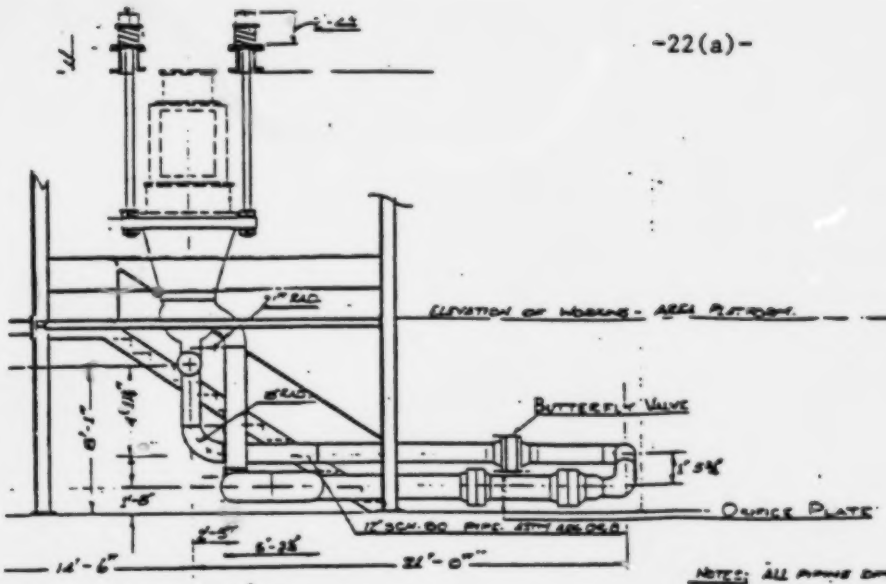


NOTES: ALL PIPING DIMENSIONS SHOWN ARE FOR REFERENCE ONLY.

GENERAL:
SEE ONTARIO DESIGN AND CONSTRUCTION MANUAL.

ERECTION:
PIPING 2-½" AND LARGER SHOWN ON THIS DRAWING TO BE FABRICATED AND ERECTED IN ACCORDANCE WITH PIPE PROCEDURE NO 1 DESIGN MANUAL.
PIPING 2" AND SMALLER SHOWN ON THIS DRAWING TO BE FABRICATED AND ERECTED IN ACCORDANCE WITH PIPE PROCEDURE NO 2 DESIGN MANUAL.

QUANTITY:
ONE PIPE SYSTEM AS SHOWN.

FILL:
A DRAINAGE FILL OF 0" FOR ROOF IS REQUIRED WHERE PRACTICABLE UNLESS OTHERWISE NOTED BY ELEVATIONS.

MATERIAL SPECIFICATION:
PIPES: ASTM A106 GR. B.
FITTINGS: ASTM A234 WPB

SUPPORTS:
SUPPORTS FOR PIPING 2-½" AND LARGER TO BE ERECTED BY CONSTRUCTION DIVISION IN ACCORDANCE WITH PROCEDURE NO 1 OF THE DESIGN MANUAL.
SUPPORTS FOR PIPING 2" AND SMALLER TO BE ERECTED BY CONSTRUCTION IN ACCORDANCE WITH PROCEDURE NO 2 OF THE DESIGN MANUAL.

INSTRUMENTS:
ALL INSTRUMENT ISOLATING VALVES TO BE INSTALLED 1' CLEAR OF INSULATION

OPERATING CONDITIONS: (AT FULL LOAD)
TEMPERATURE: 385°C PRESSURE: 15.27 MPa (2200 PSIG)
HYDROSTATIC TEST PRESSURE: 17.4 MPa (2500 PSIG)

WELDING PROCEDURES:
WELD END PREPARATION TYPE 'C' FOR PIPES 2-½" AND LARGER
SHOP FABRICATION: P 108, P 112, P 113.
FIELD FABRICATION: P 108
WELD END PREPARATION TYPE 'D' FOR PIPES 2½" AND SMALLER
SHOP FABRICATION: P 101, P 102
FIELD FABRICATION: P 101 P 102.

INSULATION:
ALL PIPING TO BE INSULATED WITH CLASS 'D' MATERIAL

NON-DESTRUCTIVE EXAMINATION:
ONTARIO HYDRO WELDING MANUAL SECTION 8 5% RDE - 1M 5 RDE - 1

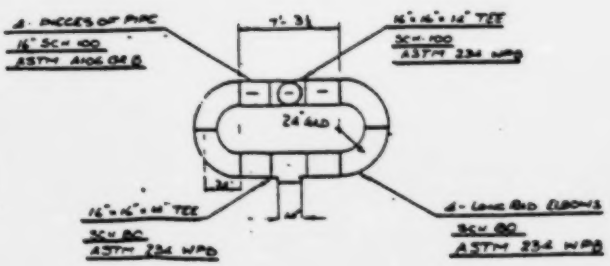


A

FIGURE 13 (REF. 11)

| | |
|---|---|
| DICKERING 'B' TEST LOOP AND STRUCTURE ARRANGEMENT | |
| PUMP TEST COMPLEX – ONTARIO HYDRO | |
| DRAWN BY- KEN RAMDIN. | CHECKED BY:- |
| DATE BY- JUNE 29, 1982 | APPROVED BY- |
| SCALE- ¼" | DWG NO: 22-151-0001 |

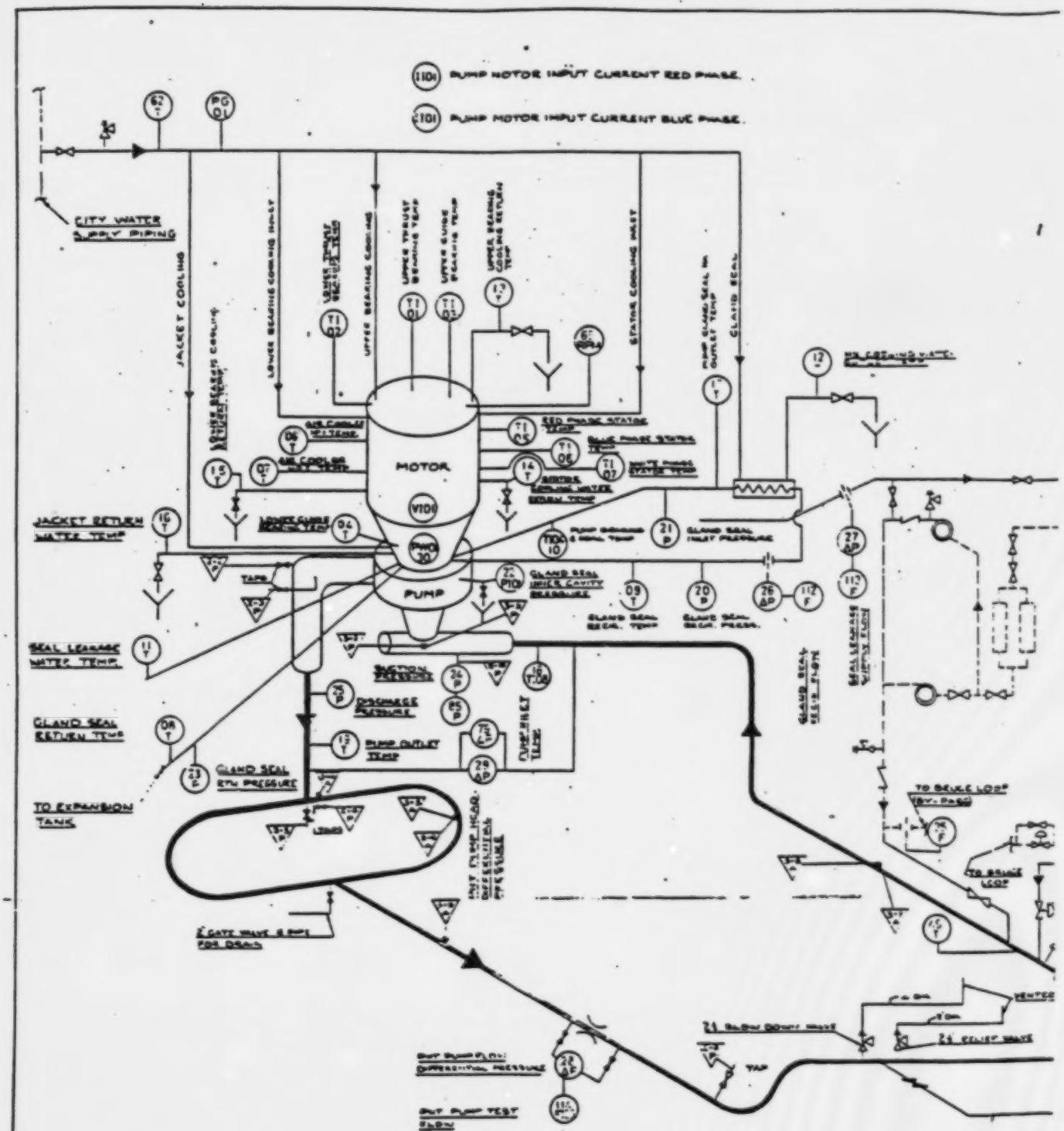


NOTES
(1) — — — — EXISTING PIPING
(2) ———— NEW PIPING
(3) INSTRUMENTATION GROUP IS NOT SHOWN.

# FIGURE 3.

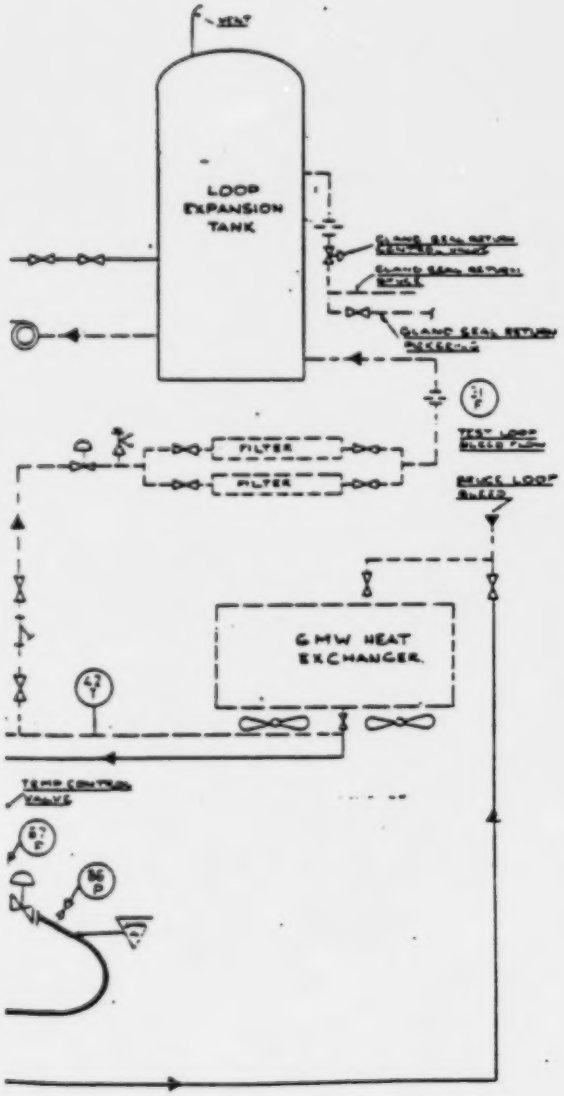


FIGURE 14 (REF. 11)

| RESEARCH PUMP TEST COMPLEX | | |
|---|---|---|
| TITLE: PICKERING 'B' PHT PUMP TEST LOOP FLOW SCHEMATIC DIAGRAM (HOBCOMP 2/45 COMPUTER PLOT) | | |
| DATE: MAY 4, 83 | PROJECT: 22-131 | SCALE: NTS |
| DWG No: 22-131-300 | DRAWN BY: A. A. | APPROVED BY: |

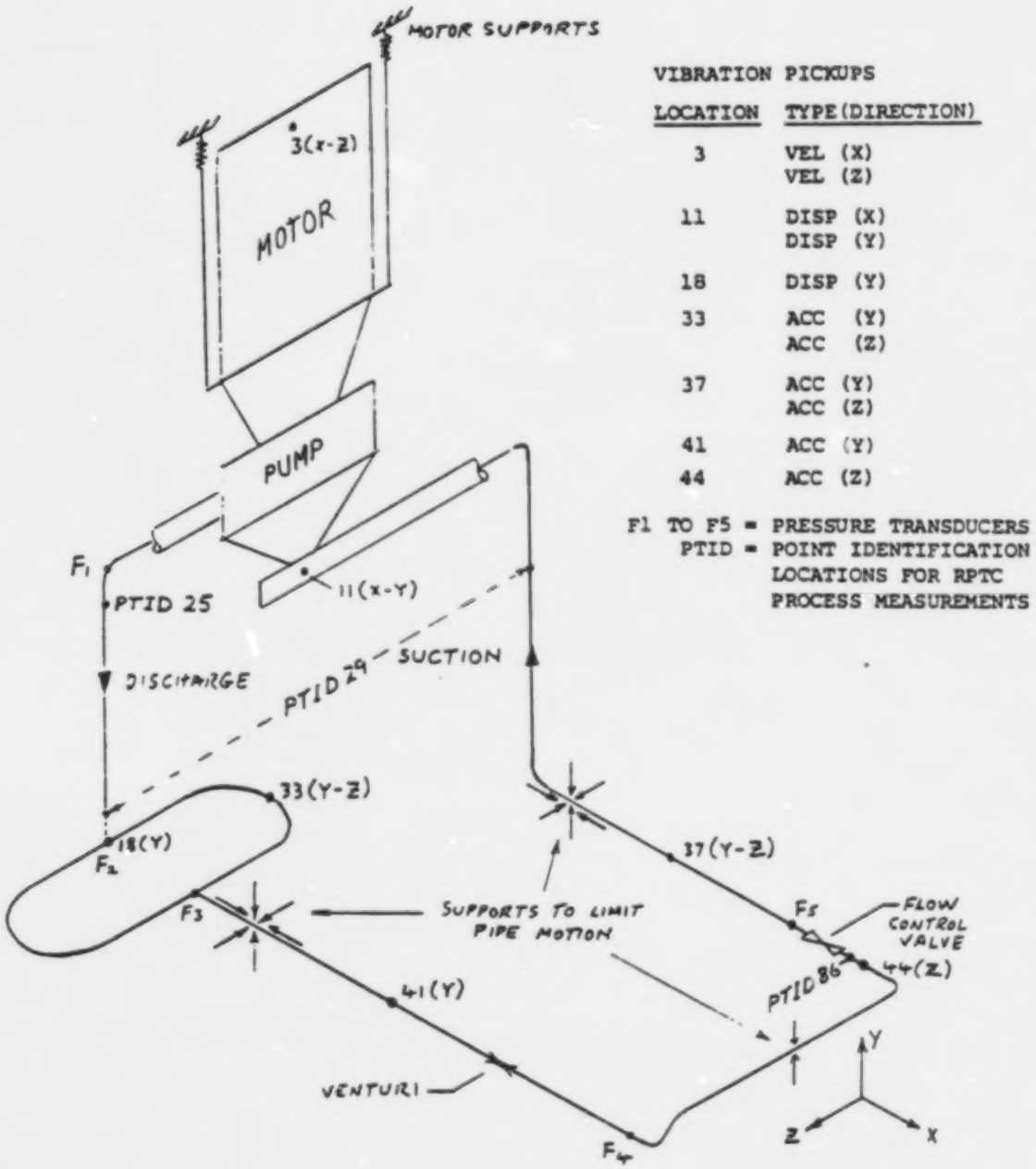


PICKERING NGS B PHT PUMP TEST AT RPTC

Figure 15 Transducer Locations on Pickering Pump Test Loop [from Ref. 10]

manner as in the Bruce pump tests, so as before, the loop average void was measured by dividing the volume of water collected in the loop expansion tank by the loop volume. Again, there was no provision for measuring local void fractions.

### A.4.4 Results of the Pickering B Pump Tests

A summary of the tests performed in the Pickering SLOCA program is given in Table 4 (taken from [Ref.10]). As shown in the table, three types of tests were performed, specifically:

(a) Void matrix tests. These were run at a constant temperature with a low bleed rate, typically 0.5 to 0.6 1/s. Because of the low bleed rates used, these tests were believed to be essentially quasi steady-state.

(b) Blowdown tests. These were high bleed rate tests performed to determine if vibration levels for high voiding rates differed significantly from those for low voiding rates.

(c) Transient tests. These were tests performed with the aim of duplicating the pump suction conditions predicted in LOCA simulations.

The test procedure followed in the void matrix tests was essentially the same as that already described for the Bruce program except that the pump was not operated during the refill period in all cases. The test procedure used in the blowdown and transient tests is described in [Ref.11].

Figure 16 shows how the pressure pulse amplitudes measured during draining varied with test tempature in the void matrix tests. At test temperatures greater than or equal to 180°C, the pressure pulsations were both non-periodic [Ref.15] and of very small amplitude (<50 kPa peak-to-peak), suggesting that they were probably churn flow-induced. At test temperatures less than or equal to 140°C, however, the pressure pulsations were both periodic, with the approximate frequencies indicated in Table 5, and of very large amplitude.

It should be mentioned that the head pulsation frequency tabulated in Table 5 for a given test corresponds to (i.e., was

Table 4

SUMMARY OF PICKERING NGS 'B' PHT PUMPSET
SIMULATED LOSS OF COOLANT ACCIDENT TESTS

| TEST NO | DATE | TYPE | TEST NO | DATE | TYPE |
|---|---|---|---|---|---|
| 189 | 83 03 24 | Commissioning 55°C | 216 | 83 04 22 | Blowdown |
| 190 | 83 03 25 | Commissioning | 217 | 83 04 22 | Blowdown |
| 191 | 83 03 29 | Commissioning 250°C | 218 | 83 04 22 | Rundown |
| 192 | 83 03 30 | Commissioning | 219 | 83 04 22 | Rundown 250°C |
| 193 | 83 04 05 | Commissioning | 220 | 83 04 22 | Rundown 250°C |
| 194 | 83 04 06 | Void Matrix 250°C | 221 | 83 04 25 | Transient 250°C |
| 195 | 83 04 07 | Void Matrix 220°C | 222 | 83 04 25 | Transient 250°C |
| 196 | 83 04 11 | Void Matrix 200°C | 223 | 83 04 25 | Transient 250°C |
| 197 | 83 04 12 | Void Matrix 250°C | 224* | 83 04 26 | Transient 250°C |
| 198 | 83 04 12 | Void Matrix 220°C | 225 | 83 04 26 | Transient 250°C |
| 199 | 83 04 13 | Void Matrix 180°C | 226 | 83 04 27 | Transient 250°C |
| 200 | 83 04 15 | Calibration | 227 | 83 04 27 | Transient |
| 201 | 83 04 18 | Void Matrix 140°C | 228 | 83 04 27 | Aborted |
| 202 | 83 04 18 | Void Matrix 100°C | 229 | 83 04 27 | Transient 250°C |
| 203 | 83 04 18 | Blowdown 250°C | 230 | 83 04 27 | Transient 250°C |
| 204 | 83 04 19 | Blowdown 250°C | 231 | 83 04 27 | Transient 250°C |
| 205 | 83 04 19 | Blowdown 250°C | 232* | 83 04 28 | Void Matrix 100°C |
| 206 | 83 04 19 | Void Matrix 100°C | 233* | 83 04 28 | Void Matrix 250°C |
| 207 | 83 04 19 | Transient | 234 | 83 04 29 | Void Matrix |
| 208 | 83 04 20 | Blowdown 250°C | 235 | 83 04 29 | Void Matrix |
| 209 | 83 04 21 | Transient | 236* | 83 05 02 | Blowdown 250°C |
| 210 | 83 04 21 | Transient | 237 | 83 05 02 | Void Matrix 56°C |
| 211 | 83 04 21 | Transient | 238 | 83 05 03 | Blowdown 250°C |
| 212 | 83 04 21 | Transient | 239 | 83 05 05 | Var Flow 120°C |
| 214 | 83 04 21 | Rundown | 240 | 83 05 05 | Var Flow 120°C |
| 215 | 83 04 22 | Blowdown | 241 | 83 05 05 | Var Flow 245°C |

The pump ran a total of 77 hours.

*Movies made.

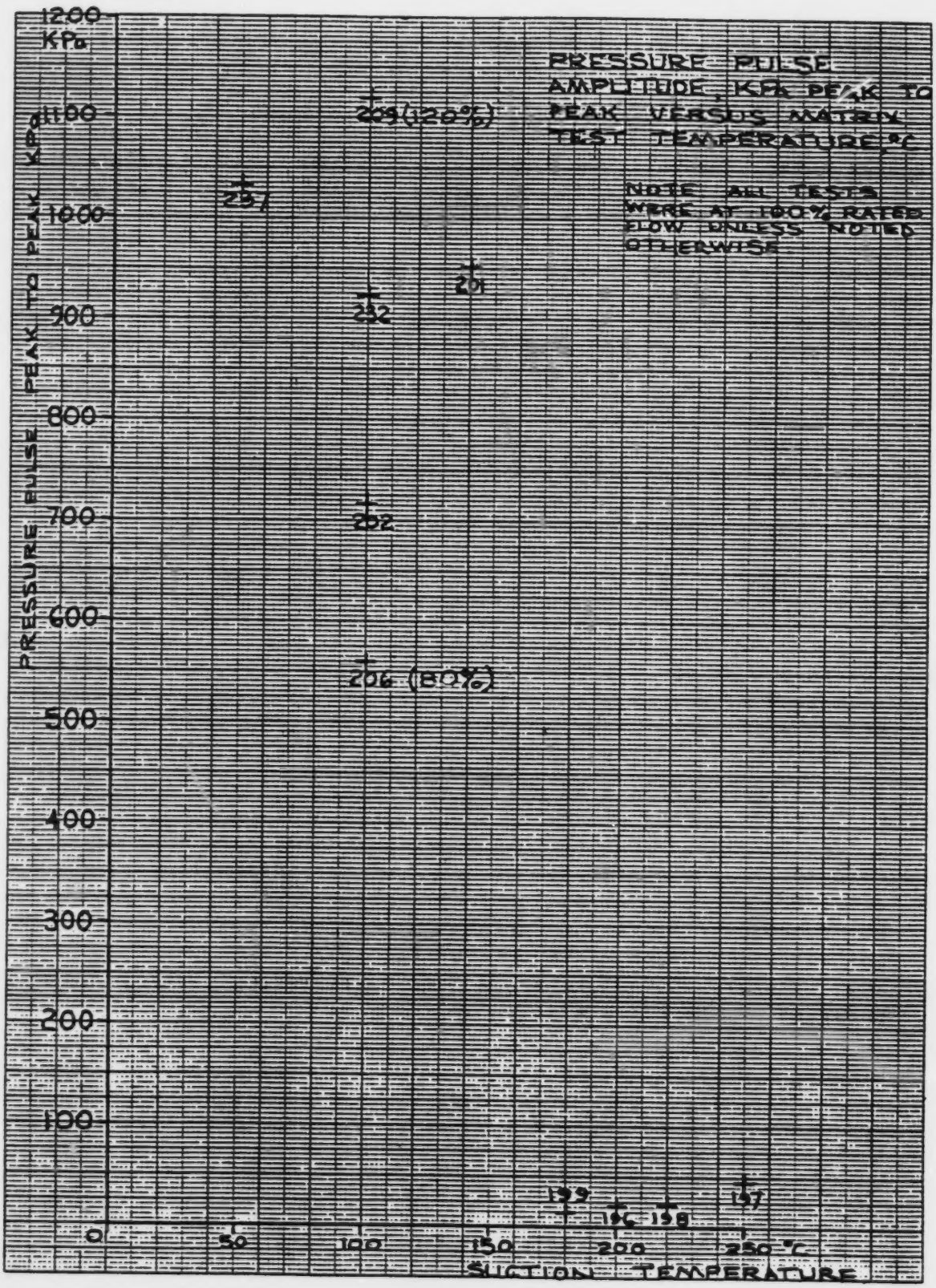


Figure 16 Pressure Pulse Amplitude vs. Test Temperature for the Pickering Void Matrix Tests [from Ref.11].

measured at the same time as) the indicated head pulsation amplitude. In test 202, for instance, the frequency of the pulsations was presumably approximately 4.5 Hz when the amplitude was 0.72 MPa. In reality, both the amplitude and frequency of the pressure pulsations varied with time during the period of instability in each test, as shown in Figure 17 for test 202

Table 5: Pressure Pulsation Data For Low Temperature Void Matrix Tests* [Ref.11]

| Test | Temp. °C | % Rated Flow | Pulse Amplitude Peak/Peak MPa | Frequency Hz |
|---|---|---|---|---|
| 201 | 140 | 100 | 0.95 | 3.9 |
| 209 | 100 | 120 | 1.12 | 4.1 |
| 202 | 100 | 100 | 0.72 | 4.5 |
| 232 | 100 | 100 | 0.92 | 3.8 |
| 206 | 100 | 80 | 0.56 | 4.4 |
| 237 | 50 | 100 | 1.04 | 3.3 |

(performed at 100°C). The frequency of the head pulsations in that test ranged from about 7.3 Hz at the beginning of the period of instability to about 2.5 Hz at the end, although the frequency was between 4 and 5 Hz most of the time, as indicated. Figure 17 shows that the amplitude of the head pulsations increased through most of the period of instability, eventually reaching a value of 2 MPa peak-to-peak or roughly 1-1/2 times the single phase (liquid) pump differential pressure of 1.35 MPa. This is quite different from the situation that existed in the Bruce pump tests where the head pulsation amplitudes produced by pump head instabilities never exceeded 450 kPa (peak-to-peak) or approximately 25% of the Bruce pump's single phase differential pressure of about 1.8 MPa.

Figure 17 shows that the amplitude of the head pulsations varied cyclically with a period of about 2.5 seconds (i.e., with a beat frequency of approximately 0.4 Hz) from 13:40:30 to 13:41:00 and

---

* All data shown were measured during draining of the loop.

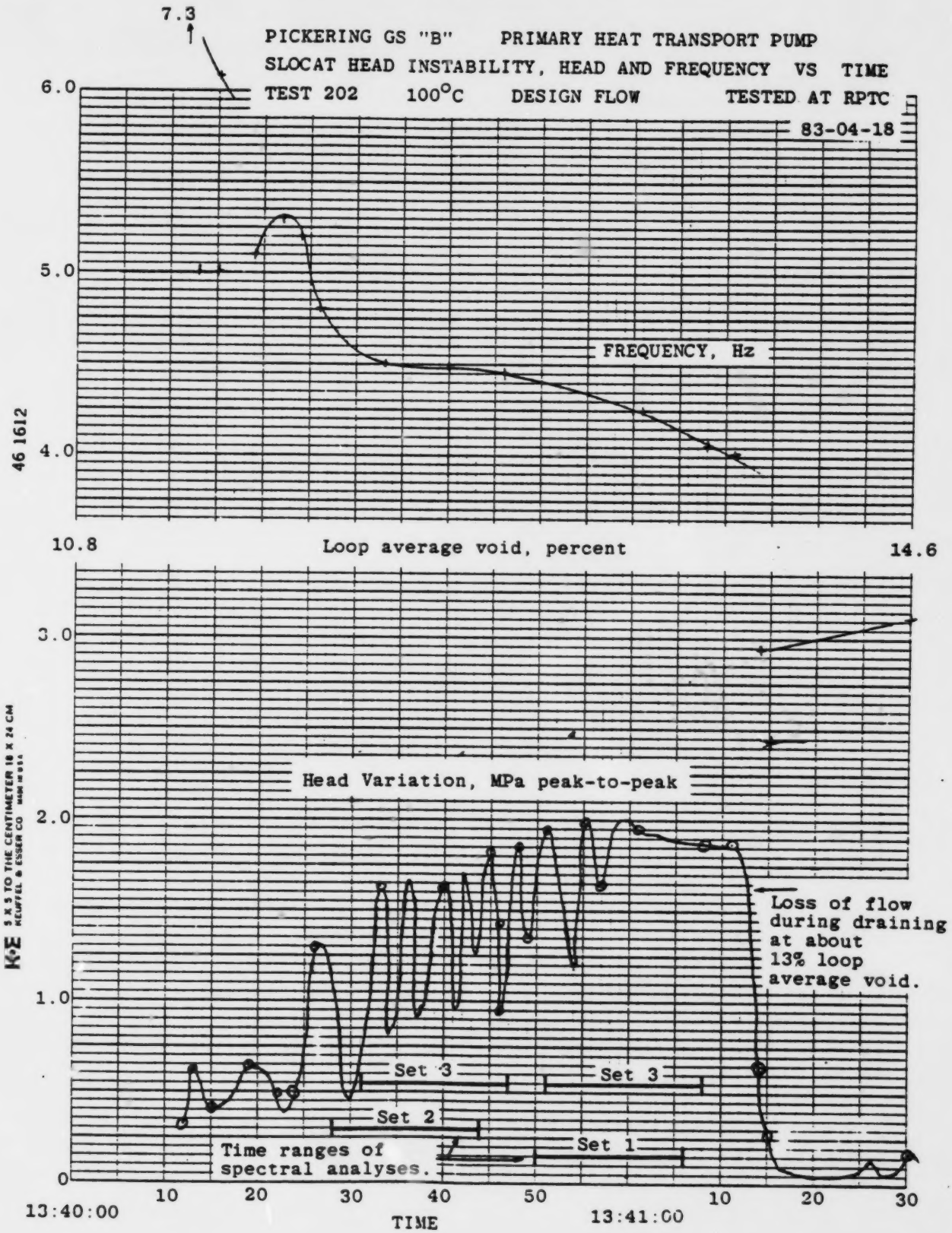


Figure 17 Head Pulsation Amplitude and Frequency vs. Time in Test 202 [from Ref. 10]

then remained fairly constant until dropping off suddenly between 13:41:11 and 13:41:16, in other words over a period of about 5 seconds. The computer printout of data for this test indicates that the average pump differential pressure dropped from an initial value of more than 1MPa to a final value of less than 100 kPa in roughly the same 5 second period, even though it had decreased only slightly from the single phase liquid value of 1.35 MPa up to that time.

High levels of vibration were also recorded while the loop was being refilled with cool (~23°C) water in those tests in which the pump was left running during refill. As in the case of the Bruce tests, the vibrations were most severe while the pump head was recovering, towards the end of the refill period. Refill rates were typically 1 l/sec. for the void matrix tests [Ref.11].

According to [Ref.11], periods of instability and high pressure pulse amplitudes were not observed in transient and blowdown tests performed at high bleed rates.

**A.5 Darlington PHT Pump Tests**

A Darlington PHT pump is a single (vertical) suction, double discharge design with hydraulic performance characteristics similar to those given previously for a Bruce pump. The rated head and flow are 224 m and 3.1 $m^3/s$ respectively vs 213 m and 3.3 $m^3/s$ for a Bruce pump, for instance. Additional characteristics of a Darlington pump can be found in [Ref.13].

A Darlington PHT pump was tested in the loop described previously for the Bruce tests. The results were reportedly similar to those of the Bruce tests in that pump head instabilities were observed at temperatures above 140°C but not below [Ref.16]. The peak-to-peak amplitude of the head pulsations was as high as 700 kPa in some instances and the most severe pulsations occurred at loop temperatures near 200°C. The pulsations at the two discharges appeared to be equal in amplitude and phase and the suction pressure remained virtually constant [Ref.16], as in the Bruce pump tests.

The abovementioned results were recorded while the loop was being drained. The pump was not operated during refill in any of the tests.

No further information about the Darlington pump tests was available at the time this report was written.

**A.6 Summary**

As discussed in Section 1.2, pump head instabilities, that is large amplitude head pulsations that occur under two-phase flow conditions while the pump head is degrading, were observed in the Bruce pump tests performed at loop temperatures greater than 170°C but not in the tests performed at temperatures of 140°C and below. Similar results were obtained in the Darlington PHT pump tests. In the Pickering pump tests, on the other hand, severe head pulsations were observed only in the low temperature (140°C and below) tests; the high temperature tests were comparatively uneventful. Also, whereas the largest peak-to-peak amplitude of the head pulsations observed in the Bruce tests was approximately 450 kPa, or 25% of the pump's single phase (liquid) differential pressure, pulsations with peak-to-peak amplitudes as high as 2 MPa were observed in the Pickering tests. This pulsation amplitude was 150% of the pump's single-phase differential pressure.

## B. FLOW INSTABILITIES IN PRESSURIZED PIPING SYSTEMS

### B.1 Introduction

There are at least four possible causes of the pump head instabilities observed in the Bruce, Darlington and Pickering PHT pump tests. The first and most obvious of these is that the head pulsations were the result of alternate slugs of liquid and pockets of vapor passing through the pump when it was operating in the slug or plug flow regime. As discussed in Section A.3, this was identified as the cause of the "interrupted flow instabilities" which were observed in the Bruce tests performed at temperatures over 170°C when the flow in the loop had almost stopped (i.e., at high void fractions). According to Heidrick [Ref.17], head pulsations produced by this mechanism occurred during steam-water tests of the SAWFT pump with an elapsed time between pressure spikes of approximately 10 seconds and pressure pulse amplitudes (peak-to-peak) that were roughly equal to the pump's single phase head of 130 m. Although the abovementioned elapsed time between pressure spikes is of the same order of magnitude as the period of the interrupted flow instabilities in the Bruce tests, i.e., 10 to 120 seconds [Ref.4], there is no obvious reason why head pulsations produced by slug or plug flow could not occur at a much higher frequency, such as one within the 0.5-3 Hz range characteristic of the pump head instabilities observed in the high temperature Bruce tests.

Another possible explanation for the head pulsations is one that was advanced by Murakami and Minemura [Ref.18] to explain instabilities observed in tests performed to determine the effect of entrained air on the cavitation characteristics of centrifugal pumps. At inlet air volume fractions of 6-9% in those tests , air was observed to accumulate in the low pressure region next to the front casing of the test pump and just past the impeller inlet, as shown in Figure 18. This is a low pressure region because the flow direction changes from axial to radial in the meridional plane at this point. When the air pocket reached a certain critical size, it momentarily elongated until it extended from the inlet to the outlet of the impeller, thereby causing a large drop in pump differential pressure. The resulting abrupt change in flow through the pump dislodged the air pocket, permitting flow to resume and a new air pocket to grow within the impeller. This process repeated itself with a period of approximately 10 seconds and caused the whole piping system to

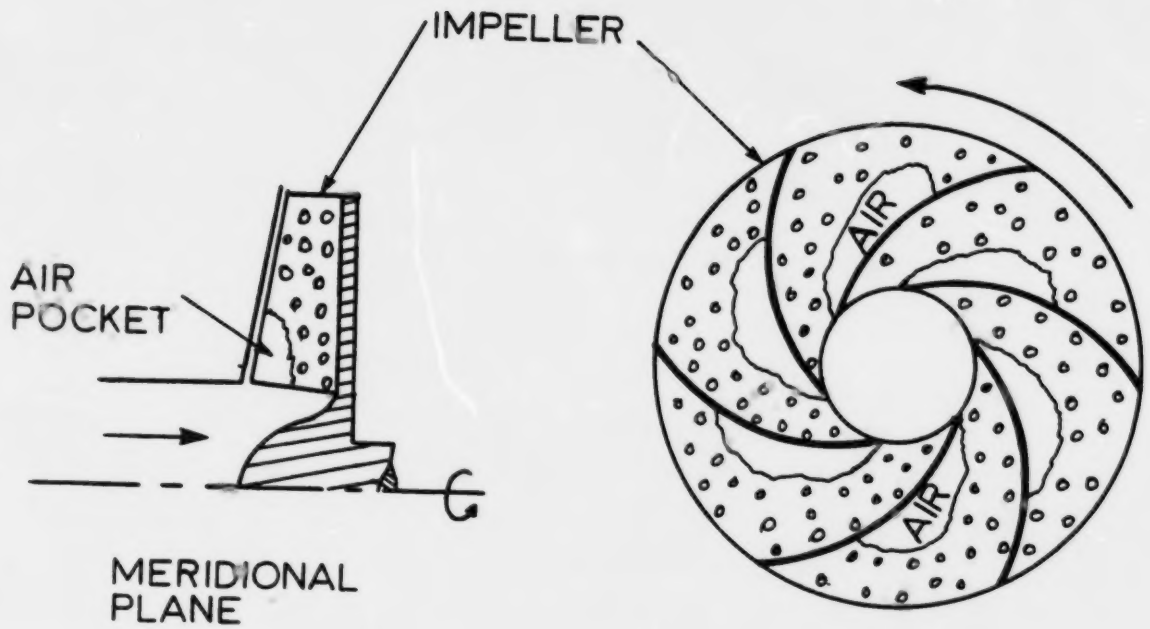


Figure 18 Location of the Air Pocket in the Impeller of the Pump Tested by Murakami and Minemura [Ref.18].

vibrate severely.

In spite of the multitude of air-water and steam-water tests of centrifugal pumps that have been performed over the years, the author knows of no other account of an instability that was obviously exactly the same as that observed by Murakami and Minemura. It is not clear whether the behaviour exhibited by the pump in their tests was due to some unusual design characteristic of the pump itself, some characteristic of the rest of the piping system, or both. The author suspects, however, that the instability described by Murakami and Minemura actually belongs to the third category, discussed below.

A third possible explanation for the head pulsations observed in the Ontario Hydro tests is that they resulted from self-excitation of a low order acoustic mode in the test loop. In contrast to the other possible causes already discussed, self-excited acoustic oscillations can occur with single-phase as well as two-phase flows.

Self-excited flow oscillations in systems in which a pump or compressor was the source of energy for the oscillations have been observed under a wide variety of circumstances [Ref.19]. In particular, it has been shown in several studies, e.g. [Refs.19, 20, 21, 22], that such oscillations readily occur in pressurized piping systems in which a cavitating turbopump is present. Since it is believed that self-excited flow oscillations of a similar nature could easily occur in a reactor primary circuit during a LOCA, the causes and characteristics of self-excited flow oscillations will be examined in detail in the next section.

A fourth phenomenon that can cause flow oscillations in a pump/piping system is choking of a flow restriction upstream of the pump, as demonstrated by Outa et al. [Ref.23]. Because this phenomenon or at least a similar one could have been responsible for the violent head pulsations that were observed in the Pickering pump tests, as will be demonstrated later, its causes and characteristics will be examined in greater detail following the discussion of acoustic flow oscillations.

## B.2 Self-Excited (Acoustic) Flow Oscillations

In order for small flow oscillations to grow in size in a system in which the only source of energy is a pump, the pump must feed

hydraulic energy into the oscillations at a rate faster than that at which it is dissipated by viscous friction. While this is a necessary and sufficient condition for instability, a necessary condition is obviously that the pump feed energy into any oscillations present in the flow, in other words increase the hydraulic energy that it delivers to the flow when oscillations are present. By applying the first law of thermodynamics to a control volume enclosing the pump, it is easily verified that the difference between the energy supplied by the pump to a flow in which oscillations of period $\tau$ are present and that supplied to a steady flow with the same average flowrate is,

$$\Delta W_p = \int_0^\tau (\dot{m}_o' h_o' - \dot{m}_i' h_i') \, dt \qquad (1)$$

over a single surge cycle, where $\dot{m}'$ and $h'$ are the oscillatory (perturbation) mass flow rate and enthalpy respectively and the subscripts i and o refer to conditions at the pump suction and discharge respectively. Changes in the kinetic energy of the flow entering and leaving the pump were assumed to be negligible in deriving Eq.1.

For isentropic pressurization of an incompressible fluid, the perturbation enthalpies in Eq.1 can be replaced by perturbation pressures ($p'$) to obtain

$$\Delta W_p = \int_0^\tau [(\dot{m}_o' p_o' - \dot{m}_i' p_i')/\rho] \, dt \qquad (\rho = \text{density}) \qquad (2)$$

Although Eq.2 is strictly only valid for an incompressible fluid, as noted previously, it is nonetheless approximately correct even when applied to the isentropic compression of a steam-water mixture of low-to-moderate void fraction (e.g., 0-40%) because the quality of such a mixture is very low except at extremely high pressures. The low quality causes the work required to compress the mixture from its initial pressure to a pressure at which it is a compressed liquid to be negligibly different from the work required to compress liquid alone between the same two pressures, as demonstrated by means of an example in Appendix A.

In order for the pump to feed energy into any oscillations present in the flow, we must have

$$\Delta W_p = \int_0^\tau [(\dot{m}_o' p_o' - \dot{m}_i' p_i')/\rho] \, dt > 0 \qquad (3)$$

To evaluate Eq.3, it must first be determined whether the pump's

performance under dynamic conditions differs significantly from its steady-state performance. If it does not, Eq.3 can be further simplified, as discussed in the next section.

### B.2.1 Quasi-Steady Pump Operation

If the mass of fluid within the pump does not change during surge and the pump behaves quasi-steadily, in other words if its performance under dynamic conditions is not significantly different from its steady-state performance, $\dot{m}_i' = \dot{m}_o' (= \dot{m}_p')$ and Eq.3 becomes

$$\Delta W_p = \int_0^\tau [\dot{m}_p' (p_o' - p_i')/\rho] \, dt$$

$$= \int_0^\tau \dot{m}_p' \frac{(\Delta p_p')}{\rho} \, dt > 0 \qquad (4)$$

where $\Delta p_p'$ is the oscillatory component of the pump differential pressure $(= p_o' - p_i')$. For small perturbations, it is assumed that

$$\Delta p_p' = \dot{m}_p' \cdot \frac{d(\Delta p_p)}{d\dot{m}_p} \qquad (5)$$

where $d(\Delta p_p)/d\dot{m}_p$ is the slope of the pump's differential pressure $(\Delta p_p)^*$ versus mass flow $(\dot{m}_p)^{**}$ characteristic. Substituting Eq.5 into Eq.4, the criterion for positive incremental energy transfer from the pump to an oscillating flow can be rewritten as

$$\Delta W_p = \int_0^\tau \frac{\dot{m}_p'^2}{\rho} (d(\Delta p_p)/d\dot{m}_p) \, dt > 0 \qquad (6)$$

When the slope of the head versus flow curve for the pump is positive at the nominal operating point, $\dot{m}_p'$ and $\Delta p_p'$ are in phase and the pump feeds energy into any oscillations present in the flow according to Eq.6. If the pump is located in a loop in

---

* $\Delta p_p = \overline{\Delta p}_p + \Delta p_p'$, where $\overline{\Delta p}_p$ is the steady component of the pump's differential pressure.

** $\dot{m}_p = \overline{\dot{m}}_p + \dot{m}_p'$, where $\overline{\dot{m}}_p$ is the steady component of the mass flow rate through the pump.

which virtually all of the pressure drop occurs across a single throttling valve, the additional hydraulic energy dissipated in the valve as the result of small perturbations in flow ($\Delta W_v$) is given by an expression similar to Eq.6 as,

$$\Delta W_v = \int_0^\tau \frac{\dot{m}_v'^2}{\rho} \left(d(\Delta p_v)/d\dot{m}_v\right) dt \qquad (7)$$

where $\dot{m}_v'$ is the oscillatory component of the mass flow through the valve ($\dot{m}_v$) and $\Delta p_v$ is the pressure upstream of the valve minus that downstream. For flow oscillations to grow, we must have both $\Delta W_p > \Delta W_v$ and $d(\Delta p_v)/d\dot{m}_v > d(\Delta p_p)/d\dot{m}_p$ since violation of the latter condition would result in a system which was statistically rather than dynamically unstable. Satisfaction of both of these conditions requires that the amplitude of $\dot{m}_v'$ (i.e., $|\dot{m}_v'|$) be less than that of $\dot{m}_p'$, a requirement that cannot possibly be satisfied unless the fluid in both the suction and discharge pipes is compressible to some extent since it is only in this case that fluid can be stored in the pipes during part of a surge cycle and later released so as to cause the flow oscillations at the valve to be smaller than those at the pump (i.e., to even out the flow through the valve). Because of this, it is unlikely that flow oscillations produced by a positively-sloped pump head vs. flow characteristic could occur in a two-phase flow loop unless the discharge pipe as well as the suction pipe contained some void, either in the form of vapor or non-condensable gases.

Since surge produced by a positively-sloped pump head-versus-flow characteristic is most likely to occur when the flow oscillations are large at the pump and small at the valve, the acoustic modes that are most likely to be excited are those for which the pump is located at a velocity loop and the valve is situated at a velocity node. For a pump and a valve located at the ends of a constant area pipe connecting two constant head reservoirs, as shown in Fig.19, such modes are the illustrated quarter-wave acoustic modes with frequencies given by the expression

$$f = \frac{n}{4}\frac{a}{\ell} \qquad n = 1, 3, 5, \ldots, \qquad (8)$$

where $\ell$ is the length of the pipe and a is the speed of sound in the pipe.

Since surge usually involves primarily the lowest order acoustic mode [Ref.26], the surge frequency for the piping system shown in Figure 19 would probably be $a/4\ell$. As shown in Appendix B, where

the stability of the system shown in Figure 19 is examined in detail, surge will occur with this frequency if the following criterion is satisfied:

$$M_v - M_p > \frac{M_v M_p}{Z_c} - Z_c > 0 \qquad \text{(Eq.B.29)}$$

where

$$M_v = \frac{d(\Delta H_v)}{dQ}$$

$$M_p = \frac{d(\Delta H_p)}{dQ}$$

$Z_c = a/gA$

$\Delta H_v$ = the head difference across the valve (positive)

$\Delta H_p$ = the pump head

$Q$ = volumetric flowrate

and

$A$ = pipe cross-sectional area.

The analysis described in Appendix B assumes that the fluid in the pipe is incompressible*, so Q is directly proportional to the mass flowrate.

According to Eq.B.29, a necessary condition for instability is that we have,

$$M_v M_p > Z_c^2 \left(= \frac{a^2}{g^2 A^2}\right) \qquad (9)$$

Since the sound speed of a fluid increases as its compressibility decreases, Eq.9 indicates that the likelihood of surge occurring decreases as the compressibility of the fluid between the pump and the valve decreases (i.e., as a increases). This result supports the observation made earlier about the importance of fluid compressibility in the suction and discharge pipes.

---

*Or at least undergoes negligible variations in density.

Although surge is most likely to involve a quarter-wave acoustic mode for the reasons given earlier, the analysis described in Appendix B indicates that a half-wave mode will be excited if

$$\frac{M_v\ M_p}{Z_c} - Z_c > M_v - M_p > 0 \qquad \text{(Eq.B.30)}$$

The lowest order half-wave mode, which is shown in Figure 20 and is the half wave mode most likely to be excited, has a frequency $f = a/2\ell$. The frequencies of higher order half-wave modes are simply integer multiples of this (for a constant area pipe).

As shown by means of a lumped parameter analysis described in Appendix C, the flow in a pipe loop such as that shown in Figure C.1 will be unstable if

$$M_v\ M_p > Z_{c1}^2\ \frac{L'}{\ell_1} + Z_{c2}^2\ \frac{L'}{\ell_2} \qquad (M_v > M_p) \qquad \text{(Eq.C.22)}$$

where

$Z_{c1} = a_1/gA$

$Z_{c2} = a_2/gA$

$a_1$ = the speed of sound in the discharge pipe

$a_2$ = the speed of sound in the suction pipe

$\ell_1$ = the length of the discharge pipe

$\ell_2$ = the length of the suction pipe

and

$L' = \ell_1 + \ell_2$

The analysis described in Appendix C also shows that the corresponding surge frequency can be estimated from the expression

$$f = \frac{\omega}{2\pi} = \frac{1}{2\pi}\sqrt{\frac{a_1^2}{\ell_1 L'} + \frac{a_2^2}{\ell_2 L'}} \qquad \text{(Eq.C.24)}$$

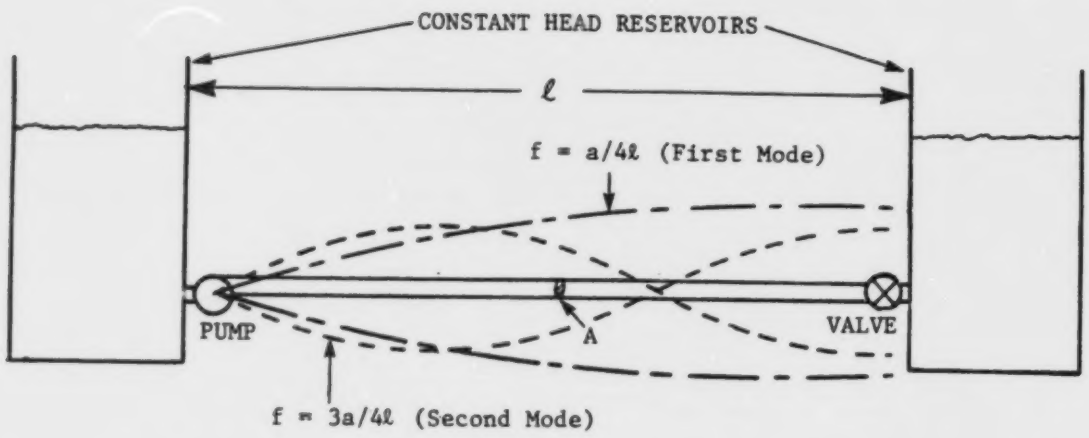


Figure 19 First and Second Quarter Wave Acoustic Modes in a Straight Pipe Connecting Two Constant Head Reservoirs.

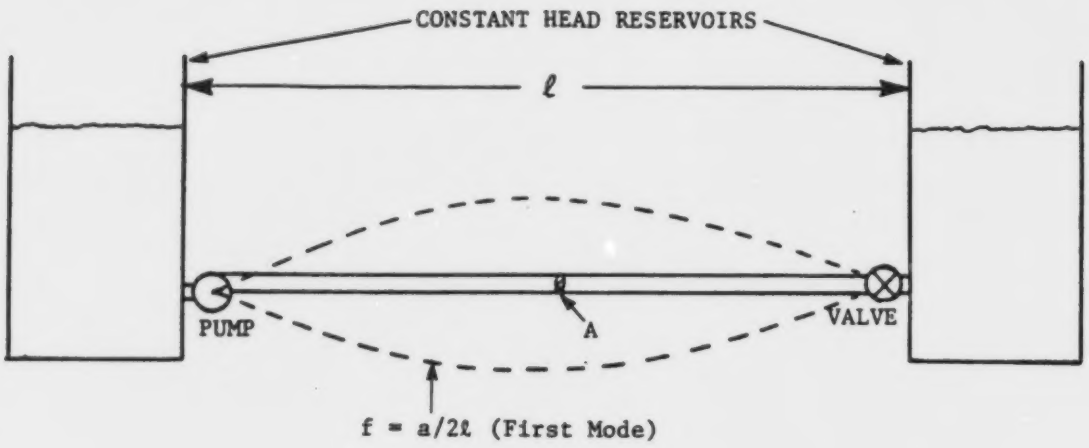


Figure 20 First Half Wave Acoustic Mode in a Straight Pipe Connecting Two Constant Head Reservoirs.

and that the ratio of the magnitude of the pressure pulsations in the discharge pipe to the magnitude of the pulsations in the suction pipe (i.e., $|p_1'|/|p_2'|$) can be obtained from the relationship

$$\frac{|p_1'|}{|p_2'|} = \left(\frac{a_1}{a_2}\right)^2 \times \frac{\ell_2}{\ell_1} \qquad \text{(Eq.C.25)}$$

Equation C.25 predicts that the largest pressure pulsations will occur in the pipe (suction or discharge) with the highest sound speed (assuming $\ell_1 \approx \ell_2$) while Eq.C.24 indicates that the highest sound speed also has the greatest effect on the surge frequency.

The surge criterion expressed by Eq.C.22 indicates once again that surge would be unlikely to occur if the fluid in the discharge and/or suction pipe had very little compressibility (i.e., a high sound speed), as would be the case if it was single phase liquid water. This does not mean that surge could not occur in a loop in which a steam-water mixture was compressed to a pressure at which it was a compressed liquid under equilibrium conditions, however, because the complete collapse of all of the vapor bubbles in the mixture would lag the pressure increase due to the finite rate of condensation of the bubbles. As a result, there would likely be a small volume of void just downstream of the pump impeller (perhaps extending into the discharge pipe) that would greatly reduce the average sound speed in the discharge pipe and thereby made surge much more likely. Any pockets of non-condensable gas in the discharge pipe would have a similar effect.

As mentioned previously, the pump differential pressure versus mass flow characteristic must be positively sloped to produce surge if the pump behaves quasi-steadily. It is well known, however, that the two-phase performance of a centrifugal pump is not a function of mass flowrate alone but rather is a function of at least two independent variables, such as either mass flowrate and inlet void fraction or volumetric flowrate and inlet void fraction. If one assumes that the inlet void fraction varies insignificantly during surge, a plot of pump head versus volumetric flowrate at constant inlet void fraction is equivalent to a plot of pump differential pressure versus mass flowrate* and is easily obtainable for any pump for which two-phase performance data are available. Such a plot was prepared by Rothe and

---

* For homogeneous flow at least.

Runstadler from the results of air-water tests of a 1/20-scale model of a nuclear reactor primary coolant pump [Ref.29] and is included here as Figure 21.

As seen in Figure 21, the head produced by the 1/20-scale pump increased with increasing flow rate when the inlet void fraction was fixed at any value between approximately 6 and 16% and the flowrate was less than approximately 110% of the design flowrate ($\phi_{des} \simeq 0.14$). During tests of the 1/20-scale pump in the open loop shown in Figure 22, the flow surged with a frequency of approximately 1 Hz when the void fraction at the pump inlet was less than 20% and the flowrate was less than about 50% of its design value [Ref.29]. The flow surged at void fractions above 20% as well, but it was apparently very difficult to determine whether the surge that was observed in those cases was really "true" surge that resulted from dynamic instability or just surge produced by slug flow passing through the pump. The difficulty in differentiating between true surge and surge produced by slug flow existed even though the loop was highly instrumented and the flow behaviour in the transparent suction and discharge pipes was recorded and studied on high speed film.

As noted previously, a plot of pump head versus volumetric flowrate at constant inlet void fraction is only equivalent to a plot of pump differential pressure versus mass flow rate if the inlet void fraction varies insignificantly during surge. Although this could have been the case in the tests performed by Rothe and Runstadler because the mass flowrates of air and water supplied to the pump suction were held constant and pressure variations at the suction were small compared to the absolute pressure level, there is no reason why this should be true in general, particularly if the void at the pump suction is condensable. In the case of surge in a closed pipe loop, numerical and frequency domain analyses performed by the author indicate that the pressure and velocity at the pump suction vary 180 degrees out of phase and that as a result the void fraction, velocity and volumetric flowrate all vary in phase. Thus these three parameters all increase and decrease together during surge, causing the conditions at the pump suction to traverse a path on the pump characteristic that is quite different from one of constant void fraction.

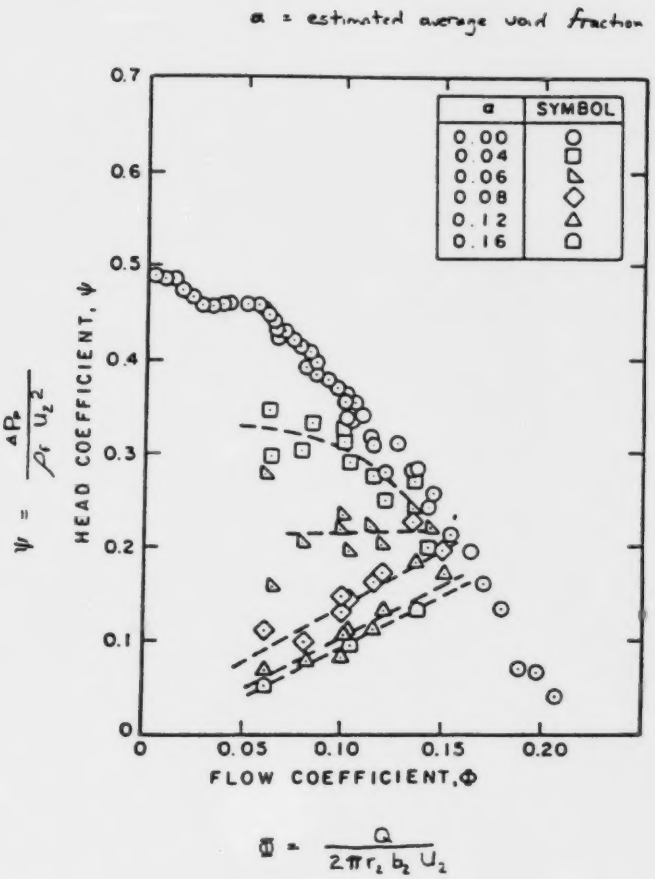


Figure 21 Crossplot of Pump Performance Data from Air-Water Tests of Rothe and Runstadler [Ref.29].

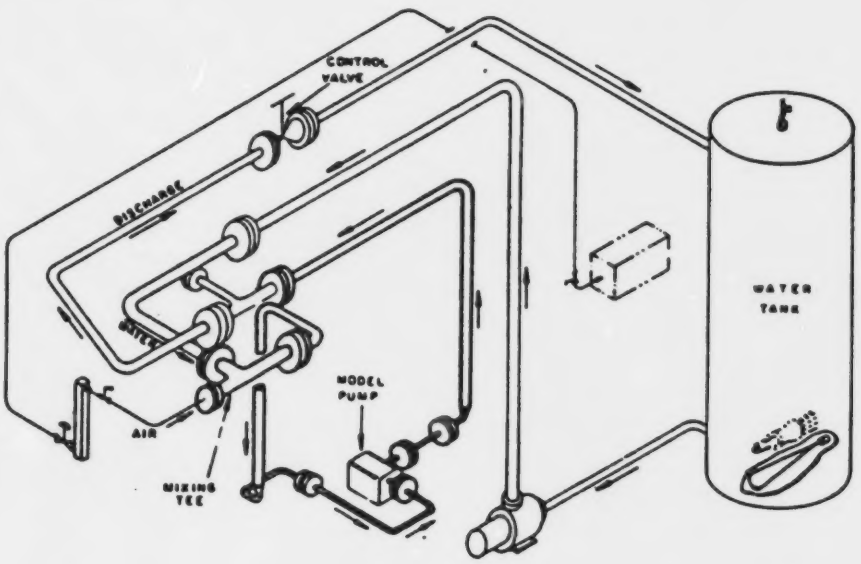


Figure 22 Test Loop Used in Air-Water Tests Performed by Rothe and Runstadler [Ref.29]

In addition to the questionable significance of curves of pump head versus volumetric flowrate which are positively-sloped at a constant inlet void fraction, it is also not known whether such curves are typical of most centrifugal and mixed flow pumps or whether they are highly atypical. The results of two-phase performance tests performed on other pumps would have to be plotted in the manner shown in Figure 21 to answer this question. There is at least some evidence that not all pumps behave in the same manner as the 1/20-scale pump to which Figure 21 applies, however, since the author was able to construct Figure 23 from data given by Kastner and Seeberger [Ref.30]for a 1/5-scale model of a Kraftwerk Union (KWU) PWR reactor coolant pump that was tested in steam-water by Combustion Engineering. As indicated, Figure 23 shows curves of normalized head (i.e., two-phase head divided by the rated head) versus void fraction for 45% and 100% of the pump's rated flow. Since the pump head produced at 45% rated flow was greater than the head produced at 100% rated flow at all void fractions, it is clear that at least the average slope of the pump head versus flowrate curve between 45% and 100% of the pump's rated flow was not positive at any void fraction.

It should be mentioned that the specific speed of the model KWU PWR pump (6500 rpm US $gpm^{1/2}/ft^{3/4}$) was approximately twice that of a Bruce PHT pump (3200) and over three times that of a Pickering pump (2000). As a result, the KWU PWR and CANDU PHT pumps could behave quite differently under two-phase conditions.

### B.2.2 Non-Steady Pump Operation

Severe flow oscillations and pipe vibrations have been observed in a variety of systems in which a cavitating turbopump served as the exciter. Among the pumps that have been known to produce flow oscillations while cavitating are boiler feed pumps [Ref.20] and the axial flow inducers used in liquid-fueled rocket motors [Ref.21, 22]. The cavitation performance of the latter type of turbopump in particular has been the subject of numerous analytical and experimental studies.

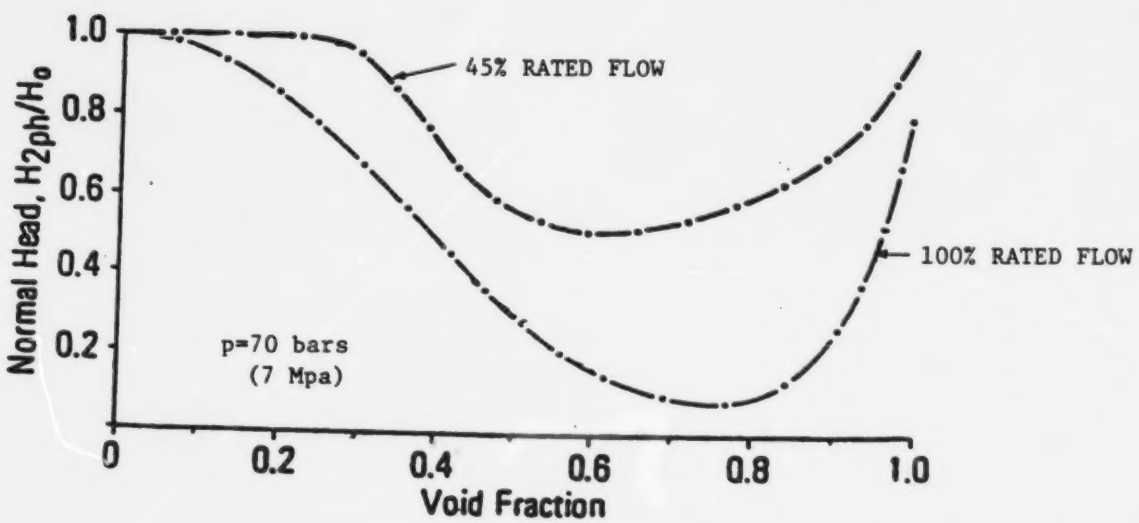


Figure 23 Head Degradation at Different Flows for a 1:5 Scale Model of a KWU PWR Pump [Ref.30]

The main conclusion of most studies of cavitating turbopumps is that their performance under dynamic conditions differs significantly from their steady-state performance, even when the frequency of the flow oscillations produced by the cavitating turbopump is only a few Hertz [Ref.19]. When a pump does not operate quasi-steadily, the oscillatory flowrates $\dot{m}_i'$ and $\dot{m}_o'$, the oscillatory pressures $p_i'$ and $p_o'$ and the fluctuating pump differential pressure $\Delta p_p'$ ($= p_o' - p_i'$) can all vary out of phase.

Another conclusion of most of the abovementioned studies is that the ability of a cavitating turbopump to act as an exciter (i.e., to feed energy into any oscillations present in the flow) is probably related to the growth and collapse of a volume of void within the pump (the cavitation volume) due to variations in pump inlet pressure and mass flow. Designating the cavitation volume by $V_c$, it is commonly assumed that for small amplitude transients about a mean operating point [Ref.19],

$$\dot{m}_o' - \dot{m}_i' = \rho \left[\frac{\partial V_c}{\partial p_i}\frac{dp_i}{dt} + \frac{\partial V_c}{\partial \dot{m}_i}\frac{d\dot{m}_i}{dt}\right] \tag{10}$$

and

$$\Delta p_p' = \frac{\partial(\Delta p_p)}{\partial \dot{m}_i}\dot{m}_i' + \frac{\partial(\Delta p_p)}{\partial p_i}p_i' \tag{11}$$

where unprimed pressures and flowrates are total (steady plus oscillatory) values, as before. Thus the pump differential pressure is assumed to be a function of two parameters, the inlet pressure and inlet mass flowrate, while the difference between the mass flow leaving and entering the pump is assumed to be a function of the time derivatives of those parameters.

As discussed in the preceding section, a positive value of $\partial(\Delta p_p)/\partial \dot{m}_i$ in Eq.11 has a destabilizing effect on the flow in a piping system but is considered to be an unlikely eventuality. Thus the first term on the right-hand side of Eq.11 should usually be stabilizing. The second term should also be stabilizing because a positive value of $\partial(\Delta p_p)/\partial p_i$ increases stability [Refs.19, 20] and $\partial(\Delta p_p)/\partial p_i$ is positive for a pump operating with a two-phase flow if a decrease in inlet void fraction (corresponding to an increase in inlet pressure) produces an increase in pump differential pressure, as is usually the case.

The term $\partial V_c/\partial p_i$ in Eq.10 is always negative while the term $\partial V_c/\partial \dot{m}_i$ is negative if an increase in inlet mass flow causes a reduction in $V_c$ and thus $\dot{m}_o - \dot{m}_i$ (due to an increase in the mass of fluid within the pump) or positive if an increase in inlet mass flow causes an increase in $V_c$ and $\dot{m}_o - \dot{m}_i$. It has been shown in several studies, e.g., [Refs.19, 20], that flow oscillations are likely to occur if $\partial V_c/\partial \dot{m}_i$ becomes sufficiently negative, i.e., negative values of $\partial V_c/\partial \dot{m}_i$ are destabilizing.

Experimental studies have indicated that $\partial V_c/\partial \dot{m}_i$ is negative for cavitating turbopumps during periods of instabilty [Ref.22]. This term is also expected to be negative for centrifugal pumps operating with two-phase mixtures of low to moderate void fraction for at least two reasons. The first of these is that at flow coefficients less than the design value, an increase in mass flow rate reduces the misalignment between the flow entering the impeller and the leading edges of the impeller blades and therefore probably also reduces the tendency of vapor bubbles to accumulate in the low pressure regions produced by such misalignment, as shown in Figures 24a and 24b. The velocity of th flow relative to the impeller (i.e., W) is shown to be aligned with the leading edge of an impeller blade at the design flow in Figure 24a and misaligned at a low flow in Figure 24b. Figure 24b also shows the resulting region of void formation and bubble accumulation that can be expected at low flowrates.

A second reason why $\partial V_c/\partial \dot{m}_i$ is expected to be negative for centrifugal pumps operating with two-phase mixtures is related to phase separation within the impeller. If phase separation occurs, as it must in order for significant head degradation to occur, vapor bubbles migrate to either the suction side or the pressure side of an impeller channel depending on the direction of the net pressure gradient. In air-water tests of model pumps with backward swept impeller blades, it has been observed that air bubbles tend to migrate more or less radially inwards and accumulate on the impeller blade pressure surfaces because of the large centrifugal (radial) pressure gradient in the impeller [Ref.31]. This type of stratification can be seen in Figure 18.

The tendency of bubbles to accumulate and coalesce within the impeller should decrease as the flowrate and hence flow velocity

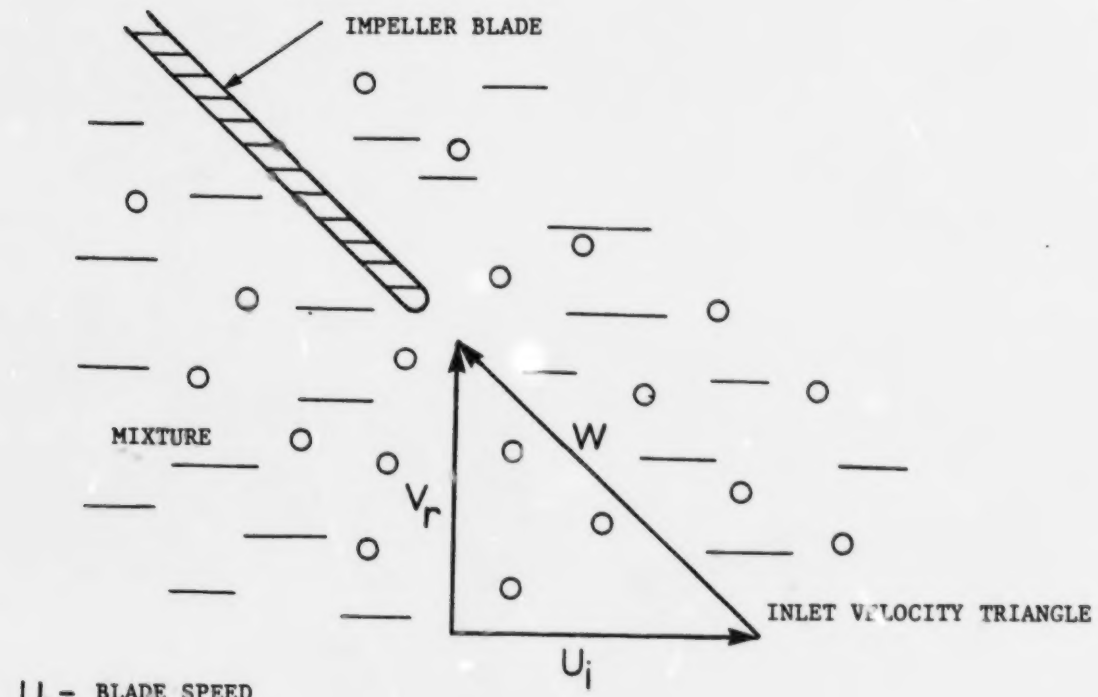


$U_i$ - BLADE SPEED

$V_r$ - RADIAL FLOW VELOCITY

W - VELOCITY OF FLOW RELATIVE TO IMPELLER BLADE

Figure 24a Flow Velocity Relative to the Impeller at Design Conditions

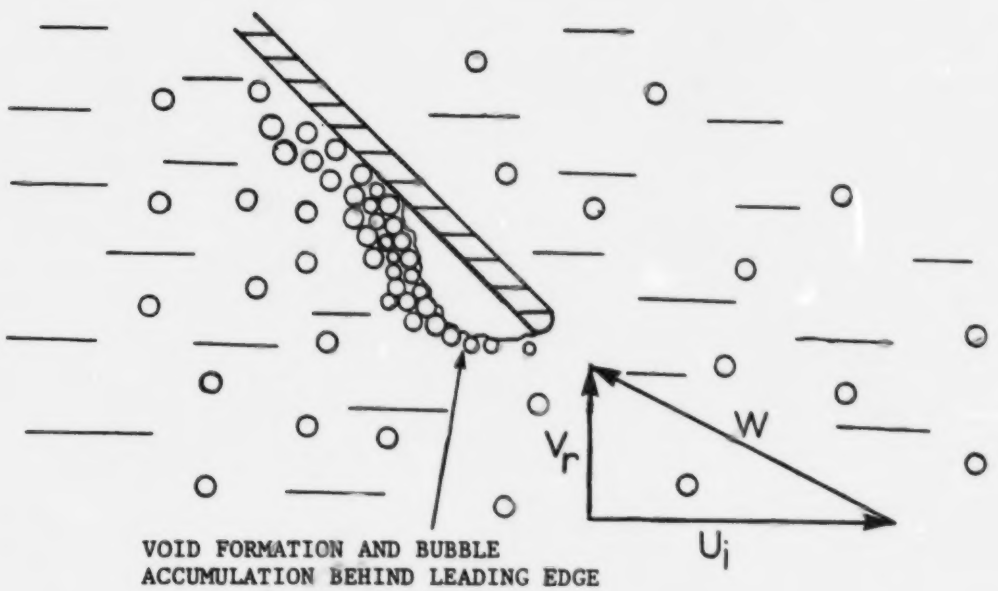


Figure 24b Void Formation and Bubble Accumulation Caused by Flow Incidence at Low Flow Coefficients.

in the impeller increases because the velocity of the bubbles relative to the fluid, which is a function of the magnitude of the net pressure gradient, will not increase proportionately and will actually probably decrease because of a reduction in the pressure gradient. Bubbles will be more readily carried through the impeller by the flow as a result. In addition, an increase in flow velocity should cause the size of the largest void pocket that can exist in the impeller without breaking up (i.e., the largest stable void pocket) to decrease.

For the reasons given above, $\partial V_c/\partial \dot{m}_i$ is more likely to be negative than positive.

Surge resulting from a negative value of $\partial V_c/\partial \dot{m}_i$ or a positively-sloped pump characteristic can be predicted either analytically if the governing differential equations are linearized by assuming small perturbations (as in Appendices B and C) or numerically. To demonstrate that surge resulting from a negative value of $\partial V_c/\partial \dot{m}_i$ can be predicted using a fairly conventional thermalhydraulics code, a homogeneous equilibrium code based on the implicit characteristic finite-difference method used in RAMA [Refs.32, 33] was used to analyze surge in the simple pipe loop shown in Figure 25. As indicated, the modelled loop consisted of 15 m constant area (0.56 m I.D.) suction and discharge pipes separated by a pump and a throttling valve. Although the geometry of the pipe loop shown in Figure 25 was chosen for its simplicity and was not intended to replicate that of the Pickering or Bruce pump test loop, the loop was nonetheless similar to the Bruce pump test loop in some respects in that (1) the suction pipe length was roughly the same as the length of the suction pipe in the Bruce loop measured from the pump to the throttling valve in the center hairpin, and (2) the pipe I.D. of 0.56 m was close to the 0.52 m I.D. of the 24" pipe from which most of the Bruce loop was fabricated (Figure 3). In addition, the pump's steady-state single-phase performance was assumed to be the same as that of a Bruce pump, shown in Figure 2.

In the numerical simulation of surge, the pump differential pressure under two-phase conditions was obtained from a pump model resembling the widely used Aerojet Nuclear Corporation (ANC) model [Ref.17] but modified using data given by McGee et al. [Ref.34] in the manner described in Appendix D. In addition, Eq.10 was enforced by approximating $dp_i/dt$ and $d\dot{m}_i/dt$ as central differences in the continuity equation for the pump and

multiplying them by user-specified values of $\partial V_c/\partial p_i$ and $\partial V_c/\partial \dot{m}_i$ respectively. Since the dependent variables in the thermalhydraulics code used to perform the simulation were the nodal values of mass velocity G ($= \dot{m}/A$), enthalphy (h) and pressure (p), as in RAMA [Ref.32], $d\dot{m}_i/dt$ was easily calculated as $AdG_i/dt$.

Figure 26 shows one cycle of the oscillations in mass flow rate and pressure that were obtained at the pump suction and discharge in a simulation performed with $\partial V_c/\partial p_i = -1.1 \times 10^{-5}$ $m^3/Pa$ and $\partial V_c/\partial \dot{m}_i = -1 \times 10^{-3}$ $m^3/kg/sec$. The nominal operating conditions in the loop during the simulation and the peak-to-peak amplitudes of the pressures and mass flowrates shown in Figure 26 are summarized in Table 6. For simplicity, the flow was assumed to be frictionless in the suction and discharge pipes in the simulation so that all of the pressure drop in the loop occurred at the valve.

The simulation was performed with a time step size of 0.5 seconds and a uniform spacing between nodes of 1 m. The flow was not perturbed in any way to initiate surge and the oscillations shown in Figure 26 were recorded after 22 seconds or approximately 20 cycles since the period of the oscillations was approximately 1.1 seconds, as seen in Figure 26. The oscillations were growing rapidly at the time the data shown in Figure 26 were recorded.

As seen in Figure 26, the variations in pump discharge pressure and mass flowrate were very close to being in phase while the variations in pump inlet pressure and mass flowrate were very close to being 180° out of phase in the simulation. When the expression for $\Delta W_p$ given in Eq.3 is rewritten in the form,

$$\Delta W_p = \left[\int_0^\tau \dot{m}_0' \, p_0' \, dt + \int_0^\tau (-\dot{m}_i' \, p_i') \, dt\right]/\rho \qquad (12)$$

it is easily verified that the integral of $\dot{m}_o' \, p_o'$ is largest (and positive-definite) when $\dot{m}_o'$ and $p_o'$ are in phase while the integral of $(-\dot{m}_i' \, p_i')$ is largest (and positive-definite) when $\dot{m}_i'$ and $p_i'$ are 180° out of phase. Thus the phase relationships seen in Figure 26 result in a value of $\Delta W_p$ which is almost the largest value possible for the given pressure and flowrate amplitudes.

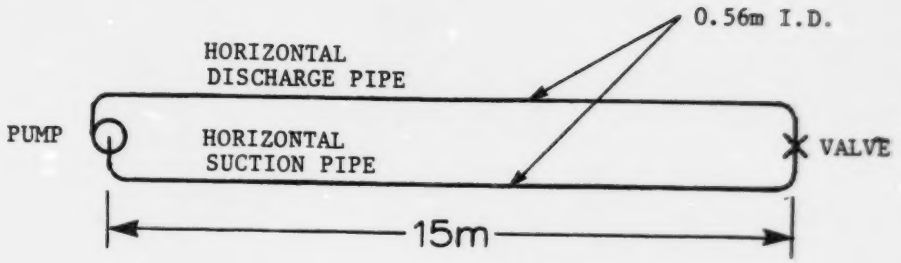


Figure 25 Loop Modelled in the Numerical Simulation of Surge.

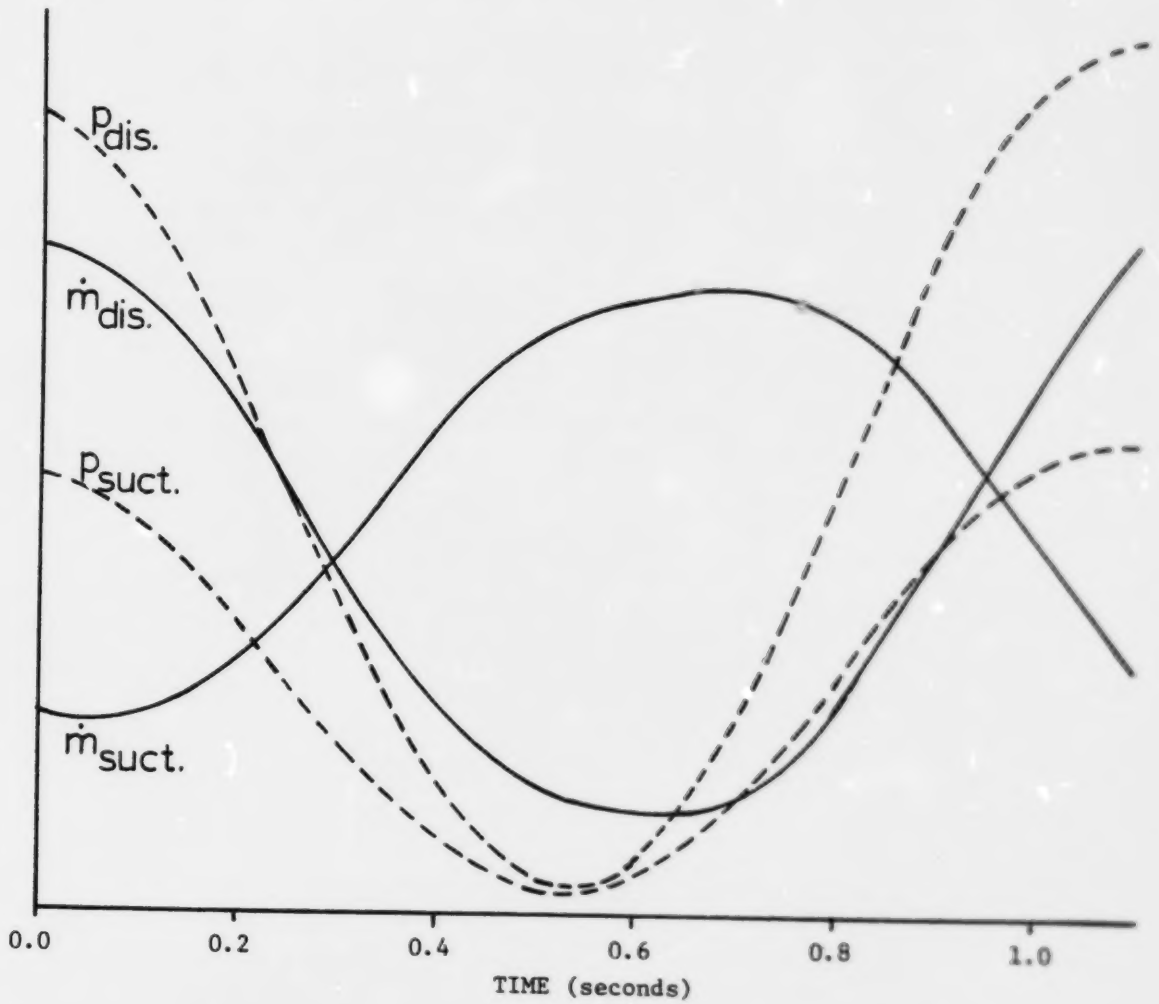


Figure 26 Results of the Numerical Simulation of Surge - Mass Flowrate ($\dot{m}$) and Pressure (p) Variations at the Pump Suction and Discharge.

Table 6: Nominal Operating Conditions and Peak-To-Peak Amplitudes of Oscillatory Parameters During Surge

Nominal Operating Conditions

| | |
|---|---|
| Mass flow rate | 940 kg/sec. |
| Pump suction pressure | 1.002 MPa |
| Pump suction temperature | 180°C |
| Pump suction void fraction | 0.28 |
| Pump discharge pressure | 2.296 MPa |
| Pump head | 206 m |
| Flow velocity in suction pipe | 6.00 m/sec |
| Flow velocity in discharge pipe | 4.33 m/sec |
| Sound speed in suction pipe | 11.5 m/sec |
| Sound speed in discharge pipe | 1358 m/sec |

Peak-to-Peak Amplitudes of Oscillatory Parameters

| | |
|---|---|
| Mass flow rate (pump suction and discharge) | 13 kg/sec (1.4% of the nominal mass flow rate) |
| Pump suction pressure | 0.9 kPa |
| Pump discharge pressure | 40.0 kPa |
| Pump inlet void fraction | 0.0072 |

When $\partial V_c / \partial p_i$ (= -1.1 x $10^{-5}$ $m^3$/Pa) is multiplied by the peak-to-peak amplitude of $p_i'$ (900 Pa) the variation in the cavitation volume ($V_c$) resulting from the variation in $p_i$ is found to be approximately 10 l. Similarly, multiplying $\partial V_c / \partial \dot{m}_i$ (= -1 x $10^{-3}$ $m^3$/kg/sec) by the peak-to-peak amplitude of $\dot{m}_i'$ (13 kg/sec) gives the variation in $V_c$ resulting from the variation in $\dot{m}_i'$ as approximately 13 l. Since $p_i'$ and $m_i'$ were close to being 180° out of phase in the simulation, a high value of one of these parameters would have corresponded to a low value of the other with the result that the net variation in $V_c$ would have been no more than about 3 l. It is not hard to imagine that such a small change in void volume could easily occur in a pump as large as a Bruce PHT pump.

To check that the surge observed in the numerical simulation was produced by a physical instability and not a numerical one, the stability of the flow in the loop shown in Figure 25 was examined by performing a small perturbation analysis, as described in Appendix E. The small perturbation analysis verified that surge would occur under the conditions assumed in the numerical simulation and yielded a value of 0.7 Hz for the surge frequency. Although this frequency is about 22% less than the surge frequency of approximately 0.9 Hz obtained in the computer simulation, the agreement is nonetheless considered satisfactory in view of the inherent limitations of a small perturbation analysis. Such an analysis is strictly only valid when (1) the flow velocity is negligible compared to the speed of sound, a proviso that was not satisfied in the numerical simulation because the flow velocity of 6 m/sec in the suction pipe was n negligible compared to the sound speed of 11.5 m/sec (Table 6), and (2) the fluid is essentially incompressible. The second condition is obviously not satisfied for a two-phase flow.

### B.3 Flow Oscillations Caused By Choking Of A Flow Restriction Upstream of a Pump

As noted previously, choking of the flow at a flow restriction upstream of a pump can cause periodic pressure and flow variations. This was demonstrated by Outa et al. [Ref.23] using an experimental facility in which an orifice located a known distance upstream of the pump served as the flow restriction, as shown in Figure 27. As illustrated, water was drawn from a

constant head reservoir and discharged to atmosphere through a control valve located at the end of the discharge pipe. The suction pipe was fabricated from clear acrylic plastic for a distance of 2.47 m (30 pipe diameters) upstream of the pump to permit observation of the flow at the pump suction.

In the tests in which flow oscillations were observed, the flowrate through the system was sufficient to cause choking of the orifice due to extensive cavitation. Because the orifice was choked, only the flowrates and pressures downstream of the orifice fluctuated; conditions upstream remained constant. This is clearly shown in Figure 28, which is an oscillograph of pressures and flowrates recorded during a period of instability. The parameters $Q_i$ and $Q_o$ in that figure are the flowrates upstream of the orifice and downstream of the pump respectively, $P_{01}$ and $P_{02}$ are pressures measured in the discharge pipe, $P_c$ is a pressure measured in the pump casing and $P_{p1}$, $P_{p2}$ and $P_{p3}$ are pressures measured between the orifice and the pump suction at the locations indicated in Figure 27.

The orifice was located 18.5 pipe diameters (1.48 m) upstream of the pump in the test to which Figure 28 applies. As indicated, the peak-to-peak amplitude of the variations in pump suction pressure ($P_{p1}$) was less than 1 m of water while the peak-to-peak amplitude of the variations in discharge pressure ($P_{01}$) was close to 4 m of water. Since the pump had a single phase head of 12 m, the peak-to-peak amplitude of the variations in pump head must have been about one-third of the pump's single-phase head.

The pulsations to which the data in Figure 28 apply had a period of approximately 5 seconds or a frequency of 0.2 Hz. In tests performed with other orifice-to-pump spacings, it was found that the frequency of the flow oscillations increased as this spacing was reduced. At an orifice-to-pump spacing of 0.34 m (4.3 pipe diameters), for instance (which is the lowest spacing for which results are given in [Ref.28]), the pulsation frequency was approximately 1.5 Hz.

According to Outa et al., the discharge flow oscillated when the upstream orifice choked because the length of pipe between the orifice and the pump cyclically voided and refilled. The pipe voided and refilled due to the backward and forward movement of a condensation shock [Ref.35] in the manner shown in Figure 29 rather than uniformly along its length. Between the orific

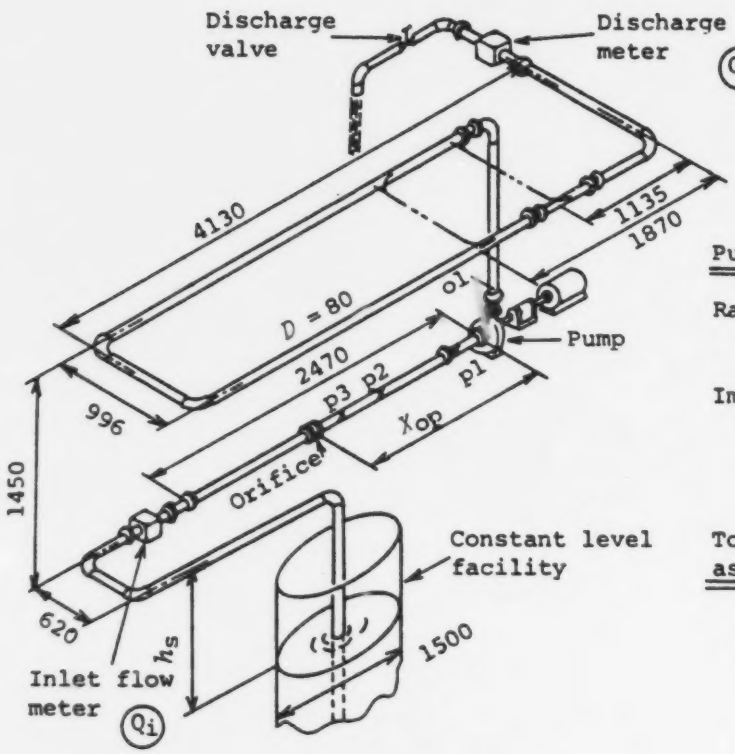


**Pump specifications**

Rating 12 mAq
0.6 $m^3$/min
1450 rpm
Impeller 3-blade centrifugal
$n_s$ = 174

**Total length of the assembly**

suction : 17 m
delivery : 13 m

Figure 27 Test Facility of Outa et al. [Ref.23]

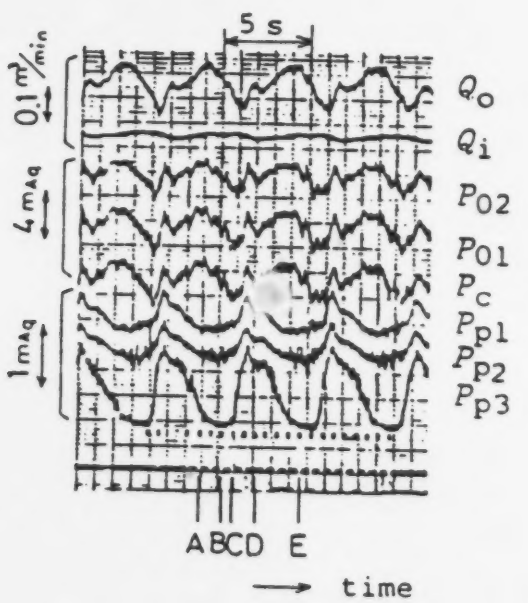


$Q_o$ = discharge flowrate

$Q_i$ = flowrate upstream of the choked orifice

$P_{o1}$ = pressure at the pump discharge

$P_c$ = pressure in pump casing

$P_{p1,p2,p3}$ = pressures measured at points p1,p2 and p3 between the orifice and the pump (see Figure 27)

Orifice-pump spacing = 1.48m (18.5 pipe diameters)

Frequency of flow oscillations = 0.2 Hz.

Figure 28 Oscillogram of Flowrates and Pressures Recorded During a Period of Instability in the Tests of Outa et al. [from Ref.23]

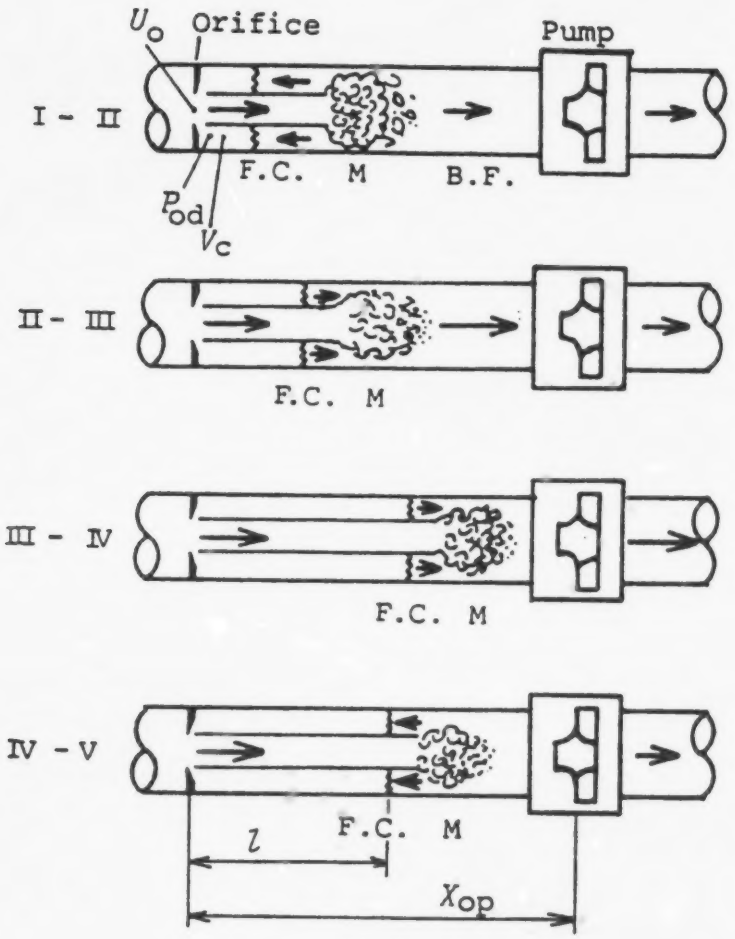


Figure 29 Sequential Flow Patterns Between the Choked Orifice and the Pump Suction in the Tests of Outa et al. [from Ref. 23]

F.C. - Front of reverse flow (condensation shock)
M - Mixing zone
B.F. - Bubbly flow
$V_c$ - Vapor cavity

and the condensation shock, the flow consisted of a central liquid jet surrounded by an annulus of largely stagnant vapor. Located immediately downstream of the forward front of the condensation shock was a highly turbulent mixing zone, designated region M in Figure 29. (Such zones are analogous to the region of intense mixing found downstream of a hydraulic pump [Ref.35]). Due to pressure recovery in the mixing zone, the flow further downstream was largely single phase liquid, although it is designated B.F. (for bubbly flow) in Figure 29.

A choked valve, orifice or other flow restriction is said to be supercavitating when the flow downstream of it consists of a liquid jet surrounded by a vapor pocket of significant length [Ref.36], as shown in Figure 29. The condensation shock at the downstream end of the vapor pocket is analogous to a compression shock in gas flow or a hydraulic pump in open channel flow and as such can be analyzed by enforcing the basic conservation relations for mass, momentum and energy [Ref.35]. As in the case of a compression shock in gas flow, a condensation shock is not uniquely located in a constant area pipe and will readily move downstream if the downstream pressure is lowered even slightly or upstream if the downstream pressure is increased by a small amount. According to Tullis [Ref.36]:

> "The condition of supercavitation is rather unstable. It is possible to cause the large vapor pocket to rapidly disappear with only a slight adjustment in downstream pressure. The transients associated with the collapse of the pocket are similar to those caused by the classical column separation problem. The pressure rise and forces on the valve can be of significant magnitude and are dependent upon the flow rate, length of the vapor pocket, and the speed with which it disappears".

The vapor pocket can be extremely long, possibly hundreds of pipe diameters [Ref.36]. According to Tullis, tests of a 12 in. valve at Colorado State University produced a vapor pocket over 100 feet long which did not collapse until it was obstructed by a partially closed downstream control valve. Tullis indicates that a pipe bend is another obstruction that can cause the void pocket produced by a supercavitating valve to collapse.

Flow oscillations produced by choking of a flow restriction upstream of a pump are fundamentally quite different from the self-excited acoustic flow oscillations described in the preceding section because they do not initiate when the pump is operating at a steady-state operating point. In the case of the tests performed by Outa et al. [Ref.28], for instance, the flow control valve was purposefully set so that the flow rate through the loop at the steady-state operating point (without choking) would exceed the flowrate required to cause the orifice to choke and thus never be achieved. As a result, the flowrate through the loop increased when the pump was first started until the orifice choked, at which point the pump suction pressure stopped decreasing as the flowrate through the pump increased (the flowrate through the orifice stopped increasing when it choked) because the vapor pocket downstream of the orifice started to grow. As noted previously, the vapor pocket downstream of a supercavitating valve or orifice can grow with almost no reduction in downstream pressure (i.e., pressure at the pump suction in this case).

Because the flowrate through the pump exceeded the flowrate through the choked orifice, the vapor pocket downstream of the orifice would have grown until it reached the pump suction. The appearance of void at the pump suction would have caused the head produced by the pump and thus the flowrate through it to decrease, permitting the vapor pocket in the suction pipe to refill to some extent and the pump head to return to normal. With the recovery of pump head, the void downstream of the orifice would have started to grow again and the sequence of events already described would have been repeated ad infinitum.

It should be mentioned that flow oscillations resulting from the growth and collapse of a vapor pocket located between a choked flow restriction and a pump cannot occur in a <u>closed</u> pipe loop unless there is an additional vapor pocket at some other location, possibly downstream of an earlier flow restriction. The second vapor pocket is needed to accommodate the fluid displaced from the vapor pocket at the pump suction as it cyclically voids and refills.

Flow oscillations produced by choking of a restriction upstream of a pump will be discussed further when the results of the Pickering pump tests are analyzed.

## C. ANALYSIS OF BRUCE PUMP TESTS

### C.1 Introduction

As described in Section A, the flow instabilities observed in the Bruce pump tests could be divided into the four categories shown in Figure 9. Of those four categories, only the head instabilities will be considered here because they are probably the most important and are certainly the most poorly understood. As noted previously, the general flow and interrupted flow instabilities were attributed to churn and/or slug flow passing through the pump and hence would likely occur to some extent in almost any piping system (including the primary circuits of Bruce and Pickering NGS) under two-phase flow conditions. The oscillating flow instabilities occurred when fluid was no longer circulating through the loop and thus could be avoided by shutting off the pump under those circumstances.

### C.2 High Temperature Tests

The head instabilities observed in the high temperature (> 170°C) Bruce tests probably resulted from slug or plug flow passing through the pump and/or from self-excitation of a low order acoustic mode. It is less likely that the oscillations were caused by choking of a flow restriction upstream of the pump because the suction pipe did not contain any restrictions downstream of the 90 degree bend leading to the pump suction. The bend would probably have collapsed any vapor pocket formed by a supercavitating flow restriction upstream even if such a restriction had been present, which is doubtful.

It is extremely difficult to determine which, if any, of the instabilities labelled head instabilities were produced by slug or plug flow and which, if any, were produced by self-excitation of a low-order acoustic mode. As noted previously, Rothe and Runstadler [Ref.29] found the flow oscillations produced by these two causes to be virtually indistinguishable even in a highly instrumented test loop with a transparent suction pipe. Although they resolved that problem by restricting their study to tests in which the pump inlet void fraction was less than 20% since this is usually assumed to be the lower limit for bubbly-to-slug flow transition in vertical flow [Ref.37], it is relatively difficult to classify the results of the Bruce tests in the same manner because pump inlet void fraction was not measured.

Without measured values, the pump inlet void fraction would have to be estimated from the loop average void in order to apply the technique used by Rothe and Runstadler to distinguish true surge resulting from dynamic instability from flow oscillations produced by plug or slug flow. This was not done for two reasons. First, it was felt that pump inlet void fraction would be virtually impossible to estimate accurately because of uncertainty in the size of the void located immediately downstream of the throttling valves. If the valves had been supercavitating during the tests, for instance, the resulting vapor pockets could easily have extended to the 36" return header (Figure 3) before collapsing. Since it is easily verified from the dimensions given in Figure 3 that the volume of piping that would have been largely steam-filled in that case (i.e., the volume located between the valves and the return header) was approximately 1.25 $m^3$ or about 4% of the total loop volume of 30.7 $m^3$*, there could have been no void anywhere else at values of loop average void less than 4%. Since the loop average void was generally in the 3% to 10% range during periods of pump head instability [Figure 5, Ref.4], the possibility that a volume of void equivalent to 4% of the loop volume could have been concentrated immediately downstream of the control valves and thus not distributed throughout the remainder of the loop (the suction pipe in particular) precludes accurate estimation of the pump suction void fraction.

Additional void could have accumulated at the top of the section of 36" pipe in the return header due to gravitational effects, further complicating the prediction of pump suction void fraction from the loop average value.

The second reason why no attempt was made to estimate pump inlet void fraction from loop average void is that it would be extremely difficult to predict the flow regime at the pump suction even if the void fraction there was known. Although the assumption that bubbly-to-slug flow transition occurs at a void fraction of 20-30% is a good rule-of-thumb for vertical flows

---

* The total loop volume was estimated from Figure 28 in [Ref.38], which shows the mass of water held by the test loop as a function of temperature.

[Ref.37], it is not really applicable to the Bruce loop where the roughly 2 m length of vertical pipe which preceded the pump was itself preceded by a 90° bend and approximately 15 m of horizontal pipe. Gravitational forces acting on the flow in the horziontal pipe and centrifugal forces acting on it in the bend could conceivably have caused transition from bubbly flow to plug or slug flow to have occurred at a void fraction less than 20%. In fully developed horizontal flows, the occurrence of plug (elongated bubble) or slug flow depends much more strongly on the liquid superficial velocity* ($U_L^S$) than on void fraction, as seen in the widely used flow regime map of Mandhane et al. [Ref.39] included here as Figure 30. Since the boundary between the dispersed bubble flow regime seen at the top of the map and the elongated bubble and slug flow regimes directly beneath it ($U_G^S$ < 50m/sec) is horizontal, there is no requirement that the plug and slug flow regimes form from bubbly flow as void fraction is increased; plug flow or even stratified flow can be the first regime to form if $U_L^S$ is sufficiently small.

The parameter ranges over which the Mandhane map is claimed to apply are summarized in Table 7. The Mandhane map is very similar to other horizontal flow regime maps proposed more recently by Weisman et al. [Ref.40] and Pearce [Ref.41]. Maps developed by Weisman and Pearce for different pressures from tests of Freon refrigerants indicate that the superficial liquid velocity at which the dispersed bubble-to-plug/slug flow transition occurs is at most a very weak function of pressure.

According to flow regime transition criteria derived by Taitel and Dukler [Ref.42] from mechanistic transition models, both the dispersed bubble-to-plug/slug flow transition boundary and the

---

* The superficial velocity of a phase is the volumetric flowrate of the phase divided by the pipe cross-sectional area.

Table 7: Parameter Ranges for the Flow Regime Map Proposed by Mandhane et al. [Ref.39]

| | | | | |
|---|---|---|---|---|
| Pipe inner diameter | 12.7 | - | 165.1 | mm |
| Liquid density | 705 | - | 1009 | $kg.m^{-3}$ |
| Gas density | 0.80 | - | 50.5 | $kg.m^{-3}$ |
| Liquid viscosity | $3\ 10^{-4}$ | - | $9\ 10^{-2}$ | $kg.m^{-1}s^{-1}$ |
| Gas viscosity | $10^{-5}$ | - | $2.2\ 10^{-5}$ | $kg.m^{-1}s^{-1}$ |
| Surface tension | 24 | - | 103 | $mN.m^{-1}$ |
| Liquid superficial velocity | 0.09 | - | 731 | $cm.s^{-1}$ |
| Gas superficial velocity | 0.04 | - | 171 | $m.s^{-1}$ |

plug/slug flow-to-stratified flow boundary move upwards on a map similar to that of Mandhane et al. as pipe diameter increases. This is clearly shown in Figure 31 (taken from [Ref.42]), which displays the former and latter boundaries, designated D and A respectively, for pipe diameters of 1.25, [illegible] and 30 cm. The results shown apply to air-water flows at 25°C and 1 atmosphere pressure. The cross-hatched boundaries are those recommended by Mandhane (Figure 30), which were determined largely from the results of air-water tests performed in 1.3 to 5 cm diameter pipes [Ref.39].

At the design flowrate of 3.3 $m^3$/sec, the flow velocity in the 24" pipe used in the Bruce loop would have been 15.5 m/sec. If this velocity had been less than the velocity needed to obtain dispersed bubble flow, that regime could have been largely supplanted by plug flow. If the flow velocity of 15.5 m /sec had been greater than that needed to obtain dispersed bubble flow, however, the path traversed by the flow conditions at the pump suction on a flow regime map could conceivably have been similar to that shown in Figure 32. As illustrated, the liquid superficial velocity would probably have remained essentially constant until the pump head started to degrade, thereby delaying the transition to plug or slug flow until after that point.

It should be stressed that neither the Mandhane map nor the flow regime transition criteria derived by Taitel and Dukler can be used to obtain quantitative results applying to the suction pipe

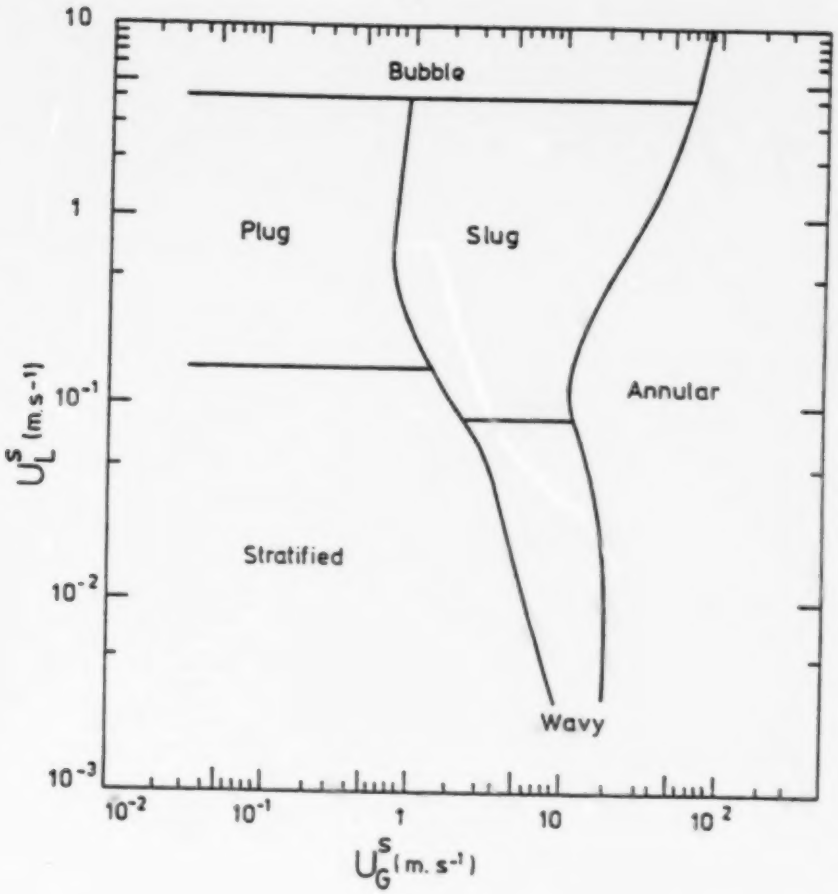


Figure 30 Flow Regime Map Proposed by Mandhane et al. [Ref.39].

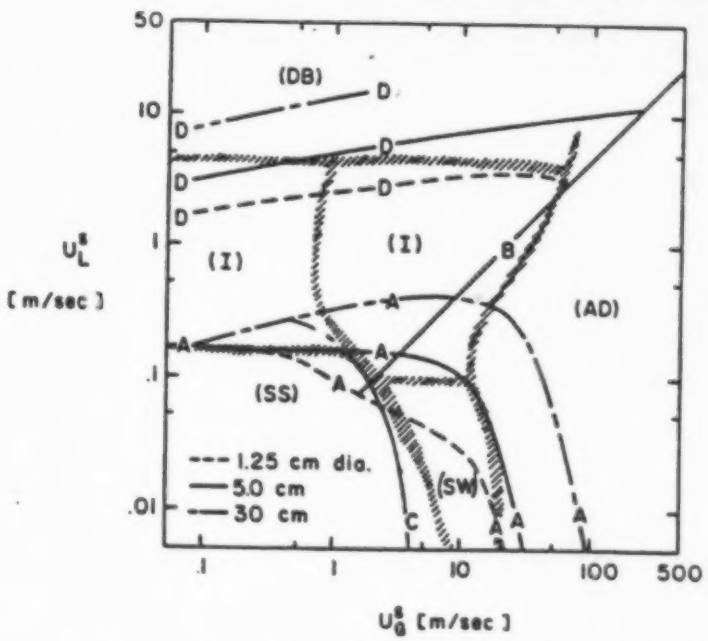


**Flow Regimes**

(AD) - annular with dispersed liquid
(DB) - dispersed bubble
(I) - intermittent (plug and slug)
(SS) - smooth stratified
(SW) - wavy stratified

**Transition Boundaries**

A - (SS) or (SS) to (I) or (AD)
B - (I) or (DB) to (AD)
C - (SS) to (SW)
D - (DB) to (I) (transition of primary interest)

Figure 31 Effect of Pipe Diameter on Transition Boundaries [from Ref.42]

—— air-water, 25°C, 1 atm.
Mandhane et al. [Ref.39]

in the Bruce pump test loop because the suction pipe was neither completely horizontal nor constant area. It's constant area sections (24" and 36") were also too short to permit the flow to become fully developed.

Although it is possible that all of the head pulsations observed in the Bruce pump tests were produced by plug or slug flow passing through the pump, there is at least some evidence to suggest that this was not the case. The head pulsation frequency was observed to change very rapidly from one fairly constant value (plateau) to another in some tests, for instance, suggesting that the acoustic mode which was being excited had changed. During refill in test 68, for example, the head pulsation frequency changed from 1 Hz to 2.2 Hz over a period of about 12 seconds [Ref.8], as shown in Figure 33 (taken from Figure RPTC V-139 in [Ref.8]). As discussed in Section B.2.1 with reference to flow oscillations in a straight pipe connecting two constant head reservoirs, either a quarter wave mode or a half wave mode can be excited in that case depending on which of the two criteria expressed by Equations B.29 and B.30 is satisfied. Thus while there is little doubt that different modes can be excited under different conditions, it is relatively difficult to imagine the frequency of head pulsations produced by plug or slug flow remaining fairly constant up until a period of very rapid change and then stabilizing again after that period.

With reference to the rapid changes in head pulsation frequency observed in some of the Bruce pump tests, Koehler notes [Figure V-106, Ref.8]:

> "It is now assumed that instabilities may occur in several modes and the frequency will depend on which unstable mode is generated. We do know whether instabilities can change from one mode to another or whether several modes can exist".

As noted above, instabilities <u>can</u> change from one mode to another as conditions change. Furthermore, different modes can undoubtedly co-exist and would normally be expected to do so.

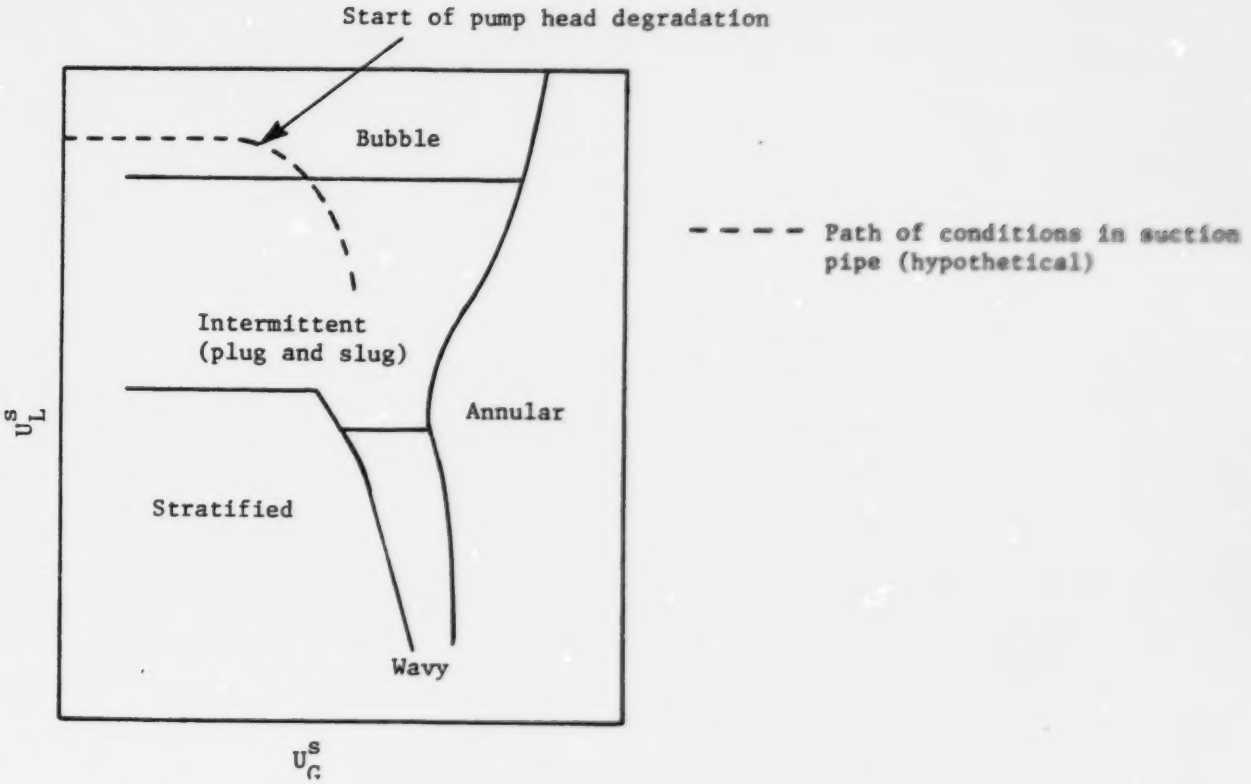


Figure 32 Possible path of conditions in the suction pipe assuming $U_L^s$ is large enough for bubbly flow to be the first flow regime to form.

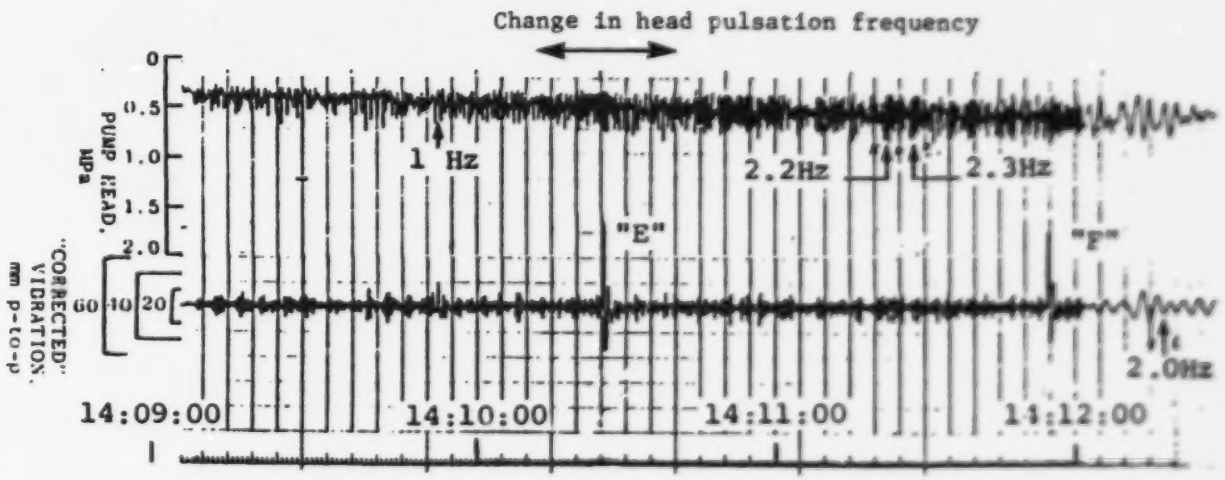


Figure 33 Rapid change in head pulsation frequency observed in Bruce GS A pump test 68 (240°C). Oscillogram was recorded during refill, starting near the time of maximum pipe vibration [from Ref.8].

### C.2.1 Possibility of Mechanical-Hydraulic Interaction

One additional point worthy of mention relates to the possibility that the head pulsations which occurred with a frequency near to the piping fundamental frequency of 1.5 Hz were caused by or at least worsened by the resulting severe pipe vibrations through some sort of mechanical-hydraulic interaction. On this question, it should be pointed out that the pulsations which occurred with a frequency of 1.5 Hz were not any larger in amplitude than the pulsations at other frequencies even though the resulting piping vibrations were the most severe. Thus it is the author's opinion that vibrations of the loop piping did not worsen the head pulsations producing those vibrations significantly, although experiments and/or analysis to confirm this might be worthwhile.

### C.3 Low Temperature Tests

As mentioned previously, head instabilities did not occur at temperatures below 170°C in the Bruce tests. Possible reasons for this are considered separately in subsequent sections, starting with reasons that would apply to any instabilities which occurred at high temperatures because of plug or slug flow and followed by reasons that would apply to any instabilities caused by self-excitation of a low order acoustic mode.

### C.3.1 Reasons for the Cessation of Any Instabilities Caused By Plug or Slug Flow

If some or all of the head instabilities observed in the high temperature Bruce tests had resulted from plug or slug flow passing through the pump, the cessation of those instabilities at low temperatures could have been due to:

a) reductions in the pump suction void fraction needed to produce almost complete head degradation, and/or,

b) decreases in the voided length present upstream of the pump before the pump head became completely degraded.

Possibilities a) and b) are discussed separately below.

### C.3.1.1 Reduction in the Pump Suction Void Fraction Required for Head Degradation

As pressure is reduced, the void fraction at which the head produced by a centrifugal or mixed flow pump starts to degrade decreases because local reductions in pressure within the pump due to flow acceleration, incidence losses, etc. produce larger vapor cavities and hence earlier decoupling of the liquid and vapor phases. The effect of pressure can be seen quite clearly in Figure 34, which shows the normalized head produced by the 1/5 scale model of a KWU PWR pump to which Figure 23 applies, as a function of inlet void fraction for 45% rated flow and pressures ranging from 20 to 69 bars (i.e., 2 to 6.9 MPa). It can be seen that in addition to causing the head to degrade at lower void fractions, reductions in pressure cause the fully degraded head (i.e., the lowest normalized head produced by the pump) to decrease as well.

If the head pulsations observed in the high temperature Bruce pump tests had been produced by plug or slug flow, it is possible that the pulsations did not occur in the low temperature tests because the pump head was severely degraded well before any of the bubbles or pockets of vapor entering the pump became large enough to cause significant variations in pump head. Stated another way, it is possible that the void fraction in the fluid separating any large bubbles in the flow was sufficient to maintain the pump head at a severely degraded value, thereby lessening the effect of the large bubbles. The fluid between large bubbles in plug or slug flow is rarely completely free of vapor bubbles.

### C.3.1.2 Decrease in the Voided Length Upstream of the Pump

In addition to causing changes in pump performance, reductions in loop pressure would also have produced quite dramatic increases in the void gradient at the pump suction and hence a concentration of void at that location. To demonstrate this, it is instructive to examine the case of a pump with a vertical suction pipe in which void starts to form at some distance L below the pump suction due primarily to the decreasing hydrostatic head, as shown in Figure 35. If the void fraction at the pump suction is specified and the momentum and frictional pressure drops in the voided length are assumed to be negligible compared to the gravitational head, the voided length L can be

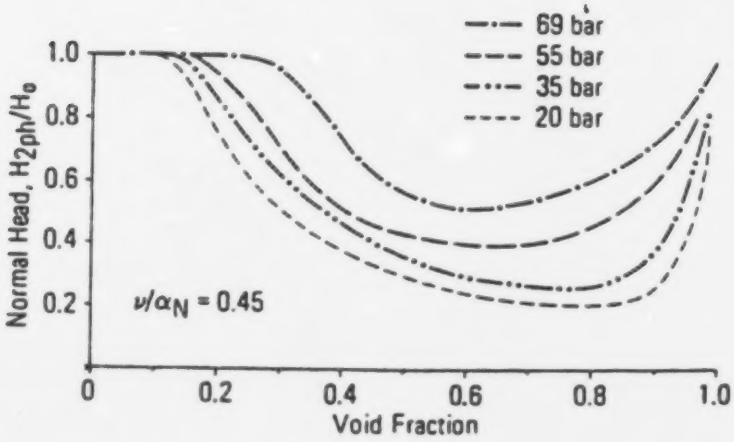


Figure 34 Effect of pressure on the two-phase performance of a 1:5 scale model of a KWU PWR pump at 45% rated flow [from Ref.30].

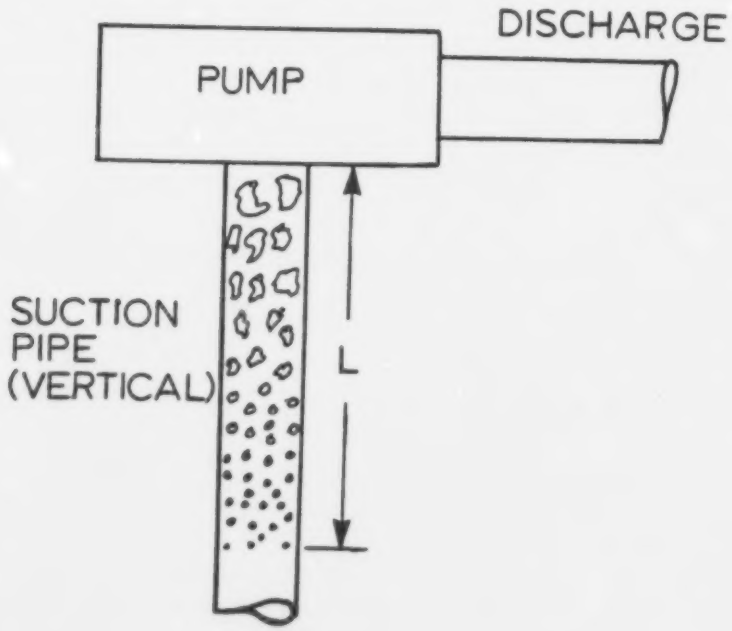


Figure 35 Voided length upstream of the pump suction (L).

calculated in the manner described in Appendix F as a function of pressure (or the corresponding saturation temperature). The results of such calculations are plotted in Figure 36 for an assumed pump suction void fraction of 30%, which is considered to be a reasonable estimate of the void fraction at which the pump head was probably fairly close to being fully degraded, or at least sufficiently degraded to preclude significant head recovery when ingesting largely liquid "slugs" in the plug or slug flow regime, in the low temperature Bruce pump tests.

Although Figure 36 applies strictly to the voided length produced by gravitational head, it can be used with negligible error to estimate the voided length resulting from frictional losses if L is assumed to be the frictional head instead. For instance, it is easily verified that a flowrate of 3.3 $m^3$/sec (Bruce pump design value) in 24" (0.52 m I.D.) pipe (similar to that used in the Bruce loop) would produce a frictional head loss of approximately 0.5 m per meter of pipe length, assuming a friction factor (Darcy) of 0.02. Since L=14 m at 220°C (Figure 36), frictional losses would result in a voided length of 14/0.5 = 28 m at this temperature for the assumed pump suction void fraction of 30%. Flows less than 3.3 $m^3$/sec would result in a smaller frictional head loss per unit length and hence a longer voided length, of course.

Since the vertical pipe leading to the pump suction in the Bruce pump test loop was about 2 m in length, as already mentioned, the horizontal return header would have been virtually void-free in the tests performed at 170°C and below when the pump suction void was less than or equal to 30% according to Figure 36. Since head instabilities did not occur at test temperatures below 170°C, this result suggests that gravitational forces in the horizontal suction pipe and/or centrifugal forces in the 90° pipe bend before the pump could have been instrumental in promoting the instabilities by causing transition to plug or slug flow. It is also probably true to say that if void had not started to form before the end of the 90° bend, the resulting voided length of less than 2 m* would have been insufficient to permit formation of the large vapor bubbles characteristic of the slug flow regime in vertical flow. Head instabilities produced by slug flow would have been impossible in that case.

---

* This voided length corresponds to fewer than four pipe diameters.

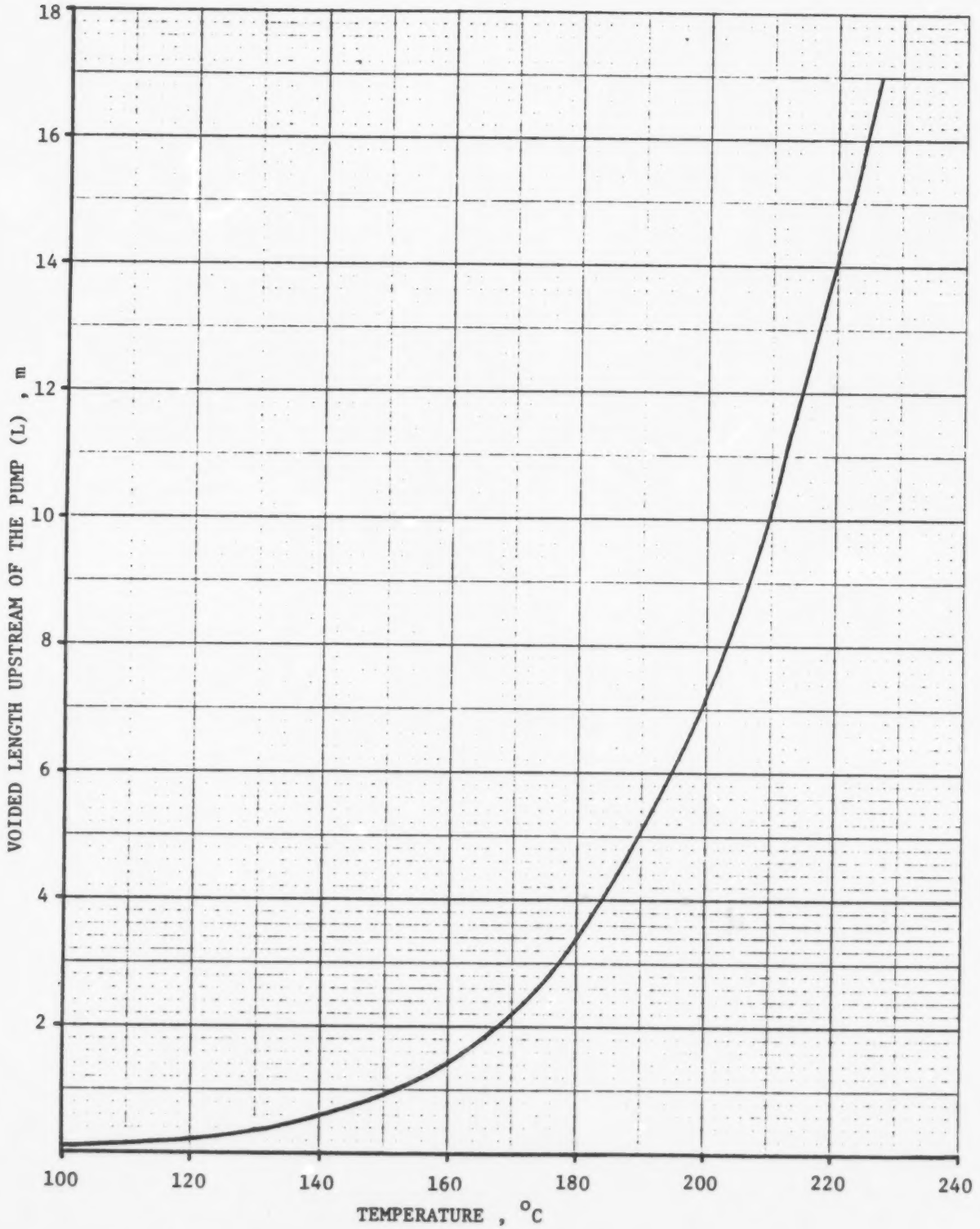


Figure 36 Voided Length Upstream of the Pump vs. Test Temperature. Results Assume Upward Flow in a Vertical Suction Pipe and a Pump Suction Void Fraction of 30%. Friction and Momentum Pressure Losses are Ignored.

### C.3.2 Reasons for the Cessation of Any Instabilities Caused By Self-Excitation of a Low Order Acoustic Mode

If some or all of the head instabilities observed in the high temperature Bruce tests had resulted from excitation of a low order acoustic mode by the pump, the cessation of the instabilities at low temperatures could have been due to:

(a) changes in the pump's two-phase performance characteristics, for instance a reduction in $-\partial V_c/\partial \dot{m}_i$ and/or an increase in $-\partial V_c/\partial p_i$ or $\partial(\Delta p_p)/\partial p_i$, all stabilizing effects assuming the pump's dynamic performance can be represented by Equations 10 and 11 (Section B) for small perturbations.

(b) the concentration of void at the pump suction, and/or

(c) reductions in the sound speed in the voided length of suction pipe to a level less than the flow velocity, inhibiting the excitation of an acoustic mode.

These possibilities are considered separately below.

#### C.3.2.1 Changes in the Pump's Two-Phase Performance Characteristics

With regard to explanation (a) above, it is considered unlikely that $-\partial V_c/\partial \dot{m}_i$ decreased as pressure decreased because hydrodynamic loss (e.g., incidence loss) variations resulting from changes in mass flow would have caused larger rather than smaller changes in $V_c$ at lower pressures. The values of $-\partial V_c/\partial p_i$ and $\partial(\Delta p_p)/\partial p_i$ would have both increased as pressure was reduced, however, thereby stabilizing the flow and offsetting to some extent the effect of any increase in $-\partial V_c/\partial \dot{m}_i$.

#### C.3.2.2 Concentration of Void at the Pump Suction

In their study of surge in boiler feed pumps, Hobson and Marshall [Ref.20] assumed that the cavitation vo[illegible] normally considered to be located within the pump itself was [illegible]ctually located in the inlet pipe immediately upstream of the pump, as shown in Figure 37. By analyzing the stability of the system shown in Figure 37 using the transfer matrix method (see Appendix B), they determined that the system's stability increased as the value of

$-\partial V_c/\partial p_i$ for the cavity increased. That result was in agreement with results obtained by other researchers who assumed the cavitation volume to be located inside the pump, as already noted. The advantage of the analysis of Hobson and Marshall in the present instance is that it shows what would happen if the small cavity shown in front of the pump in Figure 37 was increased in size by adding another cavity of volume $V_c'$ for which $\partial V_c'/\partial \dot{m}_i'$ was zero, as would normally be the case if the additional cavity was a simple accumulator. The only effect of adding the second cavity would be to increase the overall value of $-\partial V_c/\partial p_i$ for the two cavities together to $(-\partial V_c/\partial p_i - \partial V_c'/\partial p_i)$, thereby stabilizing the flow. By this reasoning, the concentration of void at the pump suction in the low temperature Bruce tests could have increased flow stability. Further evidence that a concentration of void at the pump suction probably increases stability is given in the analysis of surge in a simple pipe loop described in Appendix C, where it is shown that surge produced by a positively-sloped pump characteristic is impossible if the only compressible volumes are located at the pump suction and discharge.

Since the two preceding examples of situations in which a compressible volume located at the pump suction increases stability are very specific, it cannot be stated definitively that this would always be true.

### C.3.2.3 Supersonic Flow in the Suction Pipe

The speed of sound in a homogeneous steam-water mixture in thermodynamic equilibrium is shown as a function of saturation temperature in Figure 38 for void fractions of 0.3, 3 and 30%. As indicated, sound speed is not a strong function of void fraction for void fractions in this range.

Figue 38 shows that the flow velocity of 15.5 m/sec corresponding to the Bruce design flow of 3.3 $m^3$/sec in the 24" suction pipe would have exceeded the two-phase sound speed at loop temperatures below approximately 195°C for a void fraction of 30% and 210°C for void fractions less than 3%. When the flow velocity had dropped to say, 10 m/sec because of pump head degradation, the corresponding temperatures would have been roughly 170°C and 186°C respectively. If it is assumed that acoustic flow oscillations could not have developed when the flow in the suction pipe was supersonic, such oscillations would not

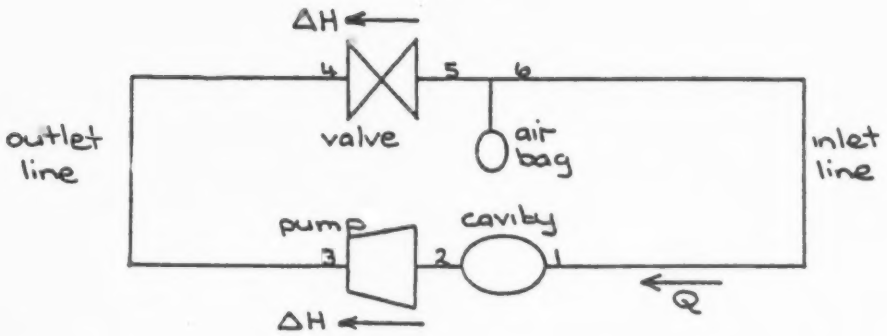


Figure 37 Loop Studied by Hobson and Marshall [Ref.20] With the Cavitation Volume Upstream of the Pump

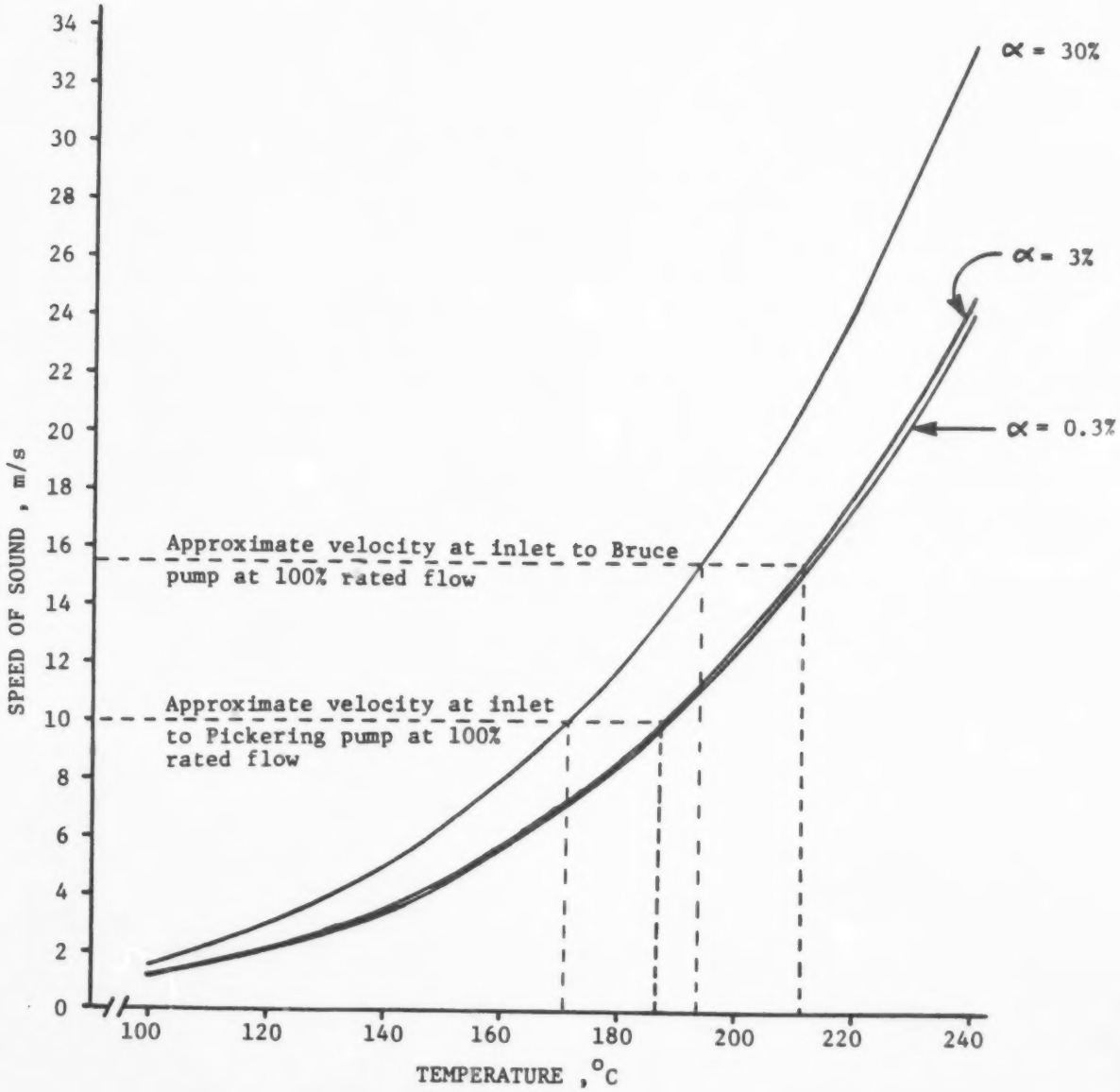


Figure 38 Speed of Sound in a Homogeneous Steam-Water Mixture in Thermodynamic Equilibrium vs. Temperature at Void Fractions of 0.3, 3 and 30%.

have occurred in the tests performed at loop temperatures below approximately 210°C until the flow velocity had dropped below the two-phase sound speed because of pump head degradation. This would have occurred much earlier (i.e., at a higher pump head) in a test performed at, say, 200°C, than in one performed at 170°C, as shown in Figure 39. It is assumed that the pump would have been unable to act as an energy source for flow oscillations once its head had become almost fully degraded, so pulsations would have ceased altogether once the test loop temperature had become low enough.

There is at least some evidence in the limited test data available to the author that the pump head at which head pulsations initiated during draining of the loop decreased as the test temperature decreased, as illustrated in Figure 39. In test 116, for instance, which was performed at a loop temperature of 206°C at 100% rated flow, head pulsations started at a loop average void of less than 2% very shortly after the start of head degradation while the pump head was still high (according to Figures RPTC V-107 and V-114 in [Ref.8]). In test 131, on the other hand, which was performed at 180°C and 80% rated flow, it is believed that head pulsations did not start until the loop average void had reached approximately 11% and the pump differential pressure had dropped to roughly 0.45 MPa or 25% of the pump's single phase (liquid) differential pressure of 1.8 MPa. These conclusions were reached after examining Figures RPTC V-160 to RPTC V-162 in [Ref.8], which show oscillograms recorded during the period of instability in test 131, along with accompanying data on the variations in loop average void and pump head during the test supplied to the author by Ontario Hydro [Ref.15]. Those same data indicate that the pulsations started to diminish at a loop average void fraction of 16-17%, by which time the pump head had dropped to 0.37 MPa.

An oscillogram showing the variations in pump head, suction and discharge annubar readings, etc. recorded during the height of the instabilities in test 131 is given in [Ref.8] as Figure RPTC V-161 and included here as Figure 40. Although scales for the different parameters are not given on the oscillogram, data furnished by Ontario Hydro indicate that the peak-to-peak

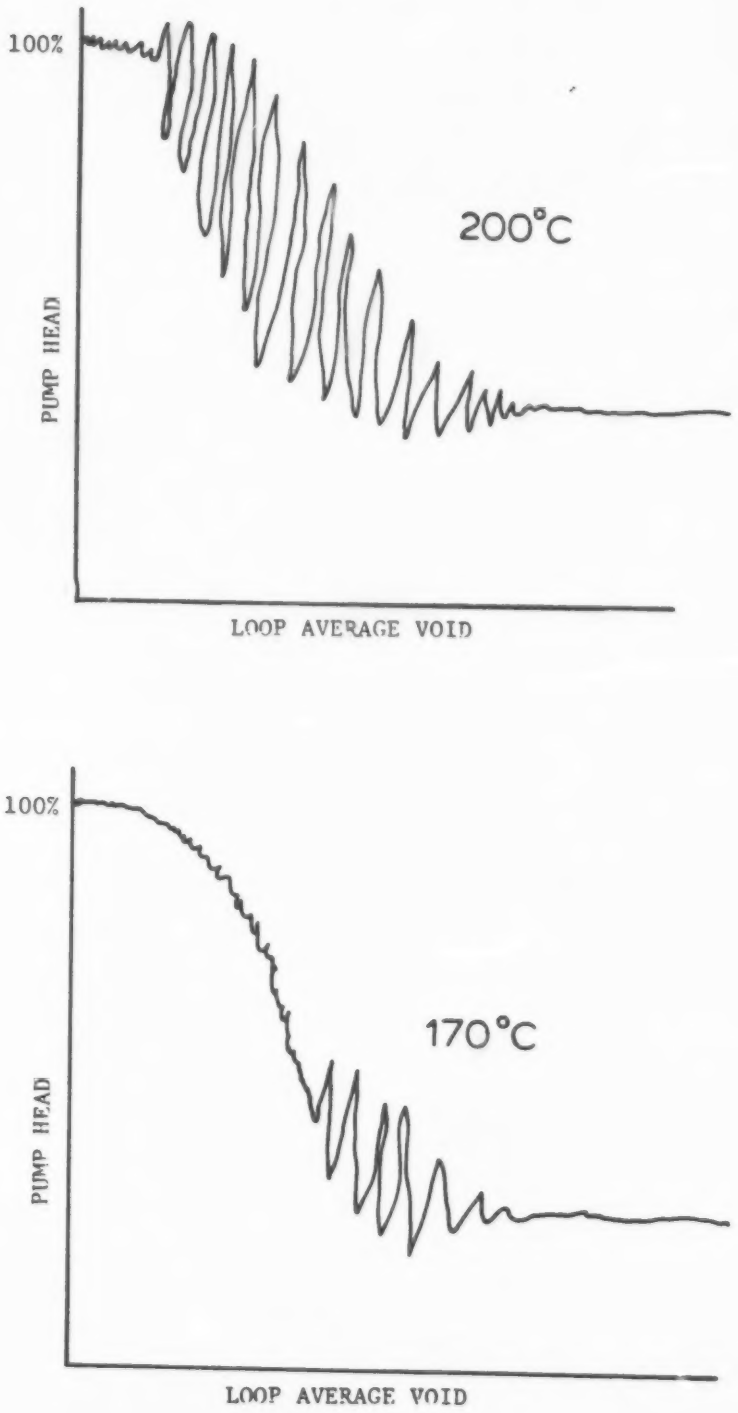


Figure 39 Possible Effect of Test Temperature on the Pump Head at Which Head Pulsations Start.

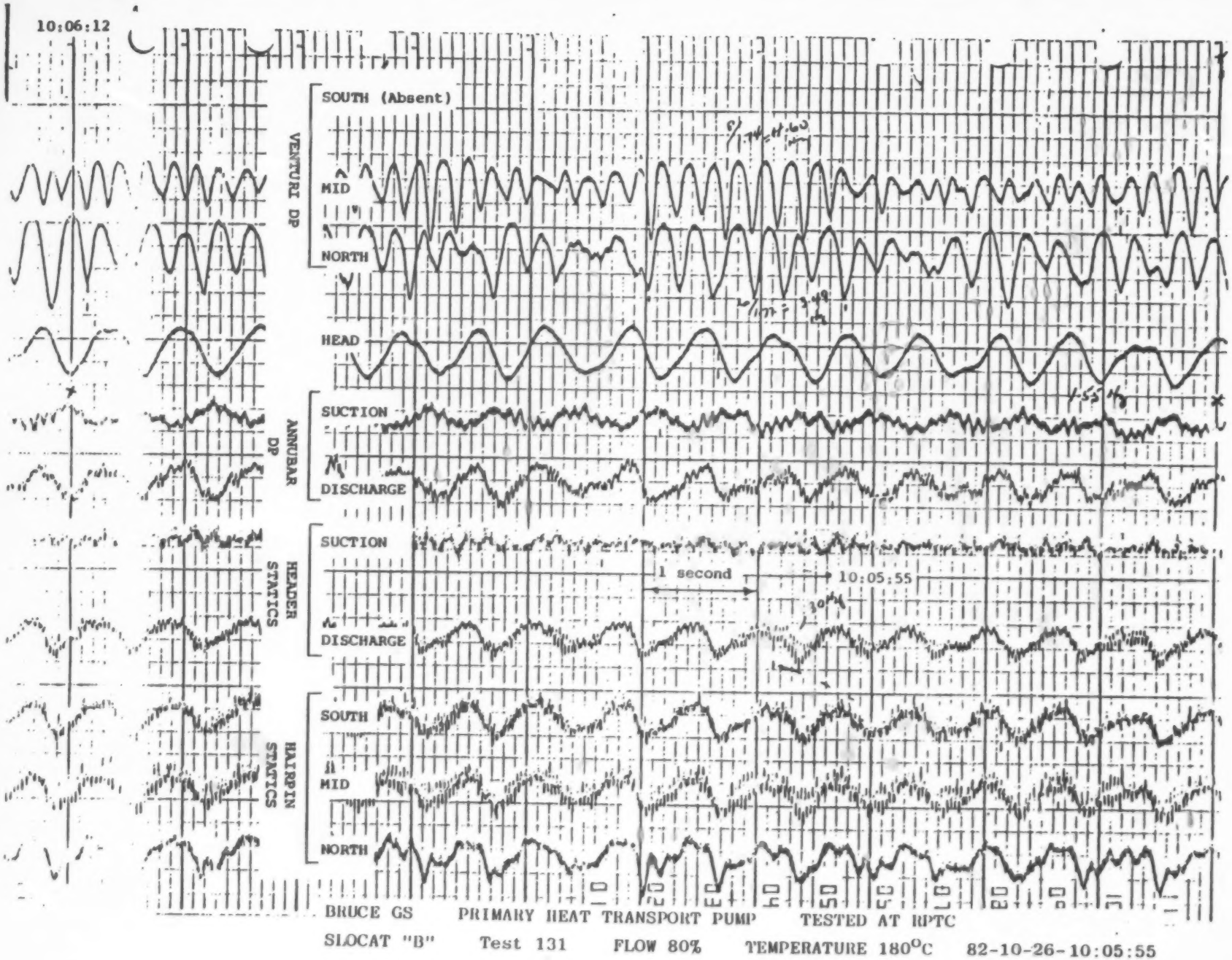


Figure 40 Oscillogram Recorded in Test 131 (Performed at 180°C) [from Ref.8]

amplitude of the head oscillations was approximately 450 kPa and that the flowrate in the discharge pipe ranged from 0.68 to 1.29 $m^3$/sec [Ref.16] at the time the oscillogram was recorded (approximately 10:06). Although these flowrates were calculated from the discharge annubar differential pressure readings by assuming that the flow through the annubar was single phase liquid, the negligible difference in phase between pressures measured at the pump discharge and the tops of the three hairpins (Figure 40) supports that assumption.

Figure 40 shows that both the suction and discharge flowrates (or at least the corresponding annubar readings) varied with the same frequency as the pump head, that is at approximately 1.5 Hz. Although the variations in the suction annubar reading could have resulted from acoustic flow oscillations, they could also have been produced by plug or slug flow. The latter cause is actually the more likely one because the loop average void of 13% that prevailed at the time the oscillogram was recorded was probably high enough to have resulted in virtually the entire suction pipe containing some void. The volume of the suction pipe in the Bruce loop was approximately 7 $m^3$ or 23% of the total loop volume of 30.7 $m^3$, so the abovementioned loop average void of 13% would have corresponded to an average void fraction in the suction pipe of 13/0.23 = 56%. This assumes that the discharge pipe did not contain any void, which was probably the case for the reason given above.

The suction annubar was located slightly less than 1 m upstream of the 90° bend before the pump suction so the flow regime of the flow passing through it would not yet have been modified by the bend. Thus if the periodic variations in the suction annubar reading seen in Figure 40 were produced by plug/slug flow, that flow regime must have formed in the horizontal length of pipe before the bend and the bend probably did not play a significant role in promoting the oscillations. This observation suggests that centrifugal forces in the bend were significantly less important than gravitational forces in the horizontal pipe in producing a flow regime capable of causing flow oscillations, assuming of course that the oscillations shown in Figure 40 resulted from plug/slug flow passing through the pump and not from self-excitation of an acoustic mode.

The manner in which supersonic flow in the suction pipe could have suppressed acoustic flow oscillations without producing head pulsations by a mechanism similar to that resulting from choking of a flow restriction upstream of the pump is not clear, although the absence of a flow restriction (i.e., throat) within direct line of sight of the pump suction in the Bruce loop could have been partly or wholly responsible for this anomaly. Certainly the fact that the pump head at the inception of pulsations in each test appeared to decrease as the loop temperature was lowered does not constitute definite proof of the theory which attributes the cessation of pulsations at temperatures below 170°C to supersonic flow in the suction pipe. The alternate theory which assumes that pulsations only occurred in those tests in which void extended into the horizontal section of the suction pipe explains that result equally well or better. The explanation in this case is that the pump suction void fraction at which the flashing front first entered the horizontal pipe would have increased as the test temperature was lowered, causing a reduction in the pump head at the inception of pulsations.

**C.4 Summary**

Although the results of the analysis of the Bruce pump tests were inconclusive, it appears that the head pulsations observed in the tests probably resulted from plug or slug flow passing through the pump and/or from excitation of a low order acoustic mode by the pump. If both of these possible causes played a role in producing the pulsations, it is likely that the former cause was responsible for the pulsations which occurred when the pump head was low (corresponding to a high pump inlet void fraction) and that the latter produced the pulsations observed when the pump head was high.

The cessation of pulsations at loop temperatures below 170°C probably resulted from a concentration of void at the pump suction. Pulsations due to plug or slug flow would have been impossible in the low temperature tests because the voided length of pipe before the pump would have been too short for plug or

slug flow to have developed* while pulsations due to self-excitation of an acoustic mode could have been inhibited by the concentration of a large part of the system's total capacitance at the pump suction. Low two-phase sound speeds at low loop temperatures could also have played a role.

With regard to the reductions in voided length that would have accompanied reductions in loop temperature, it appears that at temperatures above 170°C, the voided length upstream of the pump probably extended into the horizontal section of the suction pipe before the pump head became completely degraded. Once the flashing front had entered the horizontal section of pipe, the voided length would have increased much more rapidly with increasing loop average void because of the absence of gravitational head losses and probably quickly become long enough to permit the development of slug or plug flow.

---

* Since there were no tests performed between 140°C and 170°C, the temperature below which head pulsations would not have occurred could have been anywhere between these two temperatures. The voided length upstream of the pump would have been extremely short at 140°C, only 0.6m according to Figure 36.

## D. ANALYSIS OF PICKERING PUMP TESTS

### D.1 Introduction

As mentioned in Section A, extremely large head pulsations occurred in the Pickering pump tests performed at test temperatures of 140°C and below but not in the tests performed at 180°C and above. This behaviour was the opposite of that observed in the Bruce tests where head pulsations occurred at test temperatures above 170°C but not below. Possible reasons for this are discussed below.

### D.2 High Temperature Tests

The most obvious explanation for the differences between the results of the high temperature tests of the Pickering and Bruce pumps is that they were caused by differences between the pumps themselves. Although such differences could conceivably explain the absence in the high temperature Pickering tests of any instabilities caused by energization (self-excitation) of a low order acoustic mode by the pump, it is doubtful that they could have prevented head pulsations resulting from plug or slug flow.

Inconsistencies between the results of the Pickering and Bruce pump tests could also have been caused by differences in loop geometry. Although there were some fairly major differences in geometry between the two loops, the difference that was probably most important was that the Pickering pump was preceded by a suction tee (Figure 11) whereas the Bruce pump was not. The suction tee would have tended to homogenize the flow passing through it and thus have prevented plug or slug flow from reaching the pump inlet.

An additional effect of the tee is that the hydraulic losses across it would have caused single phase flow to persist upstream of it until the pump inlet void fraction had reached a fairly high value. The void fraction downstream of the tee at which void would have first appeared upstream is shown as a function of test temperature in Figure 41, which was obtained by assuming a loss coefficient of unity for the tee and an upstream velocity of 10 m/sec. The loss coefficient of unity was estimated from data given by Miller [Ref.43] for flow through a tee with one of the throughflow branches blocked off (as in the Pickering pump tests) while the flow velocity of 10 m/sec corresponds to a flowrate of

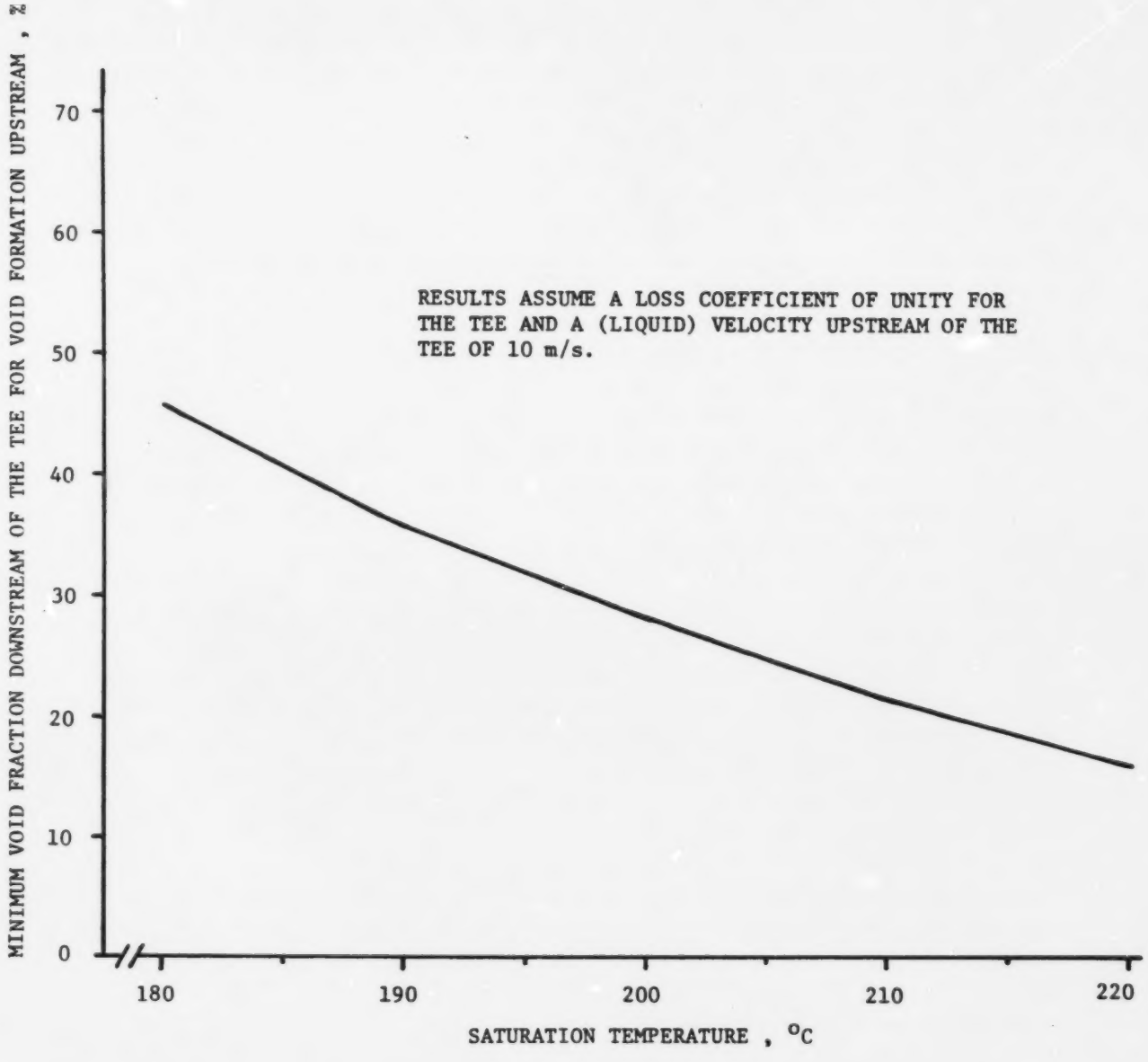


Figure 41 Void Fraction Downstream of the Suction Tee at Which Void First Appears Upstream vs. Saturation Temperature

approximately 0.7 $m^3$/sec in the suction pipe. This flowrate is slightly less than the Pickering pump's design flowrate of 0.765 $m^3$/sec but corresponds closely to the flowrate that was measured in the Pickering pump tests performed at 100°C and 140°C before the pump head started to degrade (see Figures 10-5 and 10-6 in [Ref.11]).

It should be recognized that the velocity of the liquid entering the tee would not have remained at 10 m/sec once the pump head had started to degrade so Figure 41 overestimates the pump suction void fraction at which void would have first formed upstream of the tee. The estimates shown in Figure 41 also ignore the void gradient that would have been present between the tee and the inlet to the pump impeller because of the small hydrostatic head of the intervening fluid, although the hydrostatic pressure gradient would have been offset to some extent by the pressure gradient resulting from a small amount of pressure recovery after the tee. Although the distance from the tee to the impeller inlet is not known exactly, it appears from Figure 11 to be approximately one pipe diameter or about one-third of a meter. The void gradient produced by this small vertical rise could have been significant in some of the low temperature tests, as should be apparent from the voided length estimates shown in Figure 36.

In addition to preventing head pulsations caused by plug or slug flow, the tee could thus also have prevented self-excited acoustic flow oscillations by producing a concentration of void at the pump suction. The effect that such a concentration is believed to have on the stability of flow in a closed loop was discussed in Section C.3.

### D.3 Low Temperature Tests

Because the tee upstream of the pump would have tended to homogenize the flow passing through it, the large head pulsations observed in the low temperature ($\leq$ 140°C) Pickering pump tests were probably not caused by plug or slug flow. Instead, those pulsations probably resulted from:

(a) Choking of the flow between the suction tee and the pump inlet due to low two-phase sound speeds, or

(b) Cavitation within the pump.

These possibilities are considered separately in subsequent sections.

### D.3.1 Instabilities Caused By Choking Between the Suction Tee and the Pump Inlet

When the Pickering loop was depressurized during a test, void would have formed first immediately downstream of the control valve due to pressure recovery after the valve. On further depressurization, void would eventually have formed at the pump suction while the fluid immediately upstream of the suction tee was still single phase liquid. The flow velocity downstream of the tee would have been approximately 10 m/sec in the tests performed at near to 100% rated flow, as mentioned previously. According to Figure 38, this flow velocity would have exceeded the equilibrium two-phase sound speed downstream of the tee at the instant of first void formation when the test temperature was less than approximately 180°C, suggesting that the head pulsations observed in the tests performed at temperatures below 180°C resulted from choking of the flow at the suction tee or at some point in between the tee and the impeller inlet. Since the flow would initially have been quite homogeneous after the tee, the sound speeds indicated in Figure 38 should be applicable in this instance.

According to the scenario just described, pulsations would have started as soon as the pressure at the pump suction reached the saturation pressure at the prevailing test temperature. In test 202, for instance, which was performed at 100°C, the pulsations should have started at a pump suction pressure of approximately 0.1 MPa, as they in fact did seven minutes after the start of the test, as seen in Figure 42. Similar graphs given in [Ref.11] for the tests performed at 140°C and 50°C show that pulsations started the moment the suction pressure reached the saturation value in those tests as well. These results do not constitute proof of the abovementioned choked flow theory, of course, because almost any theory would require that pulsations have started very shortly after the pump suction pressure reached saturation.

The exact manner in which the supersonic and thus unstable bubbly flow downstream of the tee would have broken up (if, in fact, it did so), is not clear at the present time, although it is possible that the anti-rotation vanes shown upstream of the impeller inlet in Figure 11 were instrumental in causing the

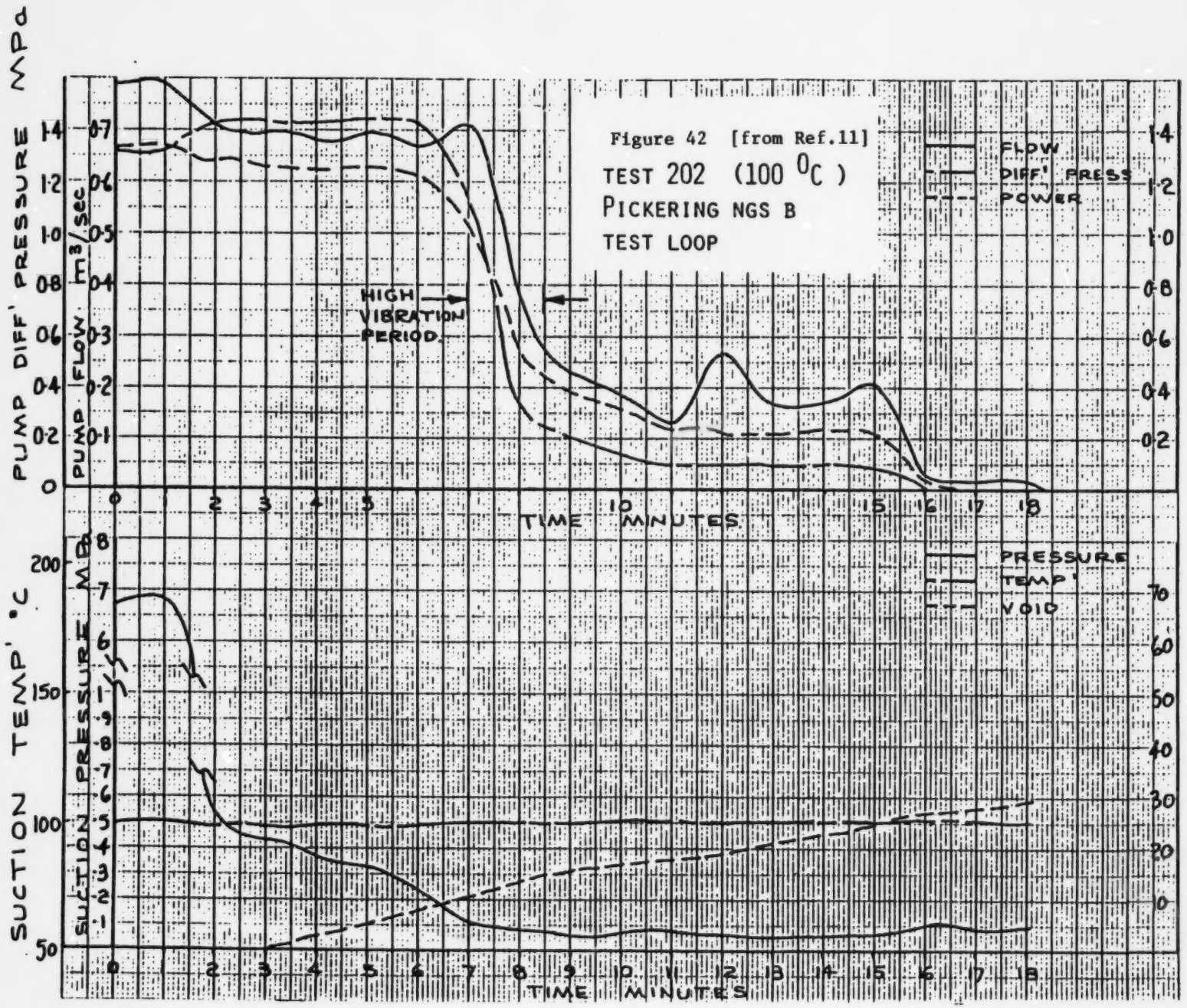


Figure 42 [from Ref.11]
TEST 202 (100 $^{0}$C )
PICKERING NGS B
TEST LOOP

breakdown since the flow would have had to have been subsonic in front of the vanes in order to turn to avoid them. This requirement could have produced a flow pattern consisting of a central core of vapor surrounded by an annulus of liquid with a thickness roughly equal to the length of the vanes. The flow impinging on the vanes would have been subsonic in this case due to the high sound speed in the liquid. There is at least some experimental evidence to support this theory since Hammitt et al. [Ref.35] detected such a flow regime downstream of the throat of a cavitating (and choked) venturi from gamma densitometer measurements even though no flow obstructions similar to the anti-rotation vanes in the Pickering suction pipe were present. Any prerotation of the fluid in the inlet pipe that occurred in spite of the anti-rotation vanes would have assisted in the formation of the abovementioned annular flow pattern since vapor would have formed preferentially in the low pressure core of the prerotation vortex [Ref.20].

Although its significance with regard to the Pickering tests is unclear at the present time, an additional point worth mentioning is that a centrifugal pump would cause the pressure of a supersonic flow to decrease instead of increase as with subsonic flow. It is easily verified that the velocity and void fraction of a two-phase supersonic flow would increase and its pressure decrease as it passed through the pump impeller. This result assumes that the flow remains homogeneous during its passage through the impeller, of course, a proviso that is unrealistic in this instance because homogeneous flow would break down once the void fraction became high enough. The large phase separating accelerations (i.e., Coriolis, centrifugal and streamline curvature [Ref.44]) that are present in a pump impeller would assist in the breakdown.

As noted in Section B.3, flow oscillations produced by choking of a flow restriction upstream of a pump cannot occur in a closed pipe loop unless two vapor cavities are present; one at the pump suction and a second one elsewhere which can accommodate fluid displaced from the first. In the case of the low temperature Pickering pump tests, the vapor cavity that would have been present immediately downstream of the control valve due to

pressure recovery after the valve* could have served as the required second cavity. The volume that this cavity must have occupied in a given test can be estimated from the experimental data for the test by recognizing that it would have accounted for virtually all of the void in the loop up until the time the pump suction pressure reached the saturation pressure for the test temperature in question. In test 202 (100°C), for example, Figure 42 shows that the loop average void at the time the pump suction pressure reached 0.1 MPa (i.e., $P_{sat}$ at 100°C) was slightly greater than 10%, so, with a total loop volume of 2.3 $m^3$ [Ref.11], the volume of void after the valve must have been approximately 0.23 $m^3$. This volume corresponds to roughly 12 diameters of the 12" schedule 80 pipe used downstream of the control valve in the Pickering loop and is significantly less than the volume of the piping located betwen the control valve and the first downstream pipe bend (Figure 13), estimated to be 0.31 $m^3$. If the valve was supercavitating during test 202, this result indicates that the vapor cavity downstream of it probably collapsed before the first pipe bend in accordance with the observation made by Tullis [Ref.36] that such cavities do not remain intact through pipe bends, partially closed valves, etc.

If the control valve had been supercavitating in the low temperature Pickering pump tests, variations in pump head and hence flow** would have had very little effect on the pressure

---

* The pressure recovery after the valve was probably approximately 400 kPa in the Pickering tests performed at 100% rated flow. This can be proven analytically or by noting that the suction pressure vs time curve in Figure 42 changes slope at suction pressures between 0.45 and 0.55 MPa (i.e., about 400 kPa above the saturation pressure of 0.1 MPa at 100°C) just before the loop average void starts to increase. Since similar changes in slope occurred in tests performed at other temperatures (see Figure 10-7 in [Ref.11] for instance), always when the suction pressure was about 400 kPa above saturation, it is assumed that the change in slope corresponds to the onset of void formation after the valve and thus that the pressure recovery was about 400 kPa.

** Note that the flowrate through a choked flow restriction responds to changes in upstream pressure even though changes in downstream pressure have no effect.

downstream of the condensation shock formed at the end of the cavitation cavity. Since the pressure would have been approximately the same as that upstream of the choked suction tee, the flowrate through the tee would have remained fairly constant, thereby creating a situation similar to that which prevailed during the tests of Outa et al. [Ref.23] described previously in Section B.3. Some variation in the pressure upstream of the tee would be expected due to the extreme violence of the head pulsations, of course.

As noted in Section A, the peak-to-peak amplitude of the head pulsations observed in the low temperature Pickering pump tests was occasionally as large as 1 1/2 times the pump's single phase (liquid) head. The most likely explanation for the large pulsation amplitudes is that they resulted from the collapse of void formed in the discharge pipe when the pump head was very low. High pressures would have been produced when the void collapsed following head recovery.

A simplified analysis undertaken to determine the approximate size of the void pocket which is assumed to have been cyclically growing and collapsing at the pump suction during periods of instability in the Pickering pump tests is described in Appendix G. The analysis considers the period in test 202 (Figure 17) during which the frequency of the oscillations and the peak-to-peak amplitude of the variations in pump differential pressure were approximately 4.5 Hz and 1 MPa respectively. (The latter value was chosen instead of the largest peak-to-peak amplitude of 2 MPa because the discharge pipe would probably have been liquid-filled at all times when the peak-to-peak amplitude was 1 MPa but not when it was 2 MPa). The analysis assumes that to a first approximation the flowrate in the discharge pipe varied sinusoidally with time and then applies the momentum equation to the oscillatory flow in the discharge pipe to determine the amplitude of the flow oscillations from the known amplitude of the head pulsations. The oscillatory void volume is then obtained by integrating the oscillatory discharge flowrate over a time interval equal to one-half of the period of the 4.5 Hz oscillations (i.e., 0.5/4.5 = 0.11 sec).

The crude analysis described in Appendix G predicts values of 25% and approximately 5 1 for the peak-to-peak amplitude of the

discharge flowrate expressed as a percentage of the mean flowrate and the oscillatory void volume respectively. Although the amplitude of the flow oscillations is quite high, the size of the resulting oscillatory void volume is very small because the period of the flow oscillations is small. The predicted size of the oscillatory void volume is so small, in fact, it could easily result from the growth and collapse of void contained solely within the pump itself instead of in the pipe upstream of the pump. Thus the flow oscillations observed in the low temperature Pickering tests could have resulted from the growth and collapse of void produced only by cavitation within the pump, as discussed in the next section.

### D.3.2 Instabilities Caused By Cavitation Within the Pump

Due to the hydrostatic head in the vertical suction pipe of the Pickering pump, vapor would have formed within the pump itself due to cavitation before it formed at any other location in the loop, excluding the region of pressure recovery after the control valve. At low temperatures, the decrease in pump head at the onset of cavitation would have been much more dramatic than at high temperatures [Ref.45], particularly if the void produced by cavitation had caused the flow to choke at some point within the pump due to the low two-phase sound speed. Assuming the flow velocity at the point where cavitation initiated was approximately equal to the flow velocity in the suction pipe, cavitation choking of the pump could have occurred at temperatures below about 180$^{o}$C at 100% rated flow for the reasons given in the preceding section. The above assumption regarding the flow velocity at the point of cavitation inception is not an unrealistic one because flow velocities in the impeller eye (where cavitation usually starts) and the suction pipe are generally similar.

If the drop in pump head due to cavitation had occurred abruptly, the resulting rapid deceleration of the flow in the loop would have caused the pressure immediately after the control valve to decrease and that at the pump suction to increase. These pressure changes would in turn have caused the void after the control valve to grow and the cavitation void within the pump to collapse, resulting in a recovery of pump head. The pump would then have started to cavitate again, starting a new cycle of flow oscillations.

Flow oscillations produced by the scenario just described would not have been self-sustaining (i.e., self-excited) unless the dynamic performance characteristics of the cavitating pump were such that it supplied the energy necessary to maintain the oscillations, as described in Section B.2. In view of the large number of instances in which cavitating turbopumps have exhibited such characteristics, however, it would not be surprising if the Pickering pump also exhibited them at low temperatures.

If the flow oscillations observed in the low temperature Pickering pump tests were self-excited, they probably involved primarily the lowest order acoustic mode. Such self-excited oscillations would have continued indefinitely if bleeding of the lop had been halted, causing the thermalhydraulic conditions to remain unchanged. If the flow oscillations were not self-excited and thus not self-sustaining but instead were feeding off of the kinetic energy of the flow in the loop as it slowed down, they probably still involved primarily the lowest order acoustic mode because that would have been the most easy mode to excite. Prediction of the oscillation frequency in either case would require the dynamic performance characteristics of the pump under cavitating and/or two-phase flow conditions.

The above theory ascribes the change in behaviour between the high temperature ($\geq 180^{o}C$) and the low temperature ($\leq 140^{o}C$) Pickering pump tests to a change in the pump's cavitation or two-phase performance characteristics. Because reductions in temperature would have increased the volume of void produced within the pump due to pressure reductions resulting from flow acceleration, hydraulic losses (e.g., incidence losses), etc. and thereby have increased the pump's sensitivity to changes in flowrate and pressure, the fact that instabilities only occurred at low temperatures is at least in accord with what one would expect. It was noted in Section B.2 that $-\partial V_c/\partial \dot{m}_i$ should increase as temperature is reduced, for instance, resulting in decreased stability. Further evidence of the effect of temperature on pump stability is given by Shafer and Simon [Ref.45], who state that "at elevated temperatures pump performance is much less sensitive to cavitation than at low temperatures".

If cavitation within the pump produced the instabilties observed in the low temperature Pickering tests, the absence of such

instabilities in the low temperature Bruce tests could have been due to the higher specific speed of the Bruce pump since a pump's sensitivity to cavitation decreases with increasing specific speed. In particular, the head produced by a high specific speed pump decreases much less rapidly with decreasing suction pressure once cavitation has started than the head produced by a lower specific speed design. With regard to the head reduction that occurs when the suction pressure is reduced after the onset of cavitation, Rao [Ref.47] notes:

"The abrupt drop for low specific speed pumps can be explained by considering the fact that the inlet passages are the narrowest for the lowest specific speed pumps, and get choked easily under moderate cavitation. In axial flow pumps, which have the highest specific speeds, the inlet passages are very large, and are not easily choked completely. Hence the gradual drop of the curves for pumps of higher specific speed".

The lessened sensitivity of high specific speed pumps to cavitation does not mean that such pumps cannot have dynamic performance characteristics capable of producing self-excited flow oscillations, of course, since even the axial flow inducers used in liquid-fueled rocket motor pumps have exhibited such characteristics, as noted previously. The more gradual head reduction exhibited by a high specific speed pump after the onset of cavitation would better explain the absence of instabilities in the low temperature Bruce tests if the instabilities in the low temperature Pickering tests had resulted from the abruptness of the head drop off after cavitation had started. The instabilities would then have been caused by the scenario described previously in which the abrupt drop in head at the start of cavitation caused the flow in the loop to decelerate, the cavitation void in the pump to collapse, etc. As noted previously, such an instability would not necessarily have been self-sustaining.

### D.3.3 Other Effects

In addition to the effects already considered to explain why instabilities occurred only at low temperatures in the Pickering tests, the shedding of vapor cavities from the anti-rotation vanes shown upstream of the pump inlet in Figure 11 could also have played a role in producing the instabilities. Since the vanes and the flow impinging on them would have been misaligned

because of swirl introduced into the flow by the suction tee and the preceding bends,* as well as a small amount of prerotation, there is a good possibility that they acted as a source of fairly large vapor cavities. This observation applies particularly to low loop temperatures, where hydraulic losses resulting from the misalignment would have resulted in greater vapor production than at high temperatures.

Prerotation of the fluid in the inlet pipe of a pump increases as the difference between the flowrate through the pump and the design flowrate increases [Ref.46], so this effect at least would have resulted in increased misalignment between the flow and the anti-rotation vanes and thus presumably increased shedding of vapor when the flowrate through the pump decreased (provided the flowrate was less than design). This could have caused the pump head to decrease as flowrate decreased (because of the increase in pump inlet void fraction) and/or have produced a negative value of $\partial V_c / \partial \dot{m}_i$ for the cavity in front of the pump, both destabilizing effects as mentioned previously.

Although the preceding observations concerning the possible effect of anti-rotation vanes assume that vapor cavities are shed from the vanes themselves due to vortex formation and flow separation, additional vapor production could also result from increased incidence losses at the impeller inlet. According to Stepanoff [Ref.46], the fitting of anti-rotation vanes to a pump increases incidence losses and worsens cavitation resulting from those losses by preventing the flow impinging on the impeller vanes from prerotating so as to lower the angle of attack. The combined effect of vapor cavities shed from the anti-rotation vanes and increased vapor production due to worsened flow incidence onto the impeller vanes (Figure 24) would have been more likely to produce a positively-sloped pump head versus mass flow characteristic and/or a negative value of $\partial V_c / \partial \dot{m}_i$ than either effect alone.

---

* It is well known that two 90° out-of-plane right-angle bends, such as those located upstream of the suction tee in the Pickering loop, cause severe swirl.

Although speculative, the foregoing observations suggest that vanes, tees, bends, etc., located close to the inlet to a pump could have a significant effect on its performance under cavitating or two-phase flow conditions. It is possible, then, that such piping elements or obstructions should be duplicated in tests aimed at determining a pump's steady-state or dynamic performance under such conditions.

**D.4 Summary**

Differences between the results of the Pickering and Bruce pump tests were probably caused by differences in loop geometry, particularly in the vicinity of the pump suction, and/or differences between the performance characteristics of the two pumps under cavitating or two-phase flow conditions. The most likely explanation for the absence of head pulsations in the tests performed at high ($\geq$ 180°C) temperatures is that the suction tee upstream of the pump inlet homogenized the flow passing through it, thereby preventing plug or slug flow from reaching the pump. A less likely explanation is that the concentration of void at the pump suction due to hydraulic losses across the tee inhibited the development of acoustic flow oscillations in some manner.

The violent head pulsations that occurred in the Pickering tests performed at loop temperatures of 140°C and below were probably caused either by choking of the flow at some point between the suction tee and the pump inlet or by a change in the pump's cavitating or two-phase performance characteristics between 140 and 180°C. Such a change could have caused either self-excited flow oscillations or transitory oscillations that would not have been self-sustaining. It is assumed that such transitory oscillations would have resulted from the abruptness of the head drop produced by cavitation at low temperatures. Choking of the flow within the pump at the point of cavitation inception could have been responsible for the above-mentioned change in pump behaviour.

It is also conceivable that the instabilities were produced by a sound speed-related phenomenon other than choking, since large hydraulic losses and hence extensive vapor production would have occurred at the pump inlet if shock waves had formed on the antirotation vanes upstream of the inlet and/or on the

leading edges of the impeller blades.

Of the different explanations offered for the instabilities observed in the low temperature tests of the Pickering pump, the one which attributes the instabilities to cavitation and perhaps cavitation choking within the pump is considered the most likely.

It is considered extremely unlikely that the instabilities observed in the low temperature Pickering pump tests resulted from the passage of slug or plug flow through the pump because the suction tee would have tended to homogenize such flow regimes before they reached the pump inlet, as noted previously. In addition, the voided length upstream of the pump would have been too short in the low temperature tests for plug or slug flow to have developed, as should be apparent upon examination of Figure 36.

## E. CONCLUSIONS

It has been shown that instabilities can occur in a pump/piping system under two-phase conditions due to:

(a) plug or slug flow passing through the pump
(b) intermittent voiding of the pump impeller, as observed by Murakami and Minemura [Ref.18]
(c) self-excitation of a low order acoustic mode, with the pump acting as the exciter, and
(d) choking of a flow restriction upstream of the pump.

Of causes (a) - (d) above, cause (a) was identified as the one most likely to have produced the pump head instabilities observed in the Bruce pump tests performed at temperatures above 170°C, although cause (c) could also have been responsible for some of the instabilities, particularly those that occurred when the pump head was high.

It was also concluded that a concentration of void at the pump suction was the most probable cause of the cessation of head instabilities that occurred in the Bruce pump tests when the test temperature was reduced below 170°C since such a concentration would have inhibited the development of acoustic flow oscillations and caused the voided length upstream of the pump to have been too short to permit the development of plug or slug flow. It was determined that in the tests performed at temperatures above 170°C, which were the tests in which head instabilities occurred, the voided length upstream of the pump would have extended into the horizontal return header before the pump head became fully degraded and thus probably have been quite long owing to the absence of the gravitational head component that would have been dominant when the void was restricted to the roughly 2m length of vertical pipe upstream of the pump. Plug or slug flow could have formed at a very low void fraction in the horizontal return header once the liquid superficial velocity became low enough.

It was concluded from the analysis of the Pickering pump tests that the suction tee upstream of the pump probably played a major role in preventing head pulsations in the tests performed at temperatures of 180°C and above. Head pulsations caused by plug or slug flow would have been prevented because the tee would have homogenized such flows before they reached the pump, while the

concentration of void at the pump suction produced by hydraulic losses across the tee would probably have inhibited the development of acoustic flow oscillations.

It was also concluded that the large head pulsations observed in the low temperature ($\leq$ 140°C) tests of the Pickering pump probably resulted from:

(a) choking of the flow between the suction tee and the pump inlet due to low two-phase sound speeds, or,
(b) cavitation within the pump.

Cause (a) is suspected because the flow velocity downstream of the tee at 100% rated flow would have exceeded the two-phase sound speed of the mixture produced by flashing at that point when the test temperature was below approximately 180°C*. Cause (b) could have produced either self-excited (acoustic) flow oscillations or oscillations which were not self-sustaining, depending on the pump's performance characteristics under cavitating conditions. Oscillations which were not self-sustaining could have been caused by the abruptness of the head drop produced by cavitation at low temperatures.

The absence of instabilities resulting from cavitation in the low temperature Bruce tests could have been due to the higher specific speed of the Bruce pump since high specific speed pumps are less affected by cavitation than ones of lower specific speed.

The instabilities observed in the low temperature Pickering tests could also have been produced by a sound speed-related phenomenon other than choking since large hydraulic losses and hence extensive vapor production and flow redistribution would have occurred at the inlet if shock waves had formed on the anti-rotation vanes upstream of the pump and/or on the leading edges of the impeller blades.

---

* Although instabilities were only observed in the tests performed at temperatures of 140°C and below, the temperature separating the temperature ranges for stable and unstable operation could equally well have been 180°C because no tests that could indicate otherwise were performed between 140 and 180°C.

Of the different explanations offered for the instabilities observed in the low temperature Pickering tests, the one which ascribes the instabilities to cavitation or cavitation choking within the pump is considered the most likely. This explanation can be modified to include most of the others mentioned, however, by considering the suction tee and the short length of pipe between the tee and the pump inlet to be effectively part of the "pump". The more general and all encompassing explanation of the low temperature instabilities that results from this modification is that they were caused by cavitation or sonic choking due to cavitation within the pump/suction tee assembly. Such cavitation could have produced self-excited flow oscillations involving a low order acoustic mode or simply transitory ones, as already mentioned.

Combining the pump and suction tee for the purpose just described is a logical simplification in any event since the presence of the suction tee approximately one pipe diameter upstream of the inlet to the pump impeller probably modifies the cavitation characteristics of the pump for the reasons noted in Section D.3.3.

It was concluded that the instabilities observed in the low temperature Pickering pump tests could not have been caused by the ingestion of plug or slug flow by the pump.

## F. RECOMMENDATIONS

The analysis of the results of the Bruce and Pickering pump tests indicates that some of the more specific results of those tests can probably be attributed to specific geometric features of the loops in which the tests were performed. In the case of the Bruce pump tests, for instance, it is believed that head instabilities did not occur in the tests performed at temperatures below 170°C because the flashing front did not enter the horizontal return header (where plug or slug flow could have developed under less restrictive conditions than in vertical flow) until the pump head was essentially fully degraded. Provided this explanation is correct, head instabilities would have occurred at temperatures below 170°C if the vertical pipe upstream of the pump had been shorter.

In the case of the Pickering pump tests, the suction tee appears to have been important.

In view of the preceding observations, it is recommended that an experimental program be initiated to investigate the effect of suction pipe geometry on the stability of flow in a closed pipe loop. The geometry of the discharge pipe should be kept as simple as possible to reduce the number of extraneous variables; only one control valve should be used, for instance, at least in the initial tests.

Tests should be performed with and without a suction tee (with one of the throughflow branches blocked off, as in the Pickering pump tests) and with different lengths of vertical pipe upstream of the pump. A length of horizontal pipe should be provided upstream of the vertical pipe and the diameter of all pipes should be as large as the budget allows to minimize scaling effects, although not so large that the measurement of void fraction with a gamma densitometer becomes difficult.

Provision should be made for depressurizing the loop by the method used in the Bruce and Pickering pump tests so as to duplicate the experimental procedure followed in those tests as closely as possible. If possible, the tests should be performed with steam-water over the full range of temperatures and pressures investigated in the Bruce and Pickering pump tests, although complementary flow-visualization studies using R-12 or R-114 should be contemplated since the plug and slug flow regimes

in horizontal flow would be relatively easy to detect in a facility with a transparent suction pipe, as would supercavitation of the control valve. The flow-visualization facility would be relatively inexpensive, of course, since it would be designed to operate at much lower pressures than the steam-water facility. The possibility of using a fully transparent pump (such as the one built by AECL and tested by Davis Engineering [Ref.31]), or at least a pump with a transparent front cover, should also be investigated.

The test loop should be equipped with annubars at the pump suction and discharge to measure the flowrates at those locations. The flow in the discharge pipe will probably be single phase liquid except under conditions of severe surging so the discharge annubar should give a reliable indication of the discharge flowrate most of the time. The suction annubar will not give a reliable indication of the flowrate at the inlet to the pump under two-phase conditions but should provide at least qualitative information about how the flow is varying with time.

If possible, the test loop should be equipped with two multi-beam gamma densitometers; one at the pump suction to determine the void fraction and flow regime at that point and another that could be traversed along the horizontal part of the suction pipe, primarily to obtain information about the flow regime. Although a turbine meter could conceivably be used in conjunction with the gamma densitometer at the pump suction to obtain an approximate measurement of the flowrate at that point under two phase conditions (since it would likely be easier to use for that purpose than the annubar), the inertia of the rotor would make measurement of the flowrate under transient conditions difficult.

If the control valve was installed at the upstream end of the horizontal length of suction pipe, the traversing gamma densitometer could be used to check for supercavitation of the control valve and to detect changes in the length of the resulting vapor cavity downstream of the valve.

Instrumentation will be required to measure the pressure at the pump discharge as well as at enough points in the suction pipe to resolve any standing wave that might be present. By locating pressure transducers along the length of the suction pipe, it should be possible to distinguish true surge resulting from dynamic instability from surge produced by plug or slug flow

passing through the pump because a significant standing wave should be present over the voided length of the suction pipe in the former case but not in the latter. It should be mentioned that it would probably be much more difficult to distinguish between these two causes of instabilities by locating pressure transducers along the length of the discharge pipe because large travelling waves* would be present in the discharge pipe in either case. Although a standing wave would be superimposed on the travelling wave if the oscillations resulted from true surge, it would be difficult to detect because the travelling wave would be relatively large.

Two pumps with different specific speeds should be tested in the loop to obtain at least some indication of the importance of pump geometry. The pumps should be fitted with anti-rotation vanes similar to those found on the Bruce and Pickering PHT pumps.

The head pulsations that occurred in the Pickering pump tests performed at temperatures of 140°C and below was occasionally as large as 1 1/2 times the single-phase pump head, as mentioned previously. Since pulsations of that magnitude could conceivably cause severe damage to the piping in a nuclear generating station, particularly if they occurred at a frequency that was closely matched to the fundamental frequency of vibration of the station's piping, it is the author's opinion that tests to identify the most probably cause of those pulsations should be given the highest priority. The possibility that the instabilities were caused by a sound speed related phenomenon (e.g., choking of the flow before or within the pump)

---

* Since standing waves are produced by identical waves travelling in opposite directions, they cannot transport energy from one point in a pipe to another. Energy is transported by travelling waves, however, since these are single waves which travel down a pipe in one direction. In the case of true surge in a pipe loop in which a pump is acting as the exciter, energy added to the oscillating flow by the pump is transported to the valve (where it is dissipated) by travelling waves. These waves travel down both the suction and the discharge pipe, although numerical simulations performed by the author indicate that they are largest in the pipe (suction or discharge) with the highest sound speed. Although standing waves are also present in both pipes, they do not transport any energy from the pump to the valve.

should be investigated first by designing the experiments to obtain flow which was supersonic downstream of the suction tee and within the passages of the pump impeller after the first appearance of void at those locations. If the loop was designed so that the design velocity after the tee was 10 m/sec, for instance, the flow would be supersonic at that location after the first appearance of void when the test temperature was less than approximately 180°C, as in the Pickering pump tests.

To investigate the possibility that the abovementioned pulsations were caused by choking of the flow at the inlet to the pump, provision should be made for inserting a constant head reservoir into the loop immediately downstream of the control valve. If choking occurred, the flowrate and pressure upstream of the suction tee (which could both be measured) would remain essentially constant in that case just as conditions remained essentially constant upstream of the choked orifice in the tests of Outa et al. [Ref.23].

Shock waves could be detected by performing detailed pressure measurements in the vicinity of the inlet to the pump.

Lastly, tests should be performed to obtain the steady-state and dynamic performance characteristics of full-scale Bruce and Pickering PHT pumps under cavitating and two-phase flow conditions. Although such tests would be very costly, they would furnish data that is badly needed to analyze a wide variety of hypothetical accidents. The pump's dynamic performance characteristics under cavitating conditions could be determined by performing tests similar to those described by Ng et al. in [Ref.22].

**REFERENCES**


1. Burchett, P.R., Brown, N.G. and Lyons, R.G., Ontario Hydro Research Center Pump Test Complex Heat Transport Pump Test Loop Facility, Ontario Hydro Design and Development Division Report 80262.

2. Tait, A.C., Review of Work Progress and Programs in 1980-81 at the Pump Test Complex, Ontario Hydro Research Division Report 81-45-K, 2/03/81.

3. Tait, A.C., Review of Work Progress and Programs in 1981-82 at the Pump Test Complex, Ontario Hydro Research Division Report 82-77-H, 26/02/82.

4. Burchett, P.R. and Sauve, R.G., Report on Pipe Vibration During Simulated Loss of Coolant Test On Bruce Pump at Kipling Avenue, Ontario Hydro Design and Development Division Report 82194.

5. Burchett, P.R. and Ellis, P.J., Assessment of Primary Heat Transport System Pump Operation During A LOCA, Ontario Hydro Design and Development Division Report 82197, 1982.

6. Stevens, T. Moffat, D.B. and Lin, T.C., Frequency Response Analysis of PHT Pump Test Loop, Bruce GS 'A' and Pickering GS 'B' PHT Piping Systems Under Loss-of-Coolant Accident Conditions, Ontario Hydro Design and Development Division Report 82236, 1982.

7. Koehler, H.P., Small Break Loss-of-Coolant Accident Test: Bruce NGS 'A' PHT Pumpset: Rotor, Hydraulic and Pipe Vibration, Ontario Hydro Research Division Report 82-239-H, 16/07/82.

8. Koehler, H.P., Simulated Loss-of-Coolant Accident Tests: Bruce NGS 'B" Pumpset: Rotor, Hydraulic and Pipe Vibration, Ontario Hydro Research Division Report, B83-64-H, 14/10/83.

9. Lin, T.C., Frequency Response Analyses of Bruce GS B PHT Pump Discharge Piping System Under Loss-of-Coolant Accident Conditions, Ontario Hydro Design and Development Division Report 83260, June 1983.

10. Boyd, J.M., Simulated Loss-of-Coolant Accident Tests: Pickering NGS 'B' PHT Pumpset: Rotor, Hydraulic and Pipe Vibration, Ontario Hydro Research Division Report 83-483-H, 12/12/83.

11. Lockett, J.C., Toong, T. and Burchett, P.R., Pickering NGS 'B' Assessment of Primary Heat Transport Pump Loss-of-Coolant Accident Tests, Ontario Hydro Design and Development Division Report 83328, 1983.

12. Fogarty, J.P. and Sauve, R.G., Frequency Response of Pickering NGS 'B' Primary Heat Transport Pump Test Loop, Ontario Hydro Design and Development Division Report 83292, 1983.

13. Guthrie, B.M. and Currie, T.C., Primary Pump Vibration Under Accident Conditions, W.R. Davis Engineering Report #C83-155, AECB Report # INFO 0168, June 1984.

14. Rivkin, S.L., Aleksandrov, A.A. and Kremenevskaya, E.A., Thermodynamic Derivatives for Water and Steam, V.H. Winston & Sons, 1978.

15. Burchett, P. (Ontario Hydro), Personal Communication to T. Currie, September 1984 - March 1986.

16. Boyd, J.M. (Ontario Hydro), Personal Communication to T. Currie, February 1986 - March 1986.

17. Heidrick, T.R. and Hancox, W.T., Centrifugal Pump Behaviour in Steady and Transient Steam-Water Flows, Polyphase Flow in Turbomachinery, ASME Winter Annual Meeting, 1978, Published by ASME, pp.139-156.

18. Murakami, M. and Minemura, K., Effects of Entrained Air on the Performance of a Centrifugal Pump, Bulletin of the JSME, Vol.17, No.110, 1974, pp.1047-1055.

19. Greitzer, E.M., The Stability of Pumping Systems, ASME Journal of Fluids Engineering, Vol.103, June 1981, pp.193-242.

20. Hobson, D.E. and Marshall, A., Surge in Centrifugal Pumps, Proceedings of the 6th Conference on Fluid Machinery, Vol.1, Budapest, 1979, pp.475-484.

21. Brennen, C.E. and Braisted, D.M., Stability of Hydraulic Systems With Focus on Cavitating Pumps, Proceedings of the 10th IAHR Symposium, Tokyo, Japan, 1980, pp.255-265.

22. Ng, S.L. and Brennen, C.E., Experiments on the Dynamic Behaviour of Cavitating Pumps, ASME Journal of Fluids Engineering, Vol.100, June 1978, pp.166-176.

23. Outa, E., Tajima, K. and Kobayakawa, H., Low Frequency Oscillation of Centrifugal Pump Discharge Due to Cavitation Choking at an Inlet Contraction, Proceedings of the 10th IAHR Symposium, Tokyo, Japan, 1980.

24. Keenan, J.H., Keyes, F.G., Hill, P.G. and Moore, J.G., Steam Tables, John Wiley & Sons, 1969.

25. Rogers, G.F.C. and Mayhew, Y.R., Engineering Thermodynamics, Work and Heat Transfer, 3rd ed., Longman, 1980.

26. VonNimitz, W.W., Low Frequency Vibrations at Centrifugal Plants, Proceedings of 4th Turbomachinery Symposium.

27. Wylie, E.B. and Streeter, V.L., Fluid Transients, McGraw-Hill Inc., 1978.

28. Rothe, P.H. and Runstadler, P.W., First-Order Pump Surge Behaviour, ASME Paper 77-WA/FE-12.

29. Rothe, P.H., Runstadler, P.W., and Dolan, F.X., Pump Surge Due to Two-Phase Flow, Polyphase Flow in Turbomachinery, ASME Winter Annual Meeting, 1978, published by ASME.

30. Kastner, W. and Seeberger, G.J., Pump Behaviour and Its Impact On A Loss-of-Coolant Accident in a Pressurized Water Reactor, Nuclear Technology, Vol.60, February 1983, pp.268-277.

31. Kim, J.H. and Belloni, P., On Centrifugal Pump Head Degradation in Two-Phase Flow, paper submitted to the Symposium on Design Methods for Two-Phase Flow in Turbomachinery, ASME Fluids Engineering Division Conference, Albuquerque, New Mexico, June 1985.

32. Hancox, W.T. and Banerjee, S., Numerical Standards for Flow Boiling Analysis, Nuclear Science and Engineering, Vol.64, 1977, pp.106-123.

33. Mathers, W.G., Zuzak, W.W., McDonald, B.H. and Hancox, W.T., On Finite-Difference Solutions to the Transient Flow Boiling Equations in Transient Two-Phase Flow, Proc. of the Committee for Safety of Nuclear Installations (CSNI) Specialists Mtg., Toronto 1976, Printed by AECL, pp.278-315.

34. McGee, G.E., Ardron, K.H. and Hobson, N., The Effect of Scale on the Behaviour of Centrifugal Pumps in Steam-Water Flow, Whiteshell Nuclear Research Establishment, Atomic Energy of Canada Ltd.

35. Hammitt, F.G., Robinson, J.M. and Lafierty, J.F., Choked-Flow Analogy for Very Low Quality Two-Phase Flows, Nuclear Science and Engineering, Vol.29, 1967, pp.131-142.

36. Tullis, P.J., Choking and Supercavitating Valves, Journal of the Hydraulics Division, ASCE, December 1971, HY12, pp.1931-1945.

37. Rogers, J.T., Two-Phase Vertical Up-Flow Regime Boundaries and Interphase Drag Models for Advanced Thermohydraulic Codes, Department of Mechanical and Aeronautical Engineering Report (prepared for the CEGB), Carleton University, August, 1985.

38. Ontario Hydro Research Report #83.420 (Graph 28).

39. Mandhane, J.M., Gregory, G.A. and Aziz, K., A Flow Pattern Map for Gas-Liquid Flow in Horizontal Pipes, Int. J. Multiphase Flow, Vol.1, 1974, pp.537-553.

40. Weisman, J., Duncan, D., Gibson, J. and Crawford, T., Effects of Fluid Properties and Pipe Diameter on Two-Phase Flow Patterns in Horizontal Lines, Int. J. Multiphase Flow, Vol.5, 1979, pp.437-462.

41. Pearce, D.L., Two-Phase Flow Regimes in Horizontal Tubes: An Experimental Investigation of Flow Regimes in Refrigerant-12, Paper presented at the European Two-Phase Flow Group Meeting, Paris, 1982.

42. Taitel, Y. and Dukler, A.E., A Model for Predicting Flow Regime Transitions in Horizontal and Near Horizontal Gas-Liquid Flow, AIChE Journal, Vol.22, No.1, January 1976, pp.47-55.

43. Miller, D.S., Internal Flow Systems, Published by BHRA Fluid Engineering, 1978.

44. Currie, T.C., A Study of Two-Phase Flow in Centrifugal Pump Impellers, Davis, Eryou and Associates Ltd. Report #79-290-1, April 1979.

45. Shafer, C. and Simon, C., Experimental Investigation of the Cavitation Behavior of Boiling Water Reactor Coolant Pumps, Kraftwerk Union, Germany.

46. Stepanoff, A.J., Pumps and Blowers: Two-Phase Flow, John Wiley & Sons, 1965.

47. Rao, N.S., Cavitation, Publication No.147, Central Board of Irrigation and Power, New Delhi, December 1980.

# APPENDICES

## APPENDIX A: COMPARISON OF THE WORK REQUIRED TO ISENTROPICALLY COLLAPSE THE VOID IN A TWO-PHASE MIXTURE WITH THE WORK REQUIRED TO COMPRESS LIQUID WATER BETWEEN THE SAME INITIAL AND FINAL PRESSURES

The work and pressure rise required to isentropically collapse the void in a homogeneous steam-water mixture with an initial void fraction ($\alpha$) of 25% at 3.344 MPa (saturation temperature = 240°C) will be calculated in this appendix and compared to the work required to compress liquid water to the same final pressure. At 3.344 MPa, the properties of saturated steam (g) and water (f) are [23],

$$v_f = 0.001229 \ m^3/kg$$

$$v_g = 0.05976 \ m^3/kg$$

$$h_f = 1037.32 \ kJ/kg$$

$$h_{fg} = 1766.5 \ kJ/kg$$

$$s_f = 2.7015 \ kJ/kg \ K$$

and

$$s_{fg} = 3.4422 \ kJ/kg \ K$$

For $\alpha = 0.25$, the quality (x) of the mixture is,

$$x = \left[\frac{v_g}{v_f}\left(\frac{1-\alpha}{\alpha}\right) + 1\right]^{-1}$$

$$= 0.006808$$

and its enthalpy and entropy are,

$$h = h_f + x h_{fg} = 1049.35 \ \frac{kJ}{kg}$$

and

$$s = s_f + x s_{fg} = 2.7249 \ \frac{kJ}{kgK}$$

Since $s_f = 2.7249 \frac{kJ}{kgK}$ when $p = 3.497$ MPa, the differential pressure $\Delta p$ required to isentropically condense the initial void in the mixture is

$$\Delta p = 3.497 - 3.344 \text{ MPa} = 153 \text{ kPa}$$

Also, since $h_f = 1049.54 \frac{kJ}{kg}$ when $s_f = 2.7249 \frac{kJ}{kgK}$ (p=3.497 MPa) the work required to isentropically collapse the void ($W_g$) is,

$$W_g = 1049.54 - 1049.35 = 0.19 \frac{kJ}{kg}$$

The work $W_f$ that would be needed to isentropically compress saturated liquid water over the same pressure range (i.e., from 3.344 MPa to 3.497 MPa) can be obtained approximately from the expression [24],

$$W_f = v_f \Delta p = 0.001229 \times 153$$
$$= 0.188 \text{ kJ/kg}$$

Thus the work required to compress a steam-water mixture with 25% void from an initial pressure of 3.344 MPa to a pressure at which all of the void has been condensed (i.e., 3.497 MPa) is negligibly different from the work required to compress liquid water between the same two pressures, essentially because of the low initial quality.

## APPENDIX B: ANALYSIS OF PUMP SURGE IN A PIPE CONNECTING TWO RESERVOIRS

Dynamic instability criteria (i.e., criteria which must be satisfied in order for surge to occur) and surge frequencies will be derived for a pumping system consisting of a single pump and a single valve in a constant area pipe connecting two constant head reservoirs, as shown in Fig.B.1. The pump and valve are assumed to be located at opposite ends of the pipe,

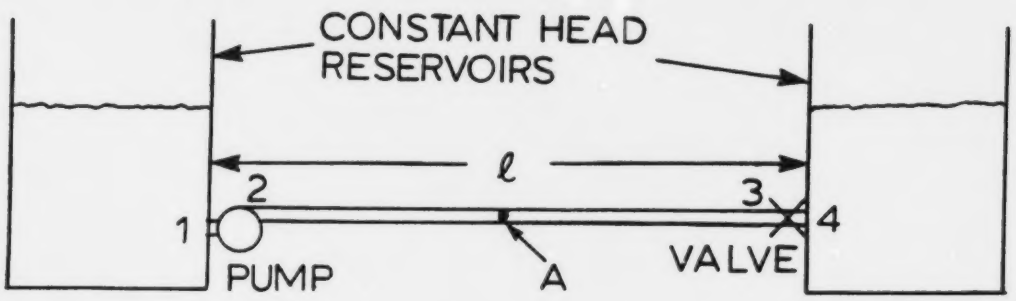


Fig.B.1: Pipe Connecting Two Constant Head Reservoirs

which has length ℓ and cross-sectional area A. The sound speed in the pipe, a, is assumed to be constant and uniform and much greater than the flow velocity V.

The stability of the simple piping system shown in Fig.B.1 will be analyzed using the transfer matrix method [25]. Essentially, this method associates a transfer matrix with each component (e.g., pipe, pump, valve) in a piping system relating the oscillatory head and flow rate downstream of the component to the same parameters upstream of it. By multiplying together the transfer matrices for the different components in a piping system, the total system transfer matrix relating the above mentioned oscillatory flow parameters at the system's inlet to those at its discharge can be obtained and the system's dynamic behaviour determined.

The transfer matrix for a constant area pipe in which the speed of sound is constant can be derived by applying the continuity and momentum

equations for the flow in the pipe. If the oscillatory head (H') and flowrate (Q') are assumed to be harmonic, it can be shown that the particular solution for the oscillatory head (H') must be of the form [25],

$$H' = e^{st} (C_1 e^{\gamma x} + C_2 e^{-\gamma x}) \tag{B.1}$$

where s = the complex frequency

$$= \sigma + i\omega \tag{B.2}$$

and $C_1$ and $C_2$ are complex constants which depend on the oscillatory head and flow at the beginning and end of the pipe (x is distance along the pipe). The constant $\gamma$ is the propagation constant defined by the expression,

$$\gamma^2 = Cs\,(Ls + R) \tag{B.3}$$

in which

C = the capacitance of the fluid in the pipe

$$= \frac{gA}{a^2} \tag{B.4}$$

L = the inertance of the fluid in the pipe

$$= 1/gA. \tag{B.5}$$

and

R = the linearized resistance/unit length

$$= \frac{f\bar{Q}}{g\,DA^2} \tag{B.6}$$

with

f = the friction factor for the flow

D = pipe diameter

A = pipe cross-sectional area

$\bar{Q}$ = mean volumetric flowrate

Similarly, it can be shown that the oscillatory flow (Q') must be defined by the expression [25],

$$Q' = \frac{-Cs}{\gamma} e^{st} (C_1 e^{\gamma x} - C_2 e^{-\gamma x}) \tag{B.7}$$

Equations (B.6) and (B.7) can be rewritten as,

$$H'(x,t) = \hat{H}(x) e^{st} \tag{B.8}$$

and

$$Q'(x,t) = \hat{Q}(x) e^{st} \tag{B.9}$$

where the complex quantities $\hat{H}(x)$ and $\hat{Q}(x)$ are defined by the expressions,

$$\hat{H}(x) = C_1 e^{\gamma x} + C_2 e^{-\gamma x} \tag{B.10}$$

$$\hat{Q}(x) = \frac{-1}{Z_c} (C_1 e^{\gamma x} - C_2 e^{-\gamma x}) \tag{B.11}$$

with,

$$Z_c = \gamma / Cs \tag{B.12}$$

At any position x in the pipe, the physical oscillations about the mean head and flowrate are the real parts of Eqs. (B.8) and (B.9).

If the upstream and downstream ends of the pipe under consideration are identified with subscripts u and D respectively, the integration constants $C_1$ and $C_2$ can be expressed in terms of $\hat{H}_u$ and $\hat{Q}_u$ at x=0 as,

$$C_1 = \frac{1}{2} (\hat{H}_u - Z_c \hat{Q}_u) \tag{B.13}$$

and

$$C_2 = \frac{1}{2} (\hat{H}_u + Z_c \hat{Q}_u) \tag{B.14}$$

Substituting Eqs.(B.13) and (B.14) into Eqs.(B.10) and (B.11), we obtain,

$$\hat{H}(x) = \hat{H}_u \cosh \gamma x - Z_c \hat{Q}_u \sinh \gamma x \tag{B.15}$$

and

$$\hat{Q}(x) = \frac{-\hat{H}_u}{Z_c} \sinh \gamma x + \hat{Q}_u \cosh \gamma x \tag{B.16}$$

If $\hat{H}(x)$ and $\hat{Q}(x)$ at the end of a pipe of length $\ell$ are designated $\hat{H}_D$ and $\hat{Q}_D$ respectively, Eqs.(B.15) and (B.16) yield,

$$\begin{Bmatrix} \hat{H}_D \\ \hat{Q}_D \end{Bmatrix} = \begin{bmatrix} \cosh \gamma\ell & -Z_c \sinh \gamma\ell \\ \frac{-1}{Z_c} \sinh \gamma\ell & \cosh \gamma\ell \end{bmatrix} \cdot \begin{Bmatrix} \hat{H}_u \\ \hat{Q}_u \end{Bmatrix}$$

$$= \left[F_{pipe}\right] \cdot \begin{Bmatrix} \hat{H}_u \\ \hat{Q}_u \end{Bmatrix} \qquad \text{(B.17)}$$

The matrix $F_{pipe}$ in Eq.(B.17) is the transfer matrix for the pipe. Further details on how $F_{pipe}$ is derived can be found in reference [25]. If the pump behaves quasi-steadily, it can be shown that its transfer matrix ($F_{pump}$) is [25],

$$F_{pump} = \begin{bmatrix} 1 & M_p \\ 0 & 1 \end{bmatrix} \qquad \text{(B.18)}$$

when the slope of its head vs. flow curve (i.e., dH/dQ) at the nominal operating point ($\bar{Q}$) is $M_p$. Similarly, the transfer matrix for a valve ($F_{valve}$) is,

$$F_{valve} = \begin{bmatrix} 1 & -M_v \\ 0 & 1 \end{bmatrix} \qquad \text{(B.19)}$$

when the slope of the valve's resistance vs. flow curve at the nominal operating point is $M_v$. Note that if the head difference across the valve ($\Delta H_v$) is related to the flowrate Q by the expression,

$$\Delta H_v = KQ^2 \quad \text{(K is the valve's loss coefficient)} \qquad \text{(B.20)}$$

then $M_v$ becomes

$$M_v = \left.\frac{d(\Delta H_v)}{dQ}\right|_{\bar{Q}} = 2K\bar{Q} = \frac{\overline{2\Delta H_v}}{\bar{Q}} \tag{B.21}$$

since $K = \frac{\overline{\Delta H_v}}{\bar{Q}^2}$ from Eq.(B.20) ($\overline{\Delta H_v}$ is the head difference across the valve when $Q = \bar{Q}$).

Using the transfer matrices given above, the complex head and flowrate at point 4 in Fig.B.1 (i.e., $\hat{H}_4$ and $\hat{Q}_4$) can be expressed in terms of the same parameters at point 1 ($\hat{H}_1$ and $\hat{Q}_1$) as,

$$\begin{Bmatrix} \hat{H}_4 \\ \hat{Q}_4 \end{Bmatrix} = [F_{valve}] \cdot [F_{pipe}] \cdot [F_{pump}] \begin{Bmatrix} \hat{H}_1 \\ \hat{Q}_1 \end{Bmatrix}$$

$$= [T] \cdot \begin{Bmatrix} \hat{H}_1 \\ \hat{Q}_1 \end{Bmatrix} \tag{B.22}$$

The first equation represented by Eq.(B.22) can be written as,

$$\hat{H}_4 = T_{1,1} \cdot \hat{H}_1 + T_{1,2} \cdot \hat{Q}_1 \tag{B.23}$$

Since the head in the reservoirs at the ends of the pipe is constant,

$$\hat{H}_1 = \hat{H}_4 = 0$$

and Eq.(B.23) indicates that we must have

$$T_{1,2} = 0 \tag{B.24}$$

in order to obtain a non-trivial solution (i.e., a solution other than $\hat{Q}_1 = 0$). Since $T_{1,2}$ is complex (i.e., $T_{1,2} = \text{Re}\,(T_{1,2}) + \text{Im}\,(T_{1,2})$) we require that

$$\text{Re}\,(T_{1,2}) = 0 \tag{B.25}$$

and

$$\text{Im}\,(T_{1,2}) = 0 \tag{B.26}$$

yielding two equations for the two unknowns $\sigma$ and $\omega$.

It will be assumed for simplicity that the flow in the pipe is frictionless (i.e., that R=0). With this assumption, it can be shown using Eqs.(B.17), (B.18) and (B.19) that

$$\text{Re}\,(T_{1,2}) = \left(\frac{M_v M_p}{Z_c} - Z_c\right) \sinh\frac{\sigma\ell}{a} \cos\frac{\omega\ell}{a} + (M_p - M_v) \cosh\frac{\sigma\ell}{a} \cos\frac{\omega\ell}{a} \tag{B.27}$$

and

$$\text{Im}\,(T_{1,2}) = i\left[\left(\frac{M_v M_p}{Z_c} - Z_c\right) \cosh\frac{\sigma\ell}{a} \sin\frac{\omega\ell}{a} + (M_p - M_v) \sinh\frac{\sigma\ell}{a} \sin\frac{\omega\ell}{a}\right] \tag{B.28}$$

Also, $Z_c = a/gA$ in this case.

Equations (B.25) and (B.26) were solved numerically with different values assigned to the coefficients $(M_v M_p/Z_c - Z_c)$ and $(M_p - M_v)$ in Eqs.(B.27) and (B.28) in order to determine the conditions under which surge will occur, that is the values of the coefficients which give $\omega > 0$ (i.e., an oscillatory solution) and $\sigma \geq 0$ (i.e., oscillations which grow with time). From those analyses, it was determined that surge will occur at frequencies ($\omega$) of approximately $n\pi a/2\ell$ (n=1,3,5...), when

$$(M_v - M_p) > \left(\frac{M_p M_v}{Z_c} - Z_c\right) > 0 \tag{B.29}$$

and with frequencies of approximately $n\pi a/\ell$ (n=1,2,3,...) when

$$\left(\frac{M_p M_v}{Z_c} - Z_c\right) > (M_v - M_p) > 0 \tag{B.30}$$

The frequencies $n\pi a/2\ell$ (n=1,3,5,...) are the frequencies of the quarter-wave acoustic modes shown in Fig. B.2a while the frequencies $n\pi a/\ell$ apply to the half-wave acoustic modes shown in Fig. B.2b. Although the pump is located at a pressure node (velocity loop) in both cases, the valve is located at a velocity node when a quarter-wave mode is excited and a velocity loop when a half-wave mode is active.

Usually surge involves primarily the lowest order acoustic mode [26], which is the first quarter-wave mode (with $\omega = (\pi/2)a/\ell$)

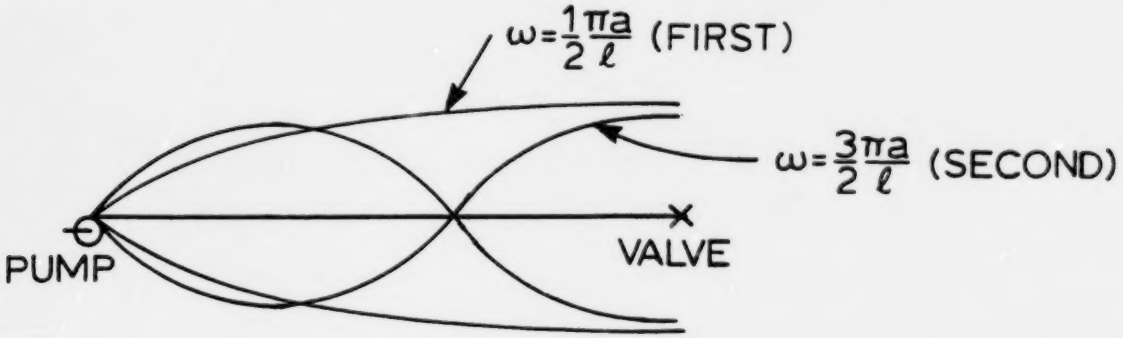


Fig.B.2a: Quarter-Wave Modes.

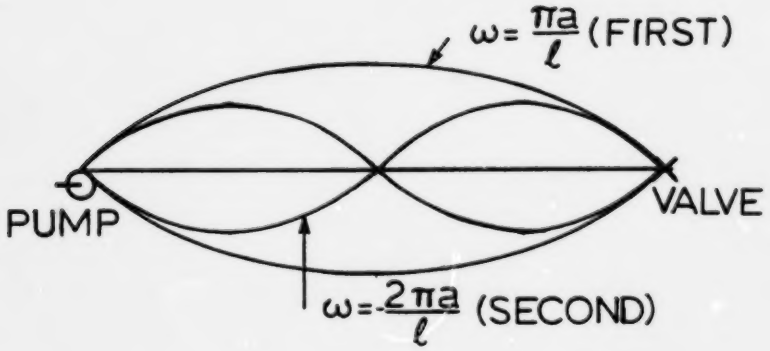


Fig.B.2b: Half-Wave Modes.

in this case. Since pressure and hence density changes are maximal at the valve for this mode, its lumped parameter representation would have an accumulator (i.e., compressible volume) located at the valve, as shown in Fig.B.3, and the fluid flowing through the system would be considered incompressible.

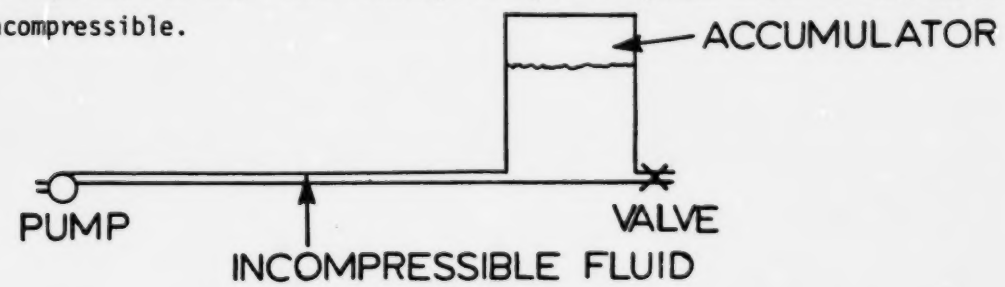


Fig.B.3: Lumped-Parameter Representation of the First-Quarter Wave Acoustic Mode in a Straight Constant-Area Pipe.

Rothe and Runstadler [27] examined the stability of the simple lumped parameter system shown in Fig.B.3 and concluded that the system would be dynamically unstable for

$$2\sqrt{M_v^2 - M_v M_p} > \frac{M_p M_v}{y} - y > 0 \tag{B.31}$$

and that the corresponding surge frequency would be approximately,

$$\omega = y \frac{gA}{\ell} \tag{B.32}$$

where

$$y = \frac{1}{g} \sqrt{\frac{P_N \ell}{\rho V_N A}} \tag{B.33}$$

with

$P_N$ = the nominal pressure of the gas in the accumulator

$V_N$ = the nominal volume of the gas in the accumulator

and

$\rho$ = the density of the fluid in the pipe.

Comparing Eq.(B.31) to Eq.(B.29), it is apparent that the two equations will predict the same minimum requirement for unstable operation (i.e., $\frac{M_p M_v}{Z_c} - Z_c > 0$ or $\frac{M_p M_v}{y} - y > 0$), if,

$$y = Z_c = a/gA \tag{B.34}$$

Since Rothe and Runstadler assumed that the gas compression process would be isothermal, the speed of sound (a) in Eq.(B.34) should be obtained from the expression,

$$a = \sqrt{\left.\frac{dP}{d\rho}\right|_T} \tag{B.35}$$

instead of the expression

$$a = \sqrt{\left.\frac{dP}{d\rho}\right|_S}$$

normally used. For isothermal compression of the gas in the accumulator,

$$PV = P_N V_N$$

so

$$dP = - \frac{P_N V_N}{V^2} dV$$

$$\simeq - \frac{P_N}{V_N} dV \qquad (B.36)$$

for small changes in volume.

The change in the total mass of fluid in the piping system resulting from the change dV in the gas volume is

$$dm = - \rho dV$$

so the change in the average density of the fluid in the piping system is

$$d\rho = \frac{dm}{V_{tot}} = - \frac{\rho dV}{A\ell} \qquad (B.37)$$

assuming $V_{tot} \simeq A\ell$, where $V_{tot}$ is the total volume of the piping system.

Using Eqs.(B.36) and (B.37), the effective speed of sound in the piping system can be written as,

$$a = \sqrt{\frac{dP}{d\rho}\Big|_T}$$

$$= \sqrt{\frac{P_N A\ell}{\rho V_N}} \qquad (B.38)$$

so

$$a = y\, gA \qquad (B.39)$$

from Eq.(B.33), or

$$y = \frac{a}{gA} = Z_c.$$

Thus the minimum requirements for unstable operation given by Eqs.(B.29) and (B.31) are equivalent. Substituting Eq.(B.39) into Eq.(B.32), we obtain

$$\omega = \frac{a}{\ell} \tag{B.40}$$

as the surge frequency predicted by the lumped parameter model. This frequency is 36% less than the frequency of the first quarter-wave acoustic mode, i.e., $\frac{\pi}{2}\frac{a}{\ell}$ .

It is not surprising that the upper limit of $\frac{M_p M_v}{Z_c} - Z_c$ seen in Eq.(B.29) (i.e., $M_v - M_p$) does not agree with that given in Eq.(B.31) because the former represents only the value of $\frac{M_p M_v}{Z_c} - Z_c$ at which the type of mode that is excited changes from quarter-wave to half-wave, not the value above which the system is no longer dynamically unstable, as in the latter case.

## APPENDIX C: ANALYSIS OF SURGE IN A SIMPLE PIPE LOOP

The dynamic instability criterion and surge frequency for first order surge in the simple piping system shown in Fig.C.1 will be obtained in this appendix. As illustrated, the loop of interest consists of a single pump and a single valve connected by constant area discharge and suction pipes of lengths $\ell_1$ and $\ell_2$ respectively. The sound speeds in the discharge and suction pipes (i.e., pipes 1 and 2) are assumed to be constant at $a_1$ and $a_2$ respectively.

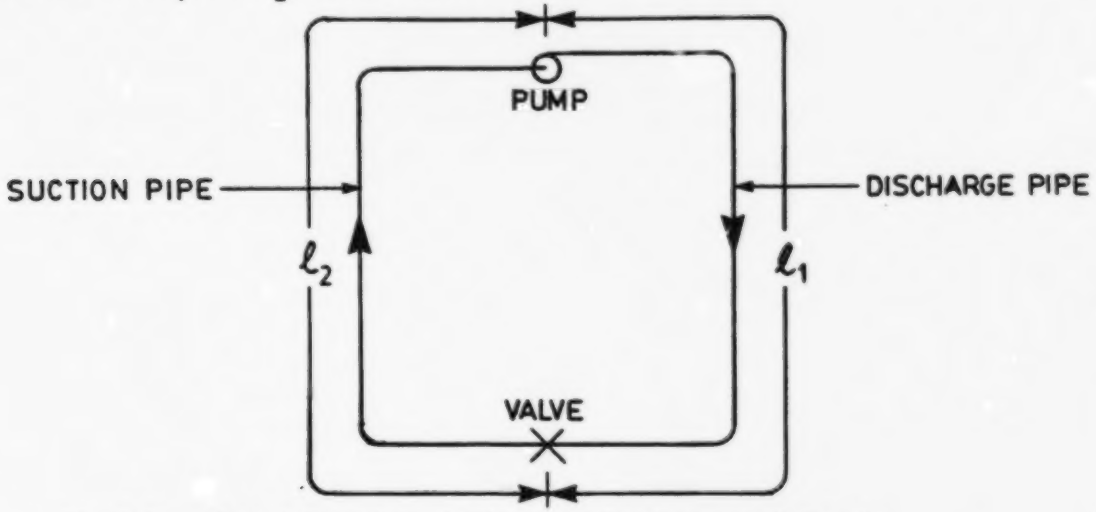


Fig.C.1: Closed Pipe Loop With A Single Pump and A Single Throttling Valve

Since first-order surge in a pipe connecting two constant head reservoirs (Fig.B.1) involves the first quarter-wave acoustic mode, shown in Fig.B.2a, it is assumed that the mode shapes in the suction and discharge pipes of a loop such as that shown in Fig.C.1 will approximate those of quarter-wave modes as closely as possible during first order surge. Provided this assumption is approximately correct, the pipe loop shown in Fig.C.1 can be replaced by the lumped parameter representation shown in Fig.C.2 for the same reason that the pipe illustrated in Fig.B.1 could be modelled with the inertance and capacitance depicted in Fig.B.2.

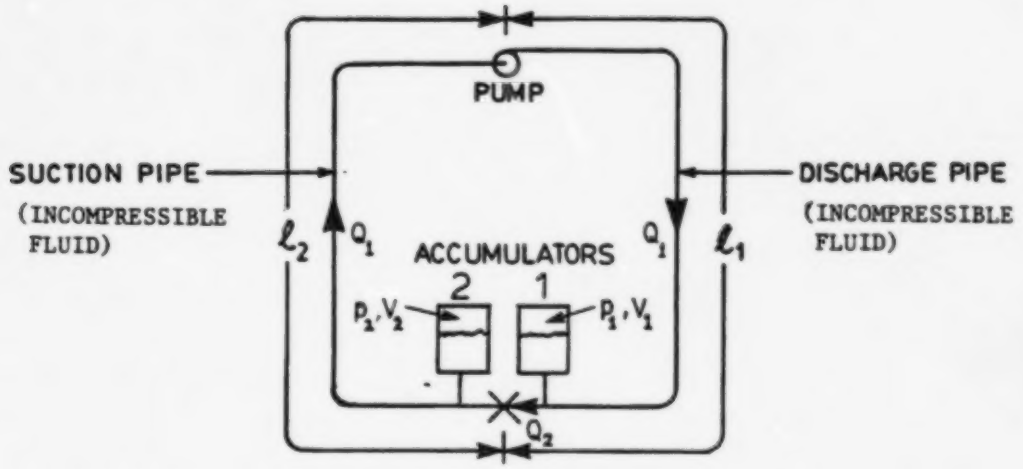


Fig.C.2: Lumped Parameter Representation of Pipe Loop

It is assumed that the flowrate through the valve is $Q_2$ and that the flowrate through the remainder of the loop is $Q_1$. It is also assumed that the two flowrates, the two accumulator volumes ($V_1$ and $V_2$) and the two accumulator pressures ($p_1$ and $p_2$) can each be written as the sum of a steady component and an oscillatory component as,

$$Q_1 = \bar{Q}_1 + Q_1'$$

$$Q_2 = \bar{Q}_2 + Q_2'$$

$$p_1 = \bar{p}_1 + p_1'$$

$$p_2 = \bar{p}_2 + p_2'$$

$$V_1 = \bar{V}_1 + V_1'$$

and

$$V_2 = \bar{V}_2 + V_2'$$

The term with the overbar on the right-hand side of each expression is the steady component while the other term on the right-hand side is the oscillatory component.

Assuming the gas in accumulator 1 is compressed polytropically with a polytropic exponent n, we have,

$$p_1 V_1^n = \bar{p}_1 \bar{V}_1^n$$

so differentiating with respect to time gives,

$$\frac{dp_1}{dt} = - n \bar{p}_1 \frac{\bar{V}_1^n}{V_1^{n+1}} \frac{dV_1}{dt}$$

For small perturbations, $V_1 = \bar{V}_1$, so

$$\frac{dp_1}{dt} = \frac{- n \bar{p}_1}{\bar{V}_1} \frac{dV_1}{dt} \tag{C.1}$$

Since the derivatives of the steady components of $p_1$ and $V_1$ are zero, Eq.(C.1) reduces to

$$\frac{dp_1'}{dt} = \frac{- n \bar{p}_1}{\bar{V}_1} \frac{dV_1'}{dt}$$

$$= \frac{- n \bar{p}_1}{\bar{V}_1} (Q_2' - Q_1') \ . \tag{C.2}$$

since $\frac{dV_1'}{dt} = Q_2' - Q_1'$ . It can be shown in a similar manner that,

$$\frac{dp_2'}{dt} = \frac{- n \bar{p}_2}{\bar{V}_2} (Q_1' - Q_2') \ . \tag{C.3}$$

Setting $L' = \ell_1 + \ell_2$, it is easily verified by applying the momentum equation to the liquid in the suction and discharge pipes that for small perturbations in $Q_1$,

$$\frac{dQ_1'}{dt} = \frac{(p_2' - p_1')\ A + M_{pp}\ Q_1'\ A}{\rho\ L'} \tag{C.4}$$

where A is the cross-sectional area of the suction and discharge pipes, $\rho$ is the density of the fluid in the pipes and $M_{pp}$ is the slope of the pump's differential pressure ($\Delta p_p$) vs. volumetric flow ($Q_1$) curve, i.e.,

$$M_{pp} = d(\Delta p_p)/dQ_1 \tag{C.5}$$

Similarly, for small perturbations in $Q_2$,

$$p_1' - p_2' = M_{vp}\ Q_2' \ . \tag{C.6}$$

where $M_{vp}$ is the slope of the valve's differential pressure ($\Delta p_v$) vs. volumetric flow ($Q_2$) curve, i.e.,

$$M_{vp} = \frac{d\ (\Delta p_v)}{dQ_2} \tag{C.7}$$

By differentiating Eq.(C.4) with respect to time and then using Eqs.(C.2), (C.3), (C.4) and (C.6) to express the resulting derivatives of $p_1'$ and $p_2'$ in terms of $Q_1'$ and its first derivative, it is possible to obtain the following second order ordinary differential equation defining $Q_1'$:

$$\frac{d^2\ Q_1'}{dt^2} + C_1\ \frac{dQ_1'}{dt} + C_2\ Q_1' = 0 \tag{C.8}$$

where

$$C_1 = \frac{n}{M_{vp}} \left(\frac{\bar{p}_1}{\bar{V}_1} + \frac{\bar{p}_2}{\bar{V}_2}\right) - \frac{M_{pp}\ A}{\rho\ L'} \tag{C.9}$$

and

$$C_2 = \frac{nA}{\rho L'} \left(\frac{\bar{P}_1}{\bar{V}_1} + \frac{\bar{P}_2}{\bar{V}_2}\right) \left(1 - \frac{M_{pp}}{M_{vp}}\right) \tag{C.10}$$

Since Eq.(C.8) is linear and homogeneous with constant coefficients, its solution depends on the roots of the corresponding characteristic equation

$$r^2 + C_1 r + C_2 = 0$$

which are

$$r = -\frac{C_1}{2} \pm \sqrt{\frac{C_1^2}{4} - C_2} \tag{C.11}$$

These roots will be complex (i.e., $r = \sigma \pm i\omega$) and thus yield an oscillatory solution when

$$C_2 - \frac{C_1^2}{4} > 0 \tag{C.12}$$

Also, the oscillations will grow with time when $\sigma > 0$, in other words when,

$$-C_1 > 0 \tag{C.13}$$

For Eqs.(C.12) and (C.13) to be satisfied simultaneously, it is easily verified that we must have,

$$2\sqrt{C_2} > -C_1 > 0 \tag{C.14}$$

From the stability criteria derived in Appendix B for a single pipe with a constant sound speed (i.e., Eqs.(B.29) and (B.30)), it can be assumed that the minimum requirement for unstable operation in the present case is that we have,

$$-C_1 > 0 \qquad (\text{with } M_{vp} > M_{pp}). \tag{C.15}$$

or

$$M_{pp}\, M_{vp} > \frac{n\, \rho\, L'}{A} \left(\frac{\bar{p}_1}{\bar{V}_1} + \frac{\bar{p}_2}{\bar{V}_2}\right) \qquad (M_{vp} > M_{pp}) \tag{C.16}$$

If $M_p = d(\Delta H_p)/dQ_1$ and $M_v = d(\Delta H_v)/dQ_2$, where $\Delta H_p$ and $\Delta H_v$ are the head differences across the pump and valve respectively as in Appendix B,

$$M_{pp} = \rho\, g\, M_p \tag{C.17}$$

and

$$M_{vp} = \rho\, g\, M_v \tag{C.18}$$

Substituting Eqs.(C.17) and (C.18) into Eq.(C.16), we obtain

$$M_p\, M_v > \frac{nL'}{\rho A g^2} \left(\frac{\bar{p}_1}{\bar{V}_1} + \frac{\bar{p}_2}{\bar{V}_2}\right) \tag{C.19}$$

or

$$M_p\, M_v > \frac{1}{g^2\, A^2} \left[\left(\frac{n\, \bar{p}_1\, \ell_1\, A}{\rho\, \bar{V}_1}\right) \frac{L'}{\ell_1} + \left(\frac{n\, \bar{p}_2\, \ell_2\, A}{\rho\, \bar{V}_2}\right) \frac{L'}{\ell_2}\right] \tag{C.20}$$

The terms in round brackets in Eq.(C.20) can be regarded as the effective sound speeds in pipes 1 and 2 (i.e., $a_1$ and $a_2$) as is easily verified by comparing them to Eq.(B.38), which was derived for the case of isothermal gas compression (i.e., for n=1). Thus it is assumed that Eq.(C.20) can be rewritten in the form,

$$M_p\, M_v > \left(\frac{a_1}{gA}\right)^2 \frac{L'}{\ell_1} + \left(\frac{a_2}{gA}\right)^2 \frac{L'}{\ell_2} \tag{C.21}$$

or as,

$$M_p\, M_v > Z_{c_1}^2 \frac{L'}{\ell_1} + Z_{c_2}^2 \frac{L'}{\ell_2} \tag{C.22}$$

where

$Z_{c_1}$ = the characteristic impedance [25] of pipe 1 = $a_1/gA$

and

$Z_{c_2}$ = the characteristic impedance of pipe 2 = $a_2/gA$.

Equation (C.22) is similar in form to the minimum requirement for unstable operation derived in Appendix B for a single pipe with a constant sound speed, i.e.,

$$M_p M_v > Z_c^2 \qquad \text{(see Eq.(B.29))}$$

When $\sigma \simeq 0$, the "natural frequency" of the lumped parameter system shown in Fig.C.2 can be obtained from the expression,

$$\omega \simeq \sqrt{-C_2} \tag{C.23}$$

If, in addition, $M_{pp} << M_{vp}$, we can write that

$$\omega \simeq \sqrt{\frac{nA}{\rho L'}\left(\frac{\bar{p}_1}{\bar{V}_1} + \frac{\bar{p}_2}{\bar{V}_2}\right)} = \sqrt{\frac{nA\ \bar{p}_1 \ell_1}{\rho\ \bar{V}_1} \times \frac{1}{\ell_1 L'} + \frac{nA\ \bar{p}_2\ \ell_2}{\rho\ \bar{V}_2} \times \frac{1}{\ell_2 L'}}$$

$$= \sqrt{\frac{a_1^2}{\ell_1 L'} + \frac{a_2^2}{\ell_2 L'}} \tag{C.24}$$

When Eq.(C.2) is divided by Eq.(C.3), we obtain,

$$\frac{p_1'}{p_2'} = -\frac{n\ \bar{p}_1}{\bar{V}_1} \Big/ \frac{n\ \bar{p}_2}{\bar{V}_2} = \frac{-\ n\ \bar{p}_1\ A\ \ell_1}{\rho\ \bar{V}_1} \times \ell_2 \Big/ \frac{n\ \bar{p}_2\ A\ \ell_2}{\rho\ \bar{V}_2} \times \ell_1$$

$$= -\frac{a_1^2}{a_2^2} \times \frac{\ell_2}{\ell_1}$$

Thus,
$$|p_1'|/|p_2'| = (a_1^2/a_2^2) \times \ell_2/\ell_1 \tag{C.25}$$

and the amplitude of the pressure pulsations will be greatest in the pipe (suction or discharge) with the highest sound speed (if $\ell_1 \simeq \ell_2$).

It is worthwhile examining the stability of a system in which the two accumulators seen in Figure (C.2) are located just before and just after the pump instead of the valve. This is easily done by substituting $-M_{vp}$ for $M_{pp}$ and $-M_{pp}$ for

$M_{vp}$ in Eqs.(C.9) and (C.10) and applying the criteria expressed by Eqs.(C.12) and (C.13), as before. With these modifications, the equation defining $C_2$ (Eq.(C.10)) becomes,

$$C_2 = \frac{nA}{\rho L'} \left(\frac{\bar{p}_1}{\bar{V}_1} + \frac{\bar{p}_2}{\bar{V}_2}\right) \left(1 - \frac{M_{vp}}{M_{pp}}\right) \qquad (C.26)$$

As seen in Eq.(C.12), there is no possibility of obtaining a dynamically unstable system unless $C_2 > 0$. For this to be the case, Eq.(C.26) indicates that we must have $M_{pp} > M_{vp}$. Since the system would be statically unstable if this condition was satisfied, dynamically unstable operation must be impossible for a system in which the only compressible volumes are located at the pump suction and discharge.

## Appendix D - Modified ANC Model for the Bruce Pump

As noted in Section B.2.2, the two-phase pump performance model that was used to predict the pump differential pressure in the numerical simulations of surge was essentially the ANC pump model [Ref.17] modified to account for the relatively high specific speed of the Bruce pump using data given by McGee et al. in [Ref.34]. In particular, it was assumed that the pump head would start to degrade and become fully degraded at void fractions of $\alpha_{ud}$ = 15% and $\alpha_{fd}$ = 50% respectively (in accordance with data given in [Ref.34]) instead of at the values of approximately 8% and 20% respectively used in the ANC model with the M2 two-phase multiplier. The fully degraded head versus flow curve was assumed to be identical in shape to the single phase head curve (again in accordance with data given in [Ref.34]) but displaced downwards by 170 m at all flowrates, as shown in Figure D.1. The head decrement of 170 m was obtained by assuming that the fully degraded head at the design flowrate would be 20% of the rated single phase head of 213 m (i.e., (1-0.2) x 213 m = 170 m), since this is a typical reduction.

The following expressions were used to obtain the head (H) at a given void fraction $\alpha^*$ and volumetric flowrate $Q^*$ from the single phase head at $Q^*(H_1(Q^*))$ and the fully degraded head ($H_2(Q^*)$):

$$H(\alpha^*,Q^*) = H_1(Q^*) \quad \text{for } \alpha^* \leq \alpha_{ud}$$

$$H(\alpha^*,Q^*) = H_1(Q^*) + \frac{(\alpha^* - \alpha_{ud})}{(\alpha_{fd} - \alpha_{ud})} (H_2(Q^*) - H_1(Q^*)) \quad \text{for } \alpha_{ud} < \alpha^* < \alpha_{fd}$$

$$H(\alpha^*,Q^*) = H_2(Q^*) \quad \text{for } \alpha^* \geq \alpha_{fd}$$

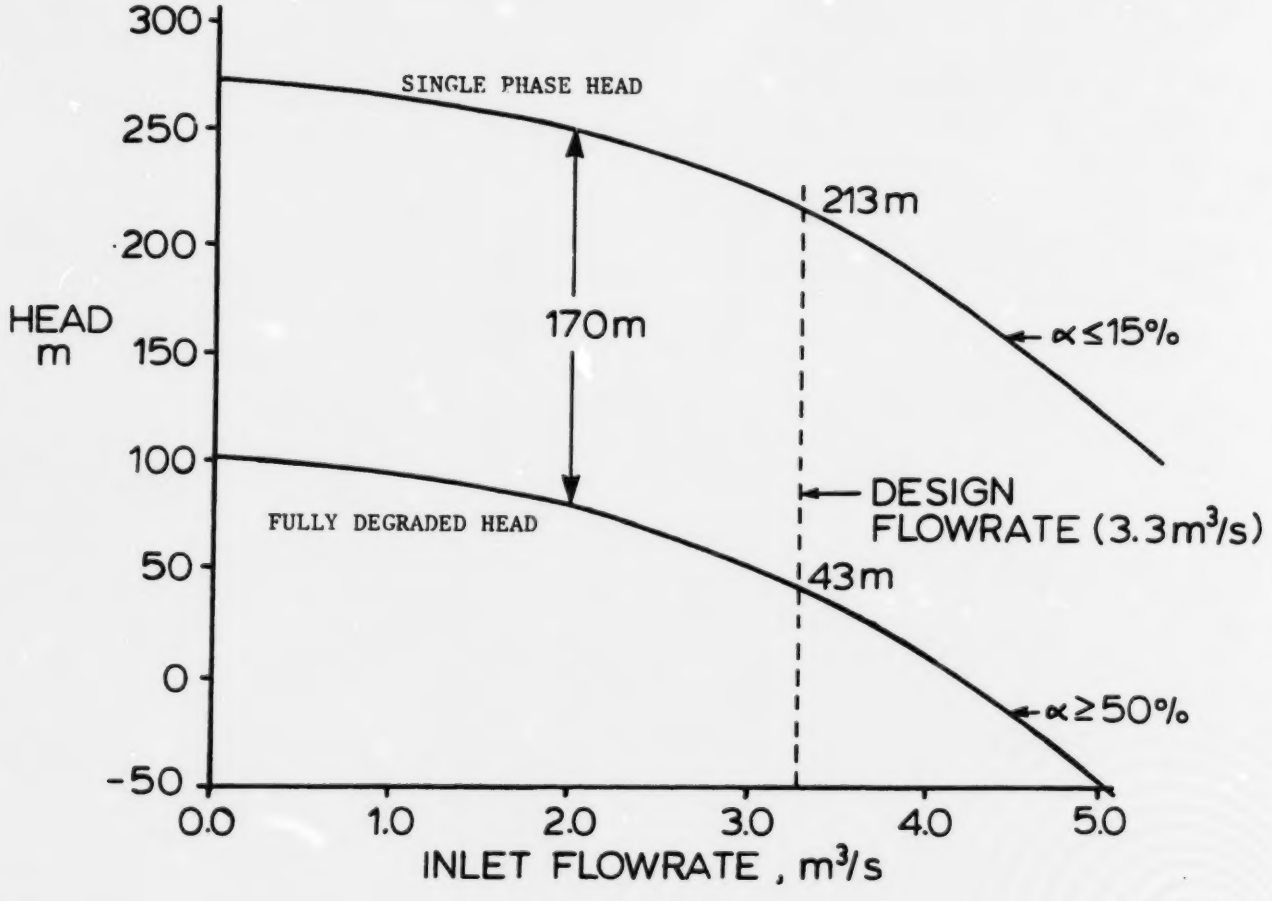


Figure D.1 Two-Phase Performance Characteristics of a Bruce PHT Pump (Assumed).

## Appendix E - Small Perturbation Analysis of Surge

The transfer matrix method described in Appendix B will be used in this appendix to examine the stability of the flow that was observed to surge in the computer simulation described in Section 2. Figure 25 shows the loop that will be modelled in the analysis and Table 6 summarizes the nominal operating conditions.

If the point immediately downstream of the value in the loop shown in Figure 25 is designated station 1, the complex head $\hat{H}_1$ and complex flowrate $\hat{Q}_1$ at that location can be written in terms of those same parameters as

$$\begin{Bmatrix} \hat{H}_1 \\ \hat{Q}_1 \end{Bmatrix} = [F_{valve}]\ [F_{dis}]\ [F_{pump}]\ [F_{suct}] \cdot \begin{Bmatrix} \hat{H}_1 \\ \hat{Q}_1 \end{Bmatrix}$$

$$= [T] \cdot \begin{Bmatrix} \hat{H}_1 \\ \hat{Q}_1 \end{Bmatrix} \qquad \text{E.1}$$

where $F_{valve}$, $F_{dis}$, $F_{pump}$ and $F_{suct}$ are the transfer matrices for the valve, discharge pipe, pump and suction pipe respectively and T is the product of those matrices. The matrix $F_{valve}$ was defined previously in Eq.B.19 while $F_{suct}$ can be obtained from Eq.B.17 by substituting the suction pipe length ($\ell_2$) for $\ell$.

Since the sound speed of the liquid in the discharge pipe is more than two orders of magnitude greater than the sound speed of the two-phase mixture in the suction pipe in the problem being analyzed, the liquid in the discharge pipe will be modelled as a lumped inertance [Ref.27]. If the flow in the discharge pipe is assumed to be frictionless, $F_{dis}$ can be written as [Ref.27]

$$F_{dis} = \begin{bmatrix} 1 & -sL\ell_1 \\ 0 & 1 \end{bmatrix} \qquad \text{E.2}$$

where s is the complex frequency ($=\sigma+i\omega$), $\ell_1$ is the length of the discharge pipe and $L = 1/gA$ (as in Eq.B.5).

Since the dependent variables in the formulation of the transfer matrix method being used here are the oscillatory head $H'$ and flowrate $Q'$ instead of $p'$ and $\dot{m}'$, Eqs.10 and 11 in Section B.2.2 defining $(\dot{m}_o' - \dot{m}_i')$ and $\Delta p_p'$ $(=p_o'-p_i')$ for the pump must be rewritten in terms of $H'$ and $Q'$ as,

$$Q_o' - Q_i' = \frac{\partial V_c}{\partial H_i} \frac{dH_i'}{dt} + \frac{\partial V_c}{\partial Q_i} \frac{dQ_i'}{dt} \qquad \text{E.3}$$

and

$$H_p' = \frac{\partial(\Delta H_p)}{\partial Q_i} Q_i' + \frac{\partial(\Delta H_p)}{\partial H_i} H_i' \qquad \text{E.4}$$

where unprimed quantities are total values, consisting of steady and oscillatory components, and $\Delta H_p'$ $(=H_o'-H_i')$ is the oscillatory component of the pump head. From Eqs.B.8 and B.9,

$$H_o' = \hat{H}_o e^{st} \qquad \text{E.5}$$

$$Q_o' = \hat{Q}_o e^{st} \qquad \text{E.6}$$

$$H_i' = \hat{H}_i e^{st} \qquad \text{E.7}$$

and

$$Q_i' = \hat{Q}_i e^{st} \qquad \text{E.8}$$

so

$$\frac{dH_i'}{dt} = s \hat{H}_i e^{st} \qquad \text{E.9}$$

and

$$\frac{dQ_i'}{dt} = s \hat{Q}_i e^{st} \qquad \text{E.10}$$

Substituting Eqs.E.6, E.8, E.9 and E.10 into Eq.E.3 and cancelling the common factor $e^{st}$, we obtain,

$$\hat{Q}_o - \hat{Q}_i = s \frac{\partial V_c}{\partial H_i} \hat{H}_i + s \frac{\partial V_c}{\partial Q_i} \hat{Q}_i \qquad \text{E.11}$$

Similarly, Eq.E.4 can be rewritten as

$$\hat{H}_o - \hat{H}_i = \frac{\partial (\Delta H_p)}{\partial Q_i} \hat{Q}_i + \frac{\partial (\Delta H_p)}{\partial H_i} \hat{H}_i \qquad \text{E.12}$$

Combining Eqs.E.11 and E.12, the transfer matrix for the pump relating $\hat{H}_o$ and $\hat{Q}_o$ to $\hat{H}_i$ and $\hat{Q}_i$ can now be written as

$$F_{pump} = \begin{bmatrix} 1 + \frac{\partial (\Delta H_p)}{\partial H_i} & \frac{\partial (\Delta H_p)}{\partial Q_i} \\ s \frac{\partial V_c}{\partial H_i} & 1 + s \frac{\partial V_c}{\partial Q_i} \end{bmatrix} \qquad \text{E.13}$$

In order to obtain a non-trivial solution to Eq.E.1 (i.e., a solution other than $\hat{H}_1 = 0$, $\hat{Q}_1 = 0$), we must have

$$\det[T-I] = 0 \qquad \text{E.14}$$

where I is the identity matrix. Since det[T-I] is complex, Eq.E.14 is equivalent to the two equations

$$\mathrm{Re}(\det[T-I]) = 0 \qquad \text{E.15}$$

and

$$\mathrm{Im}(\det[T-I]) = 0 \qquad \text{E.16}$$

applying to the real and imaginary parts respectively. Equations E.15 and E.16 can be solved simultaneously for the two unknowns $\sigma$ and $\omega$.

Table E.1 gives the values assigned to the different parameters in the transfer matrices seen in Eq.E.1.

Table E.1: Data Used in the Small Perturbation Stability Calculations

| Parameter | Assigned Value |
|---|---|
| $A$ | $0.246\ m^2$ |
| $\ell_1$ | 15 m |
| $\ell_2$ | 15 m |
| $M_v$ | $279.0\ sec/m^2$ [1] |
| $\partial(\Delta H_p)/\partial H_i$ | 42.0 [2] |
| $\partial(\Delta H_p)/\partial Q_i$ | -18.2 [3] |
| $\partial V_c/\partial H_i$ | -0.0824 [4] |
| $\partial V_c/\partial Q_i$ | -0.763 [5] |

[1] Calculated from Eq.B.21 rewritten as $M_v = 2(\overline{\Delta p_p})/g\bar{\dot{m}}$ ($\overline{\Delta p_p}$ and $\bar{\dot{m}}$ are the nominal pump differential pressure and mass flow given in Table 6).

[2] Assumed the same as $\partial(\Delta p_p)/\partial p_i$ and estimated from the variation of $\Delta p_p$ with $p_i$ in the computer simulation described in Section B.2. This derivative can also be obtained from thermodynamic relations and the variation of head with inlet void fraction in the two-phase pump performance model (e.g., ANC).

[3] Assumed equal to the slope of the head vs. flow curve at constant inlet void fraction (Figure D.1) for a flowrate calculated using the average of the suction (two-phase) and discharge (liquid) densities ($\bar{\rho}$).

[4] Calculated from the relation $\partial V_c/\partial H_i = \bar{\rho} g\ \partial V_c/\partial p_i$ with $\bar{\rho} = 763$ $kg/m^3$ and $\partial V_c/\partial p_i = -1.1 \times 10^{-5}\ m^3/Pa$ (as in the computer simulation).

[5] Calculated from the relation $\partial V_c/\partial Q_i = \bar{\rho}\ \partial V_c/\partial \dot{m}_i$ with $\bar{\rho} = 763$ $kg/m^3$ and $\partial V_c/\partial \dot{m}_i = -0.001\ m^3/kg/sec$ (as in the computer simulation).

Since the transfer matrix method assumes a constant fluid density, it was necessary to make some approximations to apply it to the present analysis where the fluids in the suction and discharge pipes have different densities. Thus in calculations where the density of the fluid was required, which was whenever a mass flowrate had to be converted to a volumetric flowrate or pressure had to be converted to head, the fluid density was taken to be the average of the fluid density in the suction and discharge pipes. Since the density of the fluid in the discharge pipe was 887 kg/m$^3$ ($\rho_f$ @180$^o$C) and the density in the suction pipe was approximately 640 kg/m$^3$ (corresponding to a void fraction of 28%), the abovementioned average density was 763 kg/m$^3$.

The first four roots of Eq.E.14 were obtained numerically and found to have the real and imaginary parts listed in Table E.2.

Table E.2 Values of $\sigma$ and $\omega$ for the First Four Roots of Eq.E.14 (i.e., modes of oscillation)

| Mode | $\sigma$ ($sec^{-1}$) | $\omega$ ($sec^{-1}$) |
|---|---|---|
| 1 | -0.434 | 2.136 |
| 2 | 0.818 | 4.367 |
| 3 | -0.227 | 7.167 |
| 4 | 0.935 | 9.316 |

Since the second mode of oscillation is the first mode with a positive value of $\sigma$, it is presumably this mode that would be excited during surge. The corresponding surge frequency of 4.367 rad/sec or approximately 0.7 Hz is roughly 22% less than the surge frequency of 0.9 Hz obtained in the numerical simulation. Because the transfer matrix method is strictly only applicable to analyses in which the flow velocity is negligible compared to the speed of sound in the fluid and the fluid is essentially incompressible, two provisos that are not satisfied in the present analysis, this agreement is considered to be acceptable.

## Appendix F - Voided Length Calculation

Assuming negligible heat loss over the voided length shown in Figure 35, the first law of thermodynamics can be written for the flow between the flashing front (station 1) and the pump suction (station 2) as,

$$h_1 + \frac{V_1^2}{2} + gz_1 = h_2 + \frac{V_2^2}{2} + gz_2 \qquad \text{F.1}$$

where h, V, z and g are enthalpy, velocity, elevation and gravitational acceleration respectively. At the flashing front, $h_1$ is equal to the enthalpy of saturated liquid water ($h_{f1}$) at a specified pressure $p_1$. Neglecting variations in kinetic energy, Equation F.1 can be rewritten as

$$h_2 = h_1 - g(z_2 - z_1)$$

$$= h_{f1} - gL \qquad \text{F.2}$$

where $L = z_2 - z_1$ .

Assuming the variation in void fraction between stations 1 and 2 is approximately linear and neglecting momentum and frictional pressure losses, the static pressure at point 2 ($p_2$) can be expressed in terms of that at point 1 ($p_1$) as

$$p_2 = p_1 - \bar{\rho}\, g\, L \qquad \text{F.3}$$

where $\bar{\rho}$ = the average density of the fluid in the voided length

$$= \frac{\rho_1 + \rho_2}{2} \qquad \text{F.4}$$

The density at the pump suction ($\rho_2$) can be calculated from the specified pump suction void fraction ($\alpha_p$) by means of the expression,

$$\rho_2 = \alpha_p\, \rho_g + (1-\alpha_p)\, \rho_\ell \qquad \text{F.5}$$

while $\rho_1 = \rho_\ell$ at $p = p_1$.

By assuming a value of L, $h_2$ and $p_2$ can be obtained from Equations F.2 and F.3 respectively for the specified values of $p_1$ and $\alpha_p$. The corresponding value of $\rho_2$ can then be obtained from the equation of state written in the form $\rho = \rho(h,p)$. If this value of $\rho_2$ agrees with that calculated initially from Equation F.5, the correct value of L has been found, otherwise the calculations are repeated with a new value of L. This procedure is repeated until the two values of $\rho_2$ are in agreement.

It should be mentioned that negligible error results if the term -gL in Equation F.2 is neglected.

## Appendix G - Oscillatory Void Volume Calculation

This appendix describes a simplified analysis undertaken to estimate the volume of void that is assumed to have been alternately forming and collapsing at the pump suction during periods of instability in the Pickering pump tests. The analysis will be performed for the period in test 202 (Figure 17) when the frequency of the oscillations and the peak-to-peak amplitude of the variations in pump differential pressure were approximately 4.5 Hz and 1 MPa respectively.

The desired oscillatory void volume will be calculated by first estimating the amplitude of the corresponding variations in discharge flowrate. For simplicity, it will be assumed that the oscillatory flowrate in the discharge pipe ($Q'$) varied sinusoidally with time according to the relationship,

$$Q' = |Q'| \sin \omega t \qquad G.1$$

in which $\omega$ and $|Q'|$ are the frequency and the amplitude of the oscillations respectively. If it is also assumed that variations in the pressure downstream of the control valve and the pressure at the pump suction were insignificant compared to the variations in pump differential pressure and that these two pressures were approximately equal (assumptions which should be valid provided vapor cavities were present at both locations), the momentum equation for the oscillatory flow in the discharge pipe can be approximated for small perturbations in pressure and flowrate as,

$$\frac{dQ'}{dt} = A(\Delta p_p' - M_v Q')/\rho_f L_d \qquad G.2$$

where

$A$ = the cross-sectional area of the discharge pipe

$\Delta p_p'$ = the oscillatory component of the pump differential pressure

$M_v$ = $d(\Delta p_v)/d\bar{Q}$, where $\Delta p_v$ is the pressure drop across the valve (and other fittings in the discharge pipe) and $\bar{Q}$ is the flowrate through it

$\rho_f$ = the density of the fluid in the discharge pipe

and

$L_d$ = the length of the discharge pipe

Substituting Equation G.1 into Equation G.2, we obtain,

$$\Delta p_p' = |Q'| \left(\frac{\rho_f L_d}{A}\right) \omega \cos \omega t + M_v \sin \omega t) \qquad G.3$$

It is assumed that $L_d$ = 16 m and A = 0.0745 $m^2$ for the discharge pipe of the Pickering loop. The former value is the length of the discharge pipe, ignoring one branch of the "donut" seen in Figure 13, while the latter is the area of the 14" schedule 100 pipe used between the donut and the pump. The discharge pipe actually contained sections of 12", 14" and 16" pipe [Ref.12] but a constant area will be used here for simplicity.

As shown in Appendix B,

$$M_v = \frac{2\Delta p_v}{\bar{Q}} \qquad G.4$$

Equation G.4 can be evaluated by noting that $\Delta p_v$ and $\bar{Q}$ were approximately 1.4 MPa and 0.7 $m^3$/sec respectively shortly after the start of test 202 (Figure 42). Since $\Delta p_v$ was approximately 1 MPa during the period of instability, as noted in Section A, it is assumed that the corresponding value of $\bar{Q}$ would have been,

$$\bar{Q} = 0.7 \times \sqrt{\frac{1}{1.4}} = 0.59 \ m^3/sec$$

Substituting $\Delta p_v$ = 1 MPa and $\bar{Q}$ = 0.59 $m^3$/sec into Equation G.3, we obtain

$$M_v = \frac{2 \times 1 \times 10^6}{0.59} = 3.39 \times 10^6 \ kg/m^4 \ sec$$

For $\omega = 2\pi \times 4.5$ Hz = 28.3 radians/sec and the values of $L_d$ and A given previously, the numerical value of the coefficient multiplying the first

term within the brackets in Equation G.3 can be evaluated as,

$$\frac{\rho_f L_d \omega}{A} = \frac{958 \times 16 \times 28.3}{0.0745} = 5.82 \times 10^6 \text{ kg/m}^4 \text{ sec}$$

Since this figure is larger than the value of $M_v$, pressure changes resulting from the inertia of the liquid in the discharge pipe were probably very important in the Pickering tests.

It is easily verified by differentiating the bracketted term in Equation G.3 with respect to $\theta(=\omega t)$ and setting the resulting derivative to zero that the term is a maximum when,

$$\omega t = \tan^{-1} \left(\frac{M_v}{\rho_f L_d \omega/A}\right)$$

$$= \tan^{-1} (3.39/5.82) = 0.53$$

Substituting this value of $\omega t$ into Equation G.3 and designating the resulting maximum value (i.e., amplitude) of $\Delta p_p'$ by $|\Delta p_p'|$, we get,

$$|\Delta p_p'| = 6.74 \times 10^6 \, |Q'|$$

from which,

$$|Q'| = 0.148 \times 10^{-6} \, |\Delta p_p'|$$

Since the peak-to-peak amplitude of the variations in pump differential pressure was 1 MPa during the period of interest, $|\Delta p_p'| = 0.5$ MPa and the above expression for $|Q'|$ gives,

$$|Q'| = 0.148 \times 10^{-6} \times 0.5 \times 10^6 = 0.074 \text{ m}^3/\text{sec}$$

This value of $|Q'|$ is 12.5% of the assumed average flowrate of 0.59 $\text{m}^3$/sec.

Assuming that the variations in flowrate in the suction pipe were negligible compared to those in the discharge pipe, the growth and collapse of the void pocket at the pump suction would have been dominated by the latter. Since the periods of growth and collapse of the void pocket would each have occupied one-half of a surge cycle, the oscillatory volume $|V_v'|$ can be calculated from the expression,

$$|V_v'| = \int_0^{\tau/2} |Q'| \sin \omega t \, dt \qquad \text{G.5}$$

where $\tau$ is the period of the oscillations. On integrating Equation G.5, we obtain,

$$|V_v'| = \frac{2|Q'|}{\omega}$$

$$= \frac{2 \times 0.074}{28.3} = 0.0052 \text{ m}^3 \simeq 51$$

as the desired oscillatory void volume.